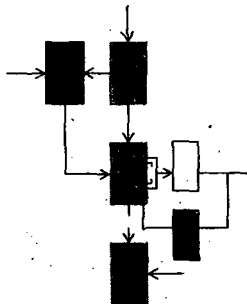


N72-12580

September, 1971

Report ESL-R-459
MIT DSR Projects 76265
and 72486

**CASE FILE
COPY**



**ON OPTIMAL SCHEDULING AND AIR TRAFFIC
CONTROL IN THE NEAR TERMINAL AREA**

Alexander H. Sarris

Electronic Systems Laboratory

MASSACHUSETTS INSTITUTE OF TECHNOLOGY, CAMBRIDGE, MASSACHUSETTS 02139

Department of Electrical Engineering

September, 1971

Report ESL-R-459

ON OPTIMAL SCHEDULING AND AIR TRAFFIC CONTROL
IN THE NEAR TERMINAL AREA

by

Alexander Hippocrates Sarris

This report is based on the unaltered thesis of Alexander H. Sarris submitted in partial fulfillment of the requirements for the degrees of Bachelor of Science and Master of Science at the Massachusetts Institute of Technology in August, 1971. The research was conducted at the Massachusetts Institute of Technology, Electronic Systems Laboratory with support extended by NASA under Grant NGL-22-009-124 and by the U. S. Air Force under Grant AFOSR-70-1941.

Electronic Systems Laboratory
Department of Electrical Engineering
Massachusetts Institute of Technology
Cambridge, Massachusetts 02139

ON OPTIMAL SCHEDULING AND
AIR TRAFFIC CONTROL IN THE
NEAR TERMINAL AREA

by

Alexander Hippocrates Sarris

SUBMITTED IN PARTIAL FULFILLMENT OF THE
REQUIREMENTS FOR THE DEGREES OF

BACHELOR OF SCIENCE

and

MASTER OF SCIENCE

at the

MASSACHUSETTS INSTITUTE OF TECHNOLOGY

August, 1971

Signature of Author *Alexander Hippocrates Sarris*
.....
Department of Electrical Engineering, August 16, 1971

Certified by *Michael Athan*
.....
Thesis Supervisor

Accepted by
Chairman, Departmental Committee on Graduate Students

ON OPTIMAL SCHEDULING AND AIR
TRAFFIC CONTROL IN THE NEAR
TERMINAL AREA

by

Alexander Hippocrates Sarris

Submitted to the Department of Electrical Engineering on August 16, 1971 in partial fulfillment of the requirements for the Degrees of Bachelor of Science and Master of Science.

ABSTRACT

There has been a lack of literature dealing with realistic deterministic air traffic control (ATC) systems. This thesis proposes a scheme for automated air traffic control of landing aircraft in the vicinity of the airport. Each aircraft is put under the control of an airport based computer as soon as it enters the near terminal area (NTA). Scheduling is done immediately thereafter. The aircraft is given a flight plan which, if followed precisely, will lead it to the runway at a prespecified time. The geometry of the airspace in the NTA is chosen so that delays are executed far from the outer marker, and violations of minimum altitude and lateral separations are avoided. Finally, a solution to the velocity mix problem is proposed.

THESIS SUPERVISOR: Michael Athans
TITLE: Associate Professor of Electrical Engineering

ACKNOWLEDGMENTS

I am grateful to Professor Michael Athans for the constant encouragement, moral support, and guidance he offered me during the various stages of this thesis.

I would also like to thank Mr. Tom Imrich for many enlightening discussions.

I am greatly obliged to Mrs. Linda Johnson for typing the thesis, Mrs. Aimee Karolyi for typing the appendix, and Mr. Arthur J. Giordani for his elegant work on the figures.

This research was carried out at the Decision and Control Sciences Group of the M.I.T. Electronic Systems Laboratory with support extended by NASA under grant NGL 22-009-124, and by AFOSR under grant 70-1941.

TABLE OF CONTENTS

	<u>Page</u>
INTRODUCTION.....	7
CHAPTER I	
Background In Air Traffic Control.....	9
1.1 The Present System and Its Problems.....	9
1.2 Summary of Previous Analytical Research.....	13
CHAPTER II	
Description of the Proposed System.....	16
2.1 Assumptions.....	16
2.2 The System Geometry.....	20
2.3 Functional Description of the Control Process	25
2.4 Why Such a System?.....	32
CHAPTER III	
Aircraft Trajectories.....	34
3.1 The Minimum Time Trajectory in the OMS.....	34
3.1.1 Problem Statement.....	35
3.1.2 Solution of the Minimum Time Problem.....	38
3.2 Delay Maneuvers.....	40
3.3 Trajectories Inside the IMS.....	45
3.4 Speed and Descent Profiles in the IMS.....	54
CHAPTER IV	
System Geometry.....	59
4.1 Minimum T_o and Minimum Radius of the IMS....	60
4.1.1 The T_o Minimum Time T_o	60
4.1.2 The Minimum Radius L_o	68
4.2 Determination of the Actual IMS Radii.....	74
4.2.1 The Velocity Mix Problem.....	75
4.2.2 Solution of the Velocity Mix Problem for One Altitude Level.....	84
4.2.3 Conclusions.....	89
4.3 Selection of Position of Altitude Levels....	90
4.4 Length of OMS and Buffer Zone.....	98
4.4.1 The Traffic "Source Points".....	98
4.4.2 The Length of the OMS.....	101
4.4.3 The Length of the Buffer Zone.....	104
4.5 Conclusions.....	112

	<u>Page</u>
CHAPTER V	
The System Algorithm.....	114
5.1 Functional Description of the Algorithm.....	114
5.2 System Subroutines.....	119
5.2.1 The Subroutine ETA-MTT.....	119
5.2.2 The Subroutine ORDER-SETA.....	119
5.2.3 The Subroutine SEQ-SCHED.....	119
5.2.4 The Subroutine DELAY-TYPE.....	125
5.2.5 The Subroutine DAA.....	127
5.2.6 The Subroutine IMS-NOM.....	131
5.2.7 The Subroutine SCHED-TAKEOFF.....	135
5.3 System Computational Requirements.....	137
CHAPTER VI	
Conclusions.....	139
CHAPTER VII	
Ideas for Further Research.....	144
APPENDIX A.....	148
BIBLIOGRAPHY.....	170

INTRODUCTION

The number of landing and take-off operations in the major airports of the United States has been increasing rapidly in the last decade as a result of the large demand for air transportation. The projected rate of growth of scheduled aircraft flights is not about to become smaller in the foreseeable future. The facilities available at commercial airports for handling in and out bound flights obviously must be made more efficient as the volume of traffic increases. Unfortunately, the rate of growth of the volume of operations in the last decade has been larger than anticipated. As a result the airports often find their traffic control systems unable to cope with the demand for landings and take-offs.

The ways to increase air transportation efficiency and capacity are:

- a) Improve the air traffic control (ATC) system presently available.
- b) Provide more runways at every airport.
- c) Build more airports.

The above suggestions are listed in order of increasing cost and increasing effectiveness. However, the difficulty of implementing the latter two suggestions is very great. Most of the airports have been surrounded by cities and the land they have is fixed thus prohibiting

the construction of more runways. The building of new airports is greatly hampered by decreasing land availability, and vigorous, negative reactions from environment and noise minded citizen groups. This leaves the first suggestion as the only solution to the short range air congestion problem. Research^{1,2,4} has proved that increased efficiency of the ATC system can delay the need to build more airports for at least two decades.

The alarm that was aroused by the unexpected growth of air traffic operations led to "patching ups" of the old ATC system. The improvements were based more or less on intuition rather than analysis. The result was the present system which consists of many ad hoc rules and procedures and a lot of intuitive guessing from the air traffic controllers, who are the sole decision makers in the process.

The aim of this work is to present a nonutopian ATC system whose major decision maker is a computer. The geometry and some of the rules of the existing system were changed to adapt them to the requirements of automation. The air traffic controllers remain as the ultimate commanders of the system, but their work load is greatly diminished. Chapter I presents the present ATC system, for comparison with the proposed scheme, and summarizes previous research relevant to this work. Chapter II presents in a non-detailed fashion the envisioned system. In Chapters III, IV and V the details of the system are analysed. Finally, Chapters VI and VII present conclusions and areas where the present work can be extended.

CHAPTER I

BACKGROUND IN AIR TRAFFIC CONTROL

This chapter presents the reader with knowledge necessary to evaluate the subsequent chapters. In section 1.1 the present ATC system is described and some of its inadequacies are pointed out. Section 1.2 summarizes the most important of the analytical research to date and previous suggestions for improvement of the present ATC system.

1.1 The Present System and Its Problems

A detailed description of the present ATC system has been treated thoroughly by Simpson¹, and for this reason will not be duplicated in this thesis. Only the aspects of the system that are relevant to this work will be summarized here.

Consider an aircraft ready for a flight. The pilot has already filed with the local FAA Flight Service Station a flight plan which is to be followed more or less closely throughout the flight.

This plan includes many bits of information, such as time of take-off, air route to be followed, altitude, speed, etc.

All the aircraft that are inside an airport are monitored by the control tower. When the pilot is ready to take-off, he contacts the tower and is put under the responsibility of one of the ground controllers. This group is in charge of every aircraft that

moves inside the airport. They guide the aircraft to and from the runways, arrange time and order of take-offs and give final clearance. They are in close communication with the departure controllers, who take charge of the aircraft after they take-off, and the approach controllers, who are in charge of the aircraft before they land.

As soon as a time interval between landings or other take-offs is available, the ground controller gives clearance to the pilot to take-off, and hands the aircraft's flight plan to one of the departure controllers. He, in turn, monitors the aircraft via radar and guides it out of the Near Terminal Area (NTA) via voice commands.--the NTA is a cylindrical region, centered at the airport, of radius 40-60 nautical miles (nmi).^{*} As soon as the aircraft is at the boundary of the NTA, its flight plan and all responsibility for control are "handed off" to the regional control center adjacent to the airport. The air route traffic control centers (ARTCC) monitor aircraft with radar and give radio commands. They "hand off" every aircraft leaving their area to the next ARTCC, and so on, until the aircraft is near its destination when it is "handed off" to one of the approach controllers. They, in turn, observe all approaching aircraft on their radar screens, determine the landing order and guide the airplanes to the runway via voice commands.

The system presented here deals with approach control; so, it is worthwhile to take a closer look at the present system and the

*The ATC system of units accepts as unit of length the nautical mile. One nmi = 1852 meters \approx 6080 feet \approx 1.153 statute mile.

interactions between the controller and the pilot, during the landing phase. If there are not too many aircraft in the NTA requiring landing service, the controller gives the pilot a "vector", or direction, to follow until the first check point called the inner fix, usually an electronic marker. Subsequently, the controller gives to the pilot another vector to follow until the final check point before landing. This check point is called the outer marker (OM) and marks the beginning of an electronically defined descent path, the glide path, which leads straight to the runway. The OM is usually located about 5-7 n.miles from the beginning, or "threshold", of the runway and at an altitude approximately 1200 feet above the level of the runway. While the aircraft is following the glide path the controller has no control over the aircraft, except when he orders a missed approach maneuver. This discussion then points out the fact that the ATC system inside the NTA aims at sequencing the aircraft safely until the OM.

If there are too many aircraft requiring landing service simultaneously, the controllers delay the aircraft they cannot handle by "stacking" them at points called the outer fixes. Each "stack" is a column of altitude levels spaced 1000 feet apart. Each altitude level can be utilized by only one aircraft at any time. As soon as the area between the OM and the outer fixes becomes decongested of traffic, some of the aircraft that are "holding" in the stacks are ordered to leave their delay positions and enter the IMS. Aircraft occupying the lower levels are serviced first. As soon as a lower level is emptied all the aircraft above move down by one level and

await their turn.

All the landings utilize the same runway. If the wind direction changes drastically then all landings are switched to a different runway, such that the direction of landing is opposite to the wind direction. The OM, which can be viewed as an extension of the runway, is shifted accordingly. The positions of the stacks remain unchanged but all aircraft that are approaching the OM are given new vectors.

The procedures outlined above constitute what is called landing under instrument flight rules (IFR). Landing under visual flight rules (VFR), which is essentially a "see and avoid" scheme, will not be considered here due to the fact that it breaks down under congestion and bad weather conditions.

The problems of the present ATC system arise because the controllers are the only system decision makers. The worst system inefficiencies occur during the landing phase. Since all the aircraft have to merge at the OM, the approach controllers have to keep in their minds future positions of the landing airplanes, and make fast decisions about future vectors to be given out. The fact that different aircraft have different speeds makes the situation worse. All routine information necessary to each pilot is transmitted via voice, a task which occupies much of the controllers' valuable time. It is understandable then, that in such an environment the human operators must be very conservative and allow large margins for the errors due to the necessarily gross estimates. It is indeed amazing that these people can keep accidents to such a low figure, and maintain in opera-

tion a system that was designed to accommodate the traffic loads of the fifties.

1.2 Summary of Previous Analytical Research

It is evident that before any suggestions for improvement of the present ATC system are made, its inefficiencies must be made explicit by studying analytically its various components.

One of the major early analytical studies of ATC was the work of Blumstein.² He analyzed mainly the capacity of a runway, i.e., the number of landings per hour the runway can support, given random arrivals of mixed speed aircraft. A result that he obtained was that with present FAA separation standards (at least 3 n.miles lateral separation over the OM and one minute time separation on the runway), a runway cannot handle more than 40 landings per hour. Given that at present, even at peak congestion, most of the runways do not handle more than 30-35 landings per hour, there is room for improvement.

The major analytical work, in the sixties was done by Simpson¹, and parts of it were recently extended by Odoni.³ They investigated analytically practically every aspect of the present ATC system. The models they reached were simulated and results indicated that the models roughly agreed with the existing system. Some of their conclusions were as follows:

a) The present holding stacks are not a very efficient delay method and in fact they lower the capacity of the airport.

b) Most of the present delays occur because of interference

of the aircraft when they are in the NTA, and not because of en-route interference.

c) The radius of the area between the outer fixes and the OM should be as small as possible so as to minimize the interval of time the aircraft fly from the stacks to the OM.

d) The best design of a terminal area ATC system should result after extensive simulation, because the terminal area cannot be analyzed mathematically accurately enough.

e) The computer can be very helpful as a control element in future systems.

The state of ATC research, projections of future air traffic volume, and propositions for improvement of the present system were recently studied^{4,5}. A major conclusion of these studies was that automation has to be introduced to relieve the controllers of the tremendous load. At present a study of a semiautomated ATC system is being conducted.⁶ The ARTS III system, as it is called, will still keep the human controller as the major decision making element.

In addition there is some recent research on concepts for completely automatic ATC. The ones the author is aware of are those of Porter⁷, Athans and Porter⁸, Telson⁹ and Erzberger and Lee¹⁰. In references 7 and 8 a method for controlling air traffic was given, based on the theory of optimal control of linear systems with quadratic criteria. References 9 and 10 presented schemes for sequencing and spacing based on minimum time trajectories of the aircraft from the

boundary of the NTA until the OM. A major simplifying assumption of the studies [7] - [10] was that all aircraft have the same speed inside the NTA. This assumption was unrealistic, but helped present some novel concepts.

To construct an ATC system that preserves some of the concepts of [7] - [10] but lifts the simplifying assumption of constant speeds was the primary motivation to undertake this research.

CHAPTER II

GENERAL DESCRIPTION OF THE PROPOSED SYSTEM

The terminal ATC system proposed in this thesis is deterministic. By this it is meant that every aircraft entering the NTA will be automatically controlled by a central, control-tower based computer. The system is structured so that the computer performs the tasks of scheduling and spacing, and determines a nominal path as well as a nominal speed profile for each aircraft.

The assumptions under which the system is analyzed are delineated in section 2.1. In section 2.2 the geometry of the airspace in the NTA is described. The geometry is suited for computer controlled ATC. Section 2.3 describes the functions that the computer will perform. The final section 2.4 discusses some of the reasons for choosing this particular system.

2.1 Assumptions

a) The identity of each aircraft in the NTA is known to the ground based control center.

b) The true position of every airplane is known accurately to the tower while the former flies inside the NTA. The ground based range measuring equipment at present have accuracy of only 1/3 n.mile (radar). However, equipment of the next two decades are projected to

bring the accuracy to about 50 feet. Azimuth at present can be measured from ground with an accuracy of 2° which is not very satisfactory. However, the technically feasible accuracy by radar is 0.5° ¹. It is to be noted that at present ground equipment cannot measure aircraft altitudes. The on-board altitude measuring devices of most aircraft are, nevertheless, fairly accurate (± 30 feet).

c) Every aircraft has a minimum turn radius which depends on its speed and passengers' comfort. At present the FAA rules specify a maximum turn rate of $3^\circ/\text{sec}$. if the speed is less than 210 Knots. If the speed is higher than 210 Knots, the maximum turn rate is specified by the speed and 30° of aircraft bank angle.

d) Only jets will be considered. It seems that in the future large commercial airports will be segregated only to jets while the smaller general aviation craft, which constitute a substantial percentage of the present fleet, will use smaller airfields.

e) The landing speed of every aircraft will be assumed to lie between 100 and 150 Knots. The landing speed depends on the load of the airplane. Table 2.1 shows typical accepted landing speeds for all the existing types of jet carriers. (Table 2.1 on page 18)

f) All landings and possibly take-offs will utilize the same runway. Thus, there will be no interference from other runways.

g) No other airports lie in the vicinity of the airport under consideration.

h) Aircraft will enter the NTA with speeds which can range from 200 Knots to 300 Knots. This is close to present practice.

TABLE 2.1¹² *

Approach Airspeed in Knots

Jet Type	Operating Empty Weight	60% Load Factor	Maximum Loading Weight
737-100	100 Knots	130 Knots	138 Knots
737-200	103 "	125 "	133 "
DC-9-30	105 "	125 "	128 "
DC-9-40	106 "	125 "	128 "
727-100	95 "	122 "	130 "
727-200	102 "	122 "	133 "
707-120	118 "	142 "	146 "
707-120B	115 "	135 "	140 "
720	102 "	123 "	128 "
707-320	117 "	140 "	143 "
707-320B	103 "	122 "	127 "
DC-8-61	118 "	137 "	143 "
DC-8-62	108 "	135 "	140 "
DC-8-63	115 "	137 "	141 "
DC-10-10	112 "	133 "	137 "
DC-10-20	117 "	135 "	140 "
747	115 "	140 "	144 "

* I would like to thank Prof. A. Odoni of M.I.T. for this table.

i) All aircraft, while in the NTA, must maintain between them a longitudinal separation of at least d_{\min} units of distance. It will be assumed that proper separation exists between jets entering the NTA. Currently, the FAA standard is $d_{\min} = 3$ n.miles. This is frequently, and deliberately violated by the controllers, especially in hours of congestion. In this report d_{\min} will be assumed equal to 2.5 n.miles.

j) It will be assumed that when the aircraft descends its groundspeed is kept constant. However, the magnitude of the groundspeed will not affect the maximum descent rate that can be achieved. In other words, an aircraft will be assumed capable of descending, e.g., 1000 feet/minute whether it flies with groundspeed equal to 250 Knots or 300 Knots or any other speed less than 300 Knots.

k) The maximum descent rate will be assumed to be 1000 feet/minute. This corresponds to a descent angle of 5.6° for an aircraft flying at 100 Knots, and a smaller angle for greater speeds. The maximum permissible deceleration will be assumed to be 1 Knot/sec.

l) Since most pilots don't like to perform many tasks simultaneously, it will be assumed that, at any particular time only one (or none) of the three tasks, namely descending, turning or decelerating will be executed.

m) It will be assumed that the wind speed is zero and that no significant variations of speed occur with changes of altitude and temperature. This is a gross simplification; however, it does not significantly affect the system concepts, and it greatly simplifies the

analysis.

2.2 The System Geometry

The structure of the airspace around the airport will now be described. First, a coordinate system (x,y,z) is defined. Its origin is the outer marker. Since the function of any terminal ATC system is to funnel aircraft to the OM, this point is picked as the origin of the coordinate system (see fig. 2.1).

The NTA will be a cylinder with its axis passing through the OM. The radius of the NTA must be picked as small as possible, so that the aircraft will be under tower control for the smallest possible time. Since the average number of aircraft in the NTA at any time is proportional to its radius (see Simpson¹), the computer at any moment will have the smallest possible number of aircraft to coordinate. The magnitude of the NTA radius will be determined at a later section (it will be of the order of 60-70 n.miles).

The NTA will be divided in three major areas each serving a specific purpose. A rough description of them follows. The outermost area, which will be called buffer zone (BZ), will be roughly an annular cylinder bounded by the boundary of the NTA and another cylindrical surface centered at the OM. The radius of this second cylinder will be about 10 n.miles smaller than the radius of the NTA cylinder, and will be determined exactly later. When an aircraft is inside the buffer zone, it is identified by the ground center, and scheduled.

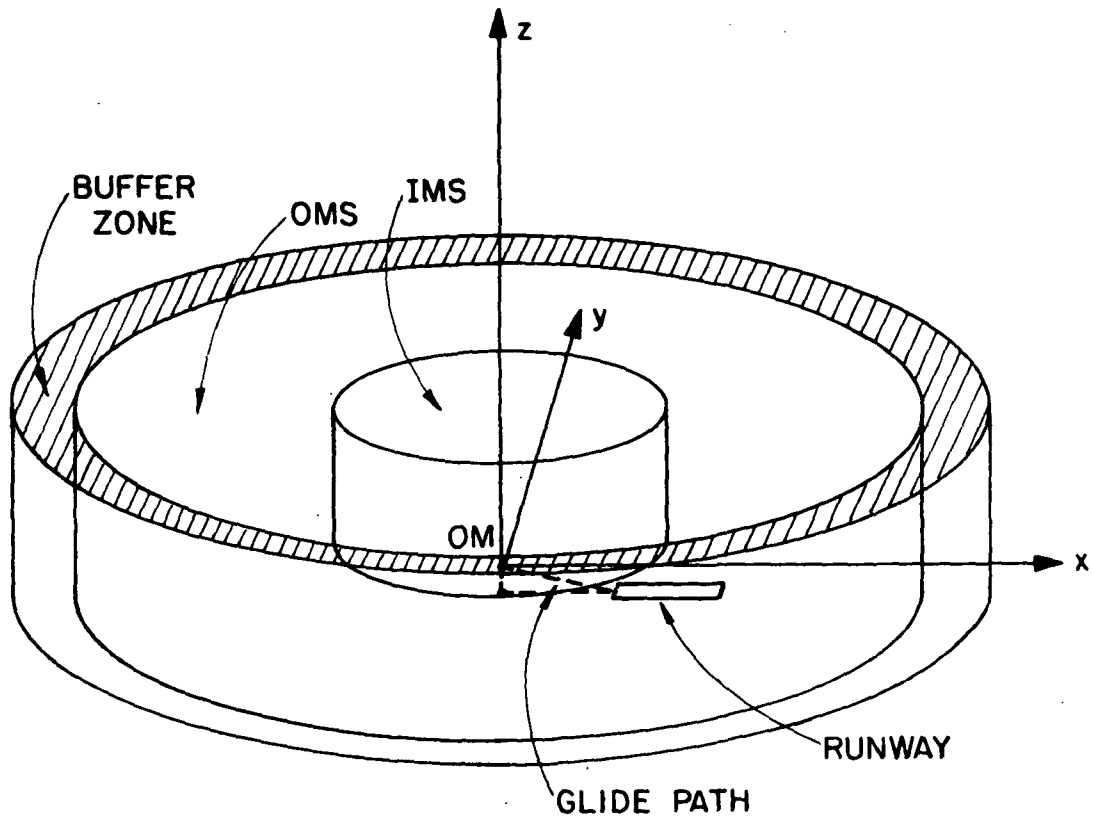


Fig. 2.1 "Rough" Description of Airspace Segregation Inside NTA

The area of the NTA the aircraft enters after it crosses the buffer zone will be called outer merging space (OMS). It is bounded by the inner boundary of the buffer zone and another roughly cylindrical surface centered at the OM--the zones are described grossly pending further details of them, to be mentioned next. The tasks of sequencing, spacing, and holding (if necessary) will be completed while the jet is in the OMS.

The remaining innermost region of the NTA will be named inner merging space (IMS). It is in this region that all aircraft will converge toward the OM. Figure 2.1 illustrates roughly how the air-space is subdivided.

Aircraft enter the NTA from air routes. We assume that inside the NTA there are no fixed air routes, but every aircraft will be assigned a nominal path that it must follow.

While in the buffer zone and the OMS, aircraft will be allowed to fly at any of a discrete number of altitude levels. Each level will carry along a speed that an aircraft must maintain while it flies on it. The higher altitude levels will allow progressively higher speeds for noise abatement reasons. The vertical separation between altitude levels will be at least 1000 feet to avoid violation of current accepted separation standards. The topmost altitude level will carry traffic at no more than the maximum entrance speed which was assumed to be of the order of 300 Knots. The lowest level will allow traffic to fly at as low as 200 Knots, the lowest assumed en-

trance speed. The exact number, specific speeds and vertical separations of the altitude levels will be determined at a later section. Any aircraft in the OMS, regardless of what altitude level it is flying at, will be allowed to specify any landing speed in the range 100 Knots to 150 Knots. Thus, there will be no segregation according to their desired landing speed.

The intersection of each altitude level with the boundary surface of the IMS will define a circle. This circle will be the check in point for entrance to the IMS (roughly corresponding to the present outer fixes). The difference, however, is that every point on the circle is a valid entrance point to the IMS. Figure 2.2 illustrates the idea. It is to be pointed out that the distances of points, A,B,C etc. from the OM are not the same as the assumption of a cylindrical IMS would imply. The same remark holds for points A',B',C' etc. That is why it was said that the IMS and the OMS are "roughly" cylindrical.

Although a particular aircraft is restricted to fly at one altitude level while it is outside the IMS, it will not be similarly segregated inside the IMS. The tasks or "objectives" the pilot will have to accomplish while in the IMS region are to descend to the level of the OM and decelerate to the landing speed. A major problem is how to avoid conflicts between aircraft entering the IMS from different altitude levels.

The way this problem will be attacked in this thesis is to demand that no matter from what altitude level an aircraft enters the IMS, and no matter what its landing speed is, it will have to traverse

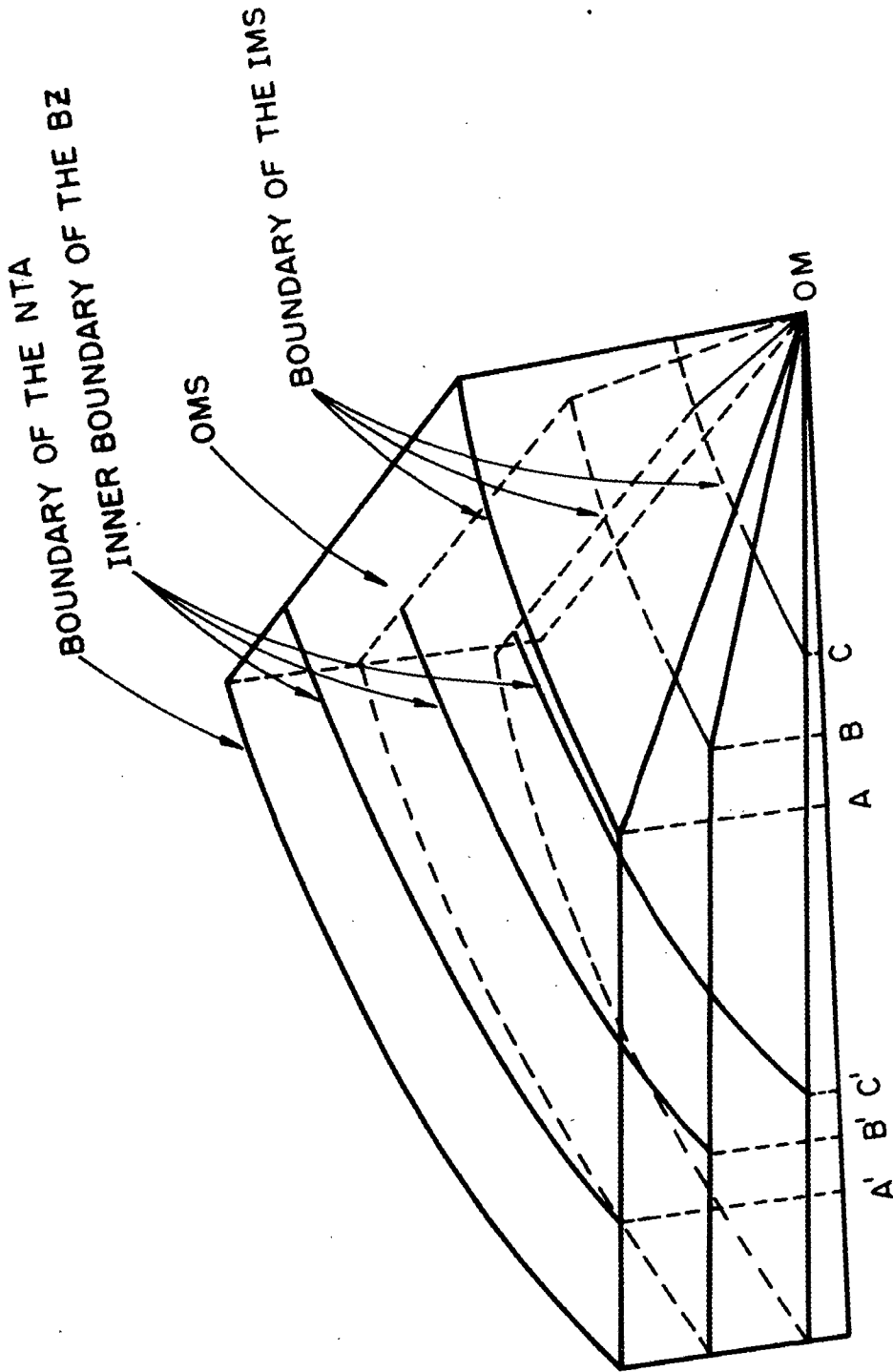


Fig. 2.2 Segregation of the BZ and OMS in Altitude Levels

the IMS in a time interval T_0 , which is the same for all aircraft.

This concept as will be seen shortly, will simplify the scheduling and spacing tasks.

In Chapter IV a method will be given for determining the minimum T_0 , and the minimum radius of each circle that separates an altitude level from the IMS.

2.3 Functional Description of the Control Process

Consider an aircraft entering the NTA. There are certain tasks that are performed by the aircraft and the automated control system while the aircraft proceeds toward the OM. These will be described in the order they take place.

A. As soon as his aircraft enters the buffer zone (BZ) of the NTA the pilot:

- a) Identifies it to the ATC system,
- b) Radioes position, heading, time of entrance and landing speed.
- c) Starts performing a simple maneuver that, if undisturbed, will lead the jet to the boundary of the IMS in minimum time.

The minimum time maneuver is simple enough, given that the aircraft flies on a particular altitude level and thus maintains constant known speed, and it can be precalculated. Its analytical description will be given in Chapter III. The advantage of this type of maneuver is that the ground computer can readily calculate the expected time

of arrival (ETA) to the boundary of the IMS. Given that the aircraft will be controlled to cross the IMS in a prespecified time T_c , and that the landing speed has been communicated to ground, the computer can readily also calculate the ETA to the runway.

B. The system now compares the most recently calculated ETA to the ETA's calculated for the aircraft that are still in the buffer zone. This is so because the BZ has been designed so that when a vehicle leaves it on its way to the OM, there is no chance that it will be superceded in landing order by any other jet subsequently entering the NTA--the details of the design will appear in Chapter IV. After the comparison the system rearranges if necessary, the landing order according to a procedure that will be described in Chapter V.

C. Once the landing order has been determined, the system assumes the task of scheduling the aircraft that are still in the buffer zone. "Scheduling" here is taken to mean the assignment of times of arrival to the boundary of the IMS (or equivalently, via a translation by T_o , to the OM). The only inputs to the scheduling algorithm are the landing order, ETA's and landing speeds. If the aircraft are spaced far from each other to begin with, the algorithm schedules them at their ETA's. If the ETA's are too close some of the aircraft have to be delayed. The algorithm decides which ones are to be delayed, and determines the kind of delay maneuvers to be performed. Take-offs can be inserted between landings, the algorithm will merely assign larger delays to the aircraft scheduled after a take-off.

D. Now, the algorithm instructs each pilot at what point of his minimum time trajectory he must initiate the delay maneuver. This final instruction is necessary because if an aircraft is closely behind another one, on the same altitude level, and if the algorithm decides that they both must be delayed considerably, then it is important that the second aircraft does not start its delay maneuver much later than the initiation of the delay maneuver of the first aircraft because a near miss might occur.

E. All the above calculations are performed by the ground system while the aircraft is still in the BZ. Thus, the nominal trajectory of every vehicle until the boundary of the IMS is calculated in an open loop manner. While the aircraft is now in the OMS no control whatsoever is applied. The system utilizes the time it will take the aircraft to reach the IMS, to calculate a nominal trajectory, or group of possible trajectories that the pilot can follow in the IMS so as to lead his aircraft to the OM in time T_0 . Notice that there are no holding stacks, since the holding maneuvers are performed along different points of the minimum time trajectory and are not all crowded in the boundary of the IMS.

Since the system has precomputed the nominal trajectory until the IMS, it "knows" the point at the boundary of the IMS where the aircraft will enter it, and the nominal heading. Given the "objectives" that must be accomplished in time T_0 , namely descent to the level of the OM and deceleration to the landing speed, there are infinitely many trajectories and speed profiles that can be used.

In this thesis, a specific type of turn-straight-turn trajectory will be postulated for all aircraft, and a speed profile will be determined for each. Descent will be performed while the aircraft is not decelerating. It will be seen later that the pilot will have some choice in picking the descent profile. The computer will help him by assigning the latest time the pilot can start his descent. The geometry of the airspace will be such that no matter how the pilot chooses to descent he will not violate separation standards with any other aircraft.

F. Now the pilot has finished traversing the OMS and has been given a range of nominal profiles to choose from when he enters the IMS. The control, however, does not stop here. Throughout the traversal of the OMS there are errors accumulating from position and velocity uncertainties which are due to inherent limitations of the measuring equipment. The control system will observe the position errors as soon as the aircraft enters the IMS. As a correction the system can immediately radio to the pilot a new turn-straight-turn type of trajectory which if followed closely will lead the aircraft to the OM with correct heading. Furthermore, a new speed profile and new range of descent profiles can be radioed to the pilot.

Figures 2.3 through 2.6 illustrate everything that was described in this section and familiarize the reader with the kind of trajectories and nominal profiles to be analyzed later.

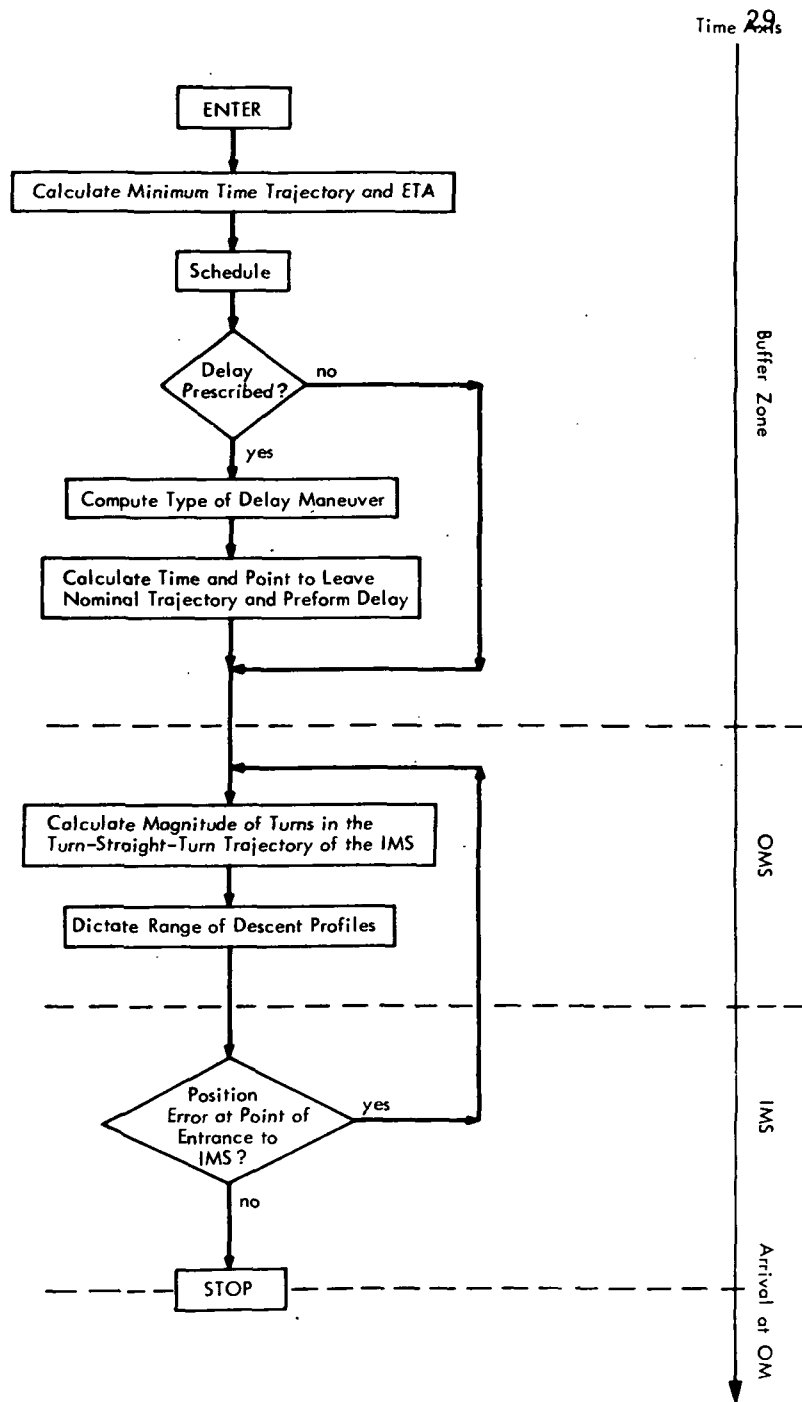


Fig. 2.3 Functional Description of the System Algorithm

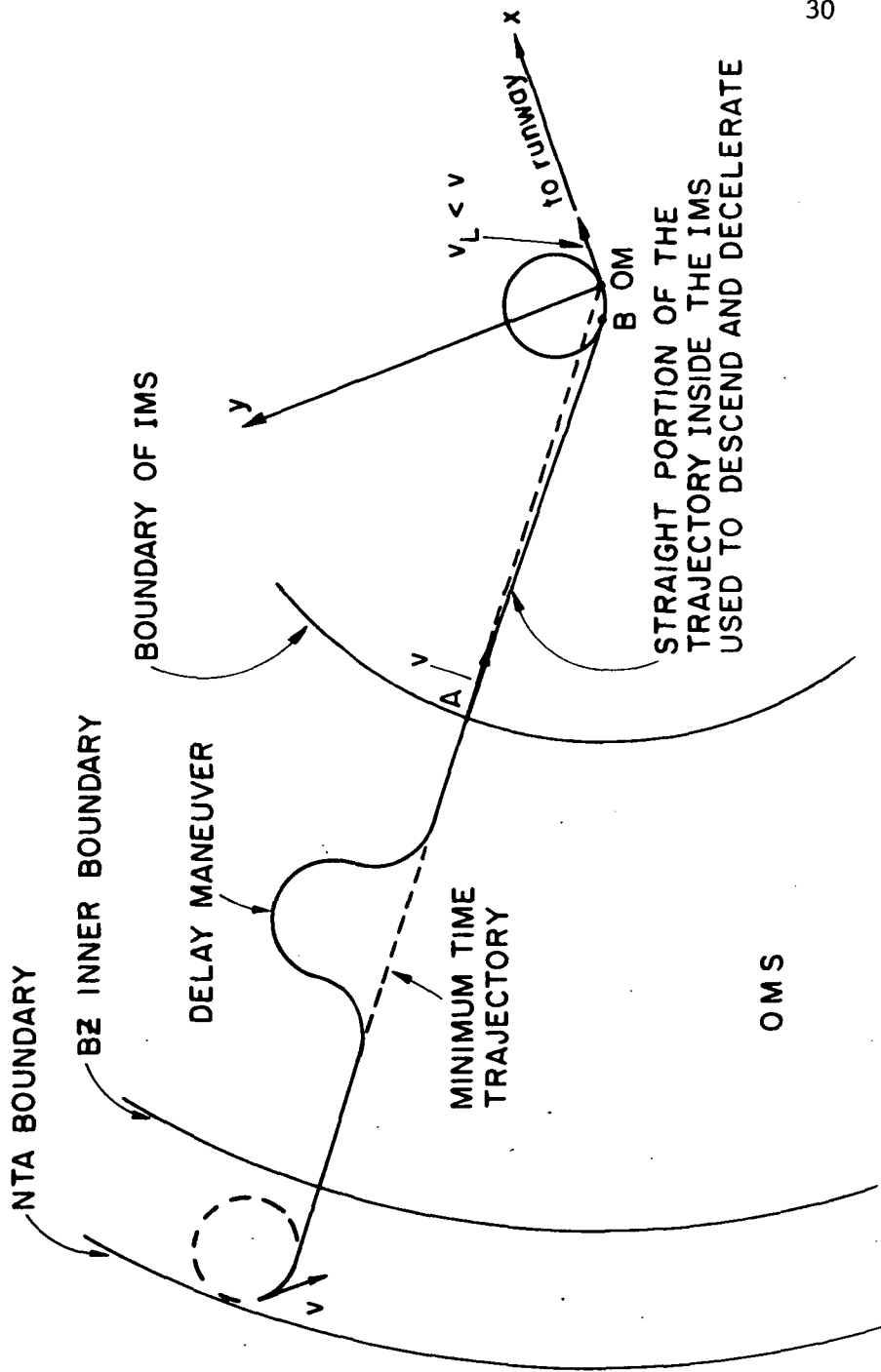


Fig. 2.4 Typical NTA Trajectory

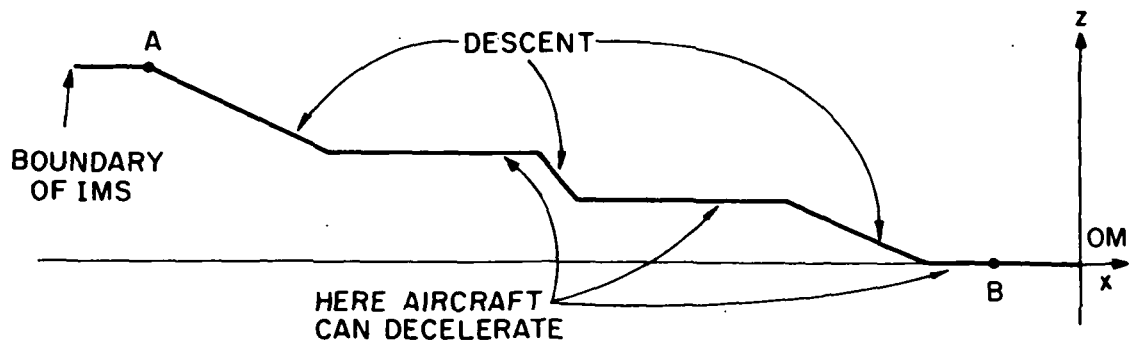


Fig. 2.5 Possible Descent Profile Between Points A and B of Fig. 2.4

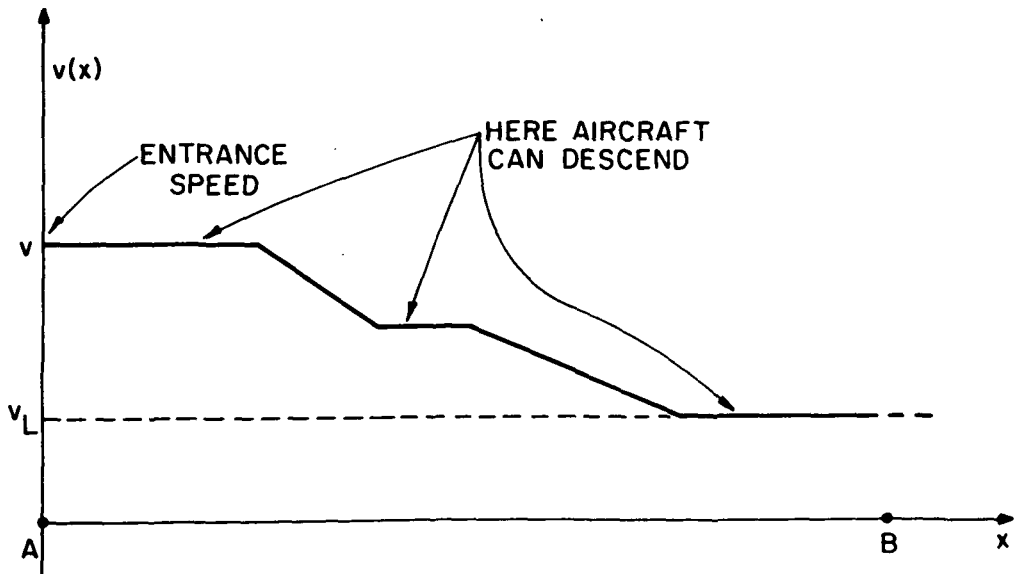


Fig. 2.6 Possible Speed Profile Inside the IMS

2.4 Why Such a System?

In this section the possible advantages of the proposed system when compared to the presently existing one are stated. Before the quality of the suggested system is discussed, its differences with the present ATC process are mentioned.

At present, the sole decision maker and co-ordinator of the terminal system is the approach controller. As such, his tasks become immensely complicated during congestion periods. In the proposed system the computer not only aids the controller in his decision making but does a lot of the deciding itself. So the machine is not only used as a fast calculator, but also as an accurate controller. The function of the human is by no means deleted. On the contrary, it is reserved to handle emergency situations, adverse weather conditions and other unpredictable cases, as well as to replace the computer if and when the latter breaks down.

At present control is concentrated in the area between the holding stacks and the OM--roughly in the IMS of the suggested scheme. This is so because, with its limited capability, the human brain cannot predict future aircraft positions far in advance. A fast computer with a large memory overrides this problem. Taking this into account the proposed scheme suggests beginning of control as soon as the jet enters the NTA. Errors, as was described above, can be monitored and corrected near the OM but by starting control early it is assured that these errors will not be large.

The holding stacks are replaced by a dynamic delaying process. At present the holding stacks are one of the bottlenecks of the terminal ATC system. This is so because the flow capacity of a holding stack is smaller than the capacity of the runway (see Simpson, p. 183). So their elimination seems likely to improve the airport capacities.

The pilot will not be confined to a very strict nominal flight plan. His flexibility is reflected in his freedom to pick the final descent profile.

Finally, computational requirements are not very large. The equations that the computer will be required to solve can be solved in faster than real time.

CHAPTER III
AIRCRAFT TRAJECTORIES

In this chapter analytical description of the nominal aircraft trajectories will be given. This is necessary before the system geometry is analyzed, because it will provide the insights into the reasons for the adoption of the particular airspace configuration. Aircraft will be treated as points moving on a plane. The trajectories that will be prescribed in the OMS will be minimum time ones. The ones that will be followed in the IMS will be such that an aircraft will arrive at the OM with proper heading.

Section 3.1 analyzes the minimum time problem. In section 3.2 the kinds of delay maneuvers that will be used are described. Section 3.3 analyzes the trajectories in the IMS. Finally, section 3.4 describes the kinds of speed profiles out of which the computer will pick the nominal one. In the last section the possible descent profiles are also described.

3.1 The Minimum-time Trajectory in the OMS

The reasons for which such a trajectory is imposed on every aircraft entering the NTA are the following:

a) If there is no interference from other aircraft, this trajectory will lead the jet under consideration to the boundary of

the IMS in the smallest possible time.

b) The equations involved are explicit, and thus the ground computer can solve them very fast.

c) The maneuver itself is simple and thus it will be easy for the pilot to execute it.

3.1.1 Problem Statement

The problem will be stated under the assumptions that the motion of the aircraft is planar, and the speed is constant. Figure 3.1 illustrates the situation. Point A represents an entering aircraft with speed V and initially at state (x_o, y_o, ϕ_o) . The problem roughly is to find a trajectory such that the aircraft arrives at the circular boundary of the IMS, and headed toward the OM, as shown in figure 3.1, in the smallest possible time.

The dynamics of the aircraft are represented by the following set of equations:

$$\dot{x}(t) = v \cos \phi(t) \quad (3.1)$$

$$\dot{y}(t) = v \sin \phi(t) \quad (3.2)$$

$$\dot{\phi}(t) = \frac{g \tan \theta(t)}{v} \quad (3.3)$$

where x and y are measured in the co-ordinate system of figure 3.1, ϕ is the aircraft heading with respect to the x -axis, g is the acceleration of gravity and $\theta(t)$ is the aircraft bank angle (see figure 3.2).

Equations 3.1 and 3.2 are simply the equations of a moving point. Equation 3.3 needs explanation. As was stated in Chapter II,

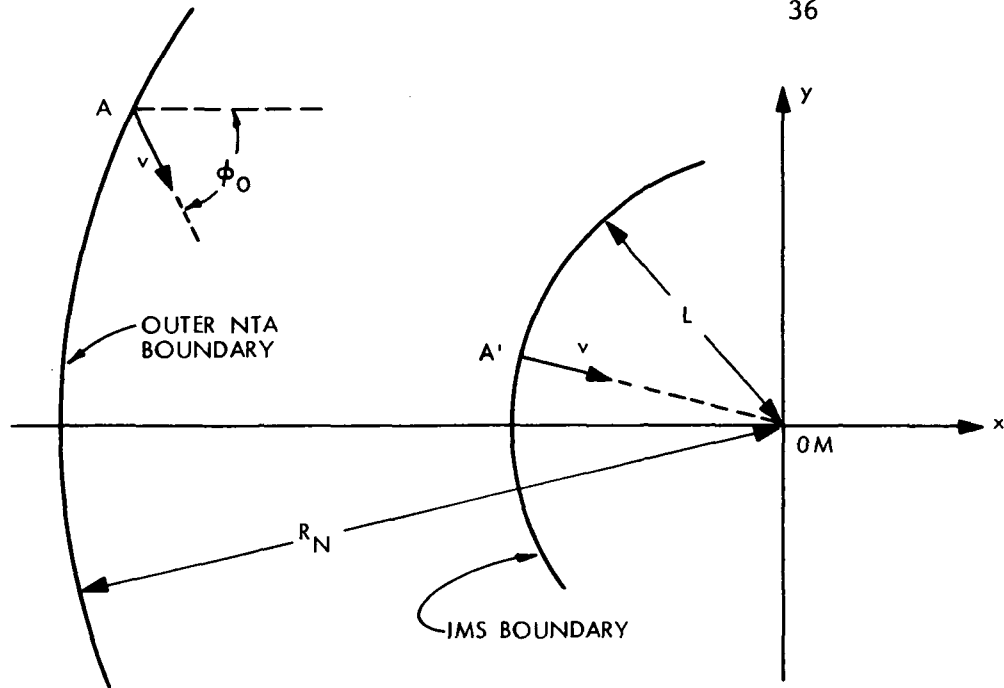


Fig. 3.1 Illustration of the Minimum Time Problem

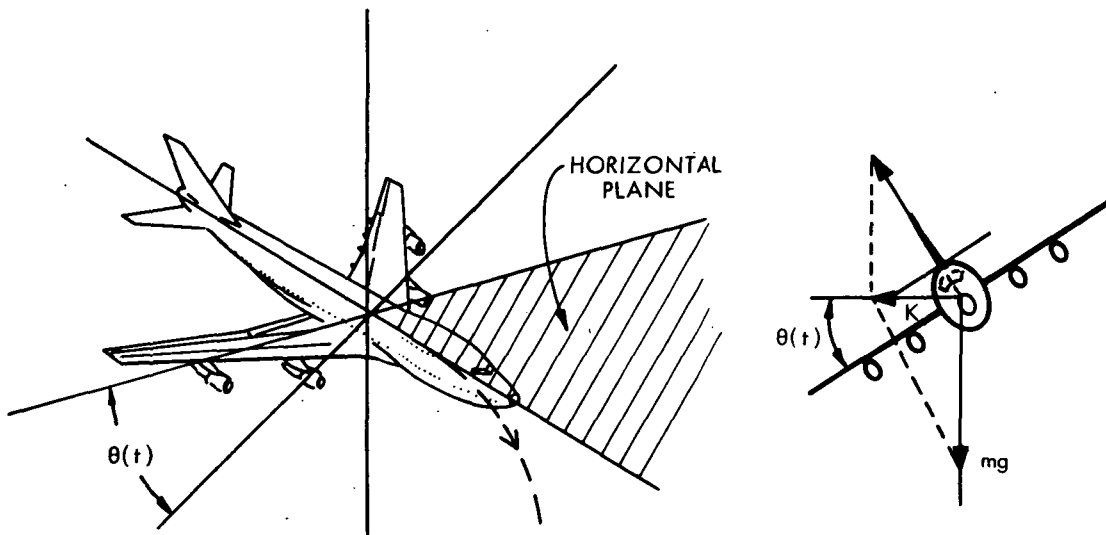


Fig. 3.2 Aircraft Turn

it is assumed that each altitude level "carries" a speed v , at which all aircraft flying at that level must fly. The value of v was assumed between 200 Knots and 300 Knots. In this speed range the turn rate is specified by the bank angle as follows:

If K, R, m denote the centrifugal force experienced during the turn by the aircraft radius of turn, and aircraft mass respectively then:

$$K = \frac{mv^2}{R} \quad (3.4)$$

Equilibrium conditions give (see fig: 3.2)

$$K = mg \tan \theta(t) \quad (3.5)$$

Thus, $\frac{mv^2}{R} = mg[\tan \theta(t)]$

implies $\frac{v}{R} = \frac{g[\tan \theta(t)]}{v} \quad (3.6)$

Since $\dot{\phi}(t) = \frac{d\phi(t)}{dt} = \frac{v}{R}$, equation (3.3)

Equation (3.3) can be simplified by setting

$$u(t) = g[\tan \theta(t)] \quad (3.7)$$

Since the maximum bank angle currently allowed is 30° $u(t)$ is restricted

by: $|u(t)| \leq g \tan \frac{\pi}{6} = \frac{g}{\sqrt{3}} = A$

Since the heading of the aircraft at the final time must be along a radius of the IMS the end-time condition on ϕ is:

$$\tan \phi(t) = \frac{y(t)}{x(t)} \quad (3.8)$$

We now formulate an optimal control problem.

Given the state equations:

$$\dot{x}(t) = v \cos \phi(t)$$

$$\dot{y}(t) = v \sin \phi(t)$$

$$\dot{\phi}(t) = \frac{u(t)}{v}$$

the initial conditions,

$$[x(0) \ y(0) \ \phi(0)] = [x_0 \ y_0 \ \phi_0]$$

the final condition:

$$x(T) + y^2(T) = L^2 ; \quad \tan \phi(T) = \frac{y(T)}{x(T)}$$

and the cost functional:

$$J = \int_0^T dt.$$

Find the control $u_{[0,T]}$ such that $|u(t)| \leq A$, and such that it minimizes J .

3.1.2 Solution of the Minimum-time Problem

In Appendix A the problem formulated above is solved. The answer is the following.

a) If $\tan \phi_0 = \frac{y_0}{x_0}$, then the optimal control law is $u^0 = 0$. The aircraft trajectory is a straight line and the cost functional J is trivially found by:

$$J = T_{\min} = \frac{R_n - L}{v} \quad (3.9)$$

b) If $\tan \phi_0 > \frac{y_0}{x_0}$, then the optimal control law is

$u^0 = (-A, 0)$. The aircraft turns clockwise and "hard" for time t_s given by:

$$t_s = \frac{v}{A} \left[\phi_0 - \tan^{-1} \frac{y_0 - \frac{v^2}{A} \cos \phi_0}{x_0 + \frac{v^2}{A} \sin \phi_0} - \sin^{-1} \frac{\frac{v^2}{A}}{\left[(y_0 - \frac{v^2}{A} \cos \phi_0)^2 + (x_0 + \frac{v^2}{A} \sin \phi_0)^2 \right]^{1/2}} \right] \quad (3.10)$$

Then it continues along a straight line until it reaches the boundary of the IMS. The value of the minimum time is:

$$T_{\min} = \frac{[x^{o^2}(t_s) + y^{o^2}(t_s)]^{1/2} - L}{v} \quad (3.11)$$

where

$$x^o(t) = x_0 + \frac{v^2}{A} \sin \phi_0 - \frac{v^2}{A} \sin \left(\phi_0 - \frac{A}{v} t \right) \quad (3.12)$$

$$y^o(t) = y_0 - \frac{v^2}{A} \cos \phi_0 + \frac{v^2}{A} \cos \left(\phi_0 - \frac{A}{v} t \right) \quad (3.13)$$

c) If $\tan \phi_0 < \frac{y_0}{x_0}$, then the optimal control law is $u^0 = (A, 0)$.

The aircraft turns counterclockwise and "hard" for time t_s given by:

$$t_s = \frac{v}{A} \left[\tan^{-1} \frac{y_0 + \frac{v^2}{A} \cos \phi_0}{x_0 - \frac{v^2}{A} \sin \phi_0} - \sin^{-1} \frac{\frac{v^2}{A}}{\left[(y_0 + \frac{v^2}{A} \cos \phi_0)^2 + (x_0 - \frac{v^2}{A} \sin \phi_0)^2 \right]^{1/2}} - \phi_0 \right] \quad (3.14)$$

Then it continues on a straight line until it reaches the boundary of the IMS. The value of the minimum time is:

$$T_{\min} = \frac{[x^{o^2}(t_s) + y^{o^2}(t_s)]^{1/2} - L}{v} \quad (3.15)$$

where

$$x^0(t) = x_0 - \frac{v^2}{A} \sin \phi_0 + \frac{v^2}{A} \sin \left(\phi_0 + \frac{A}{v} t \right) \quad (3.16)$$

$$y^0(t) = y_0 + \frac{v^2}{A} \cos \phi_0 + \frac{v^2}{A} \cos \left(\phi_0 + \frac{A}{v} t \right) \quad (3.17)$$

3.2 Delay Maneuvers

The scheduling algorithm, which is described later, will, in general and especially under congestion, arrange that each aircraft be delayed by some time t_D . In this section the maneuvers necessary to perform delays for any $t_D > 0$ are described.

The topic of delays has been treated in [1], and from a different viewpoint in [7], [8] and [9]. The philosophy in [1] is to evaluate the effectiveness of any proposed delay maneuver by examining the ratio t_D/T , where t_D is the desired delay and T is the total time it takes the aircraft to perform the maneuver. The larger the ratio $\frac{t_D}{T}$, for a given t_D , the more effective is the delay maneuver. In [7], [8] and [9] the philosophy was to delay the aircraft by trying to minimize the time the aircraft stays away from its air-route, while it is performing the delay maneuver. Some of the optimal maneuvers arrived at, via the two philosophies were identified.

In this thesis the delay maneuvers described in [7],[8] and [9] will be adopted with one modification. All the delay maneuvers will be of the "path stretch" type and will be initiated while the aircraft fly on the straight line parts of their minimum time trajectories.

The objective has been to pick delay maneuvers that take up both little time and space.

We define D to be the time it takes an aircraft flying at speed v to perform a circle of minimum radius.

$$D = \frac{2\pi R}{v} \quad (3.18)$$

where

$$R = \frac{v^2}{g(\tan 30^\circ)} = \frac{v^2 \sqrt{3}}{g} \quad (3.19)$$

and g is the acceleration of gravity.

The following types of delay maneuvers are now adopted.

a) If $t_D < D$, then the delay is performed via an oscillation maneuver (or θ -delay). See figure 3.3 for illustration. The magnitude of θ is calculated by:

$$t_D = \frac{4R}{v} (\theta - \sin \theta)$$

or

$$\theta - \sin \theta = \frac{vt_D}{4R} \quad (3.20)$$

(3.20) is a transcendental equation and can be solved only numerically. The quantity of interest is the maximum excursion from the straight line path. This is shown in figure 3.3 to be $2(R - R \cos \theta)$. The maximum angle θ occurs when $t_D \approx D$. Then the maximum excursion receives the largest possible value it can have, about $3.4R$.

b) If $t_D = D$ then the delay maneuver to be used is the circle

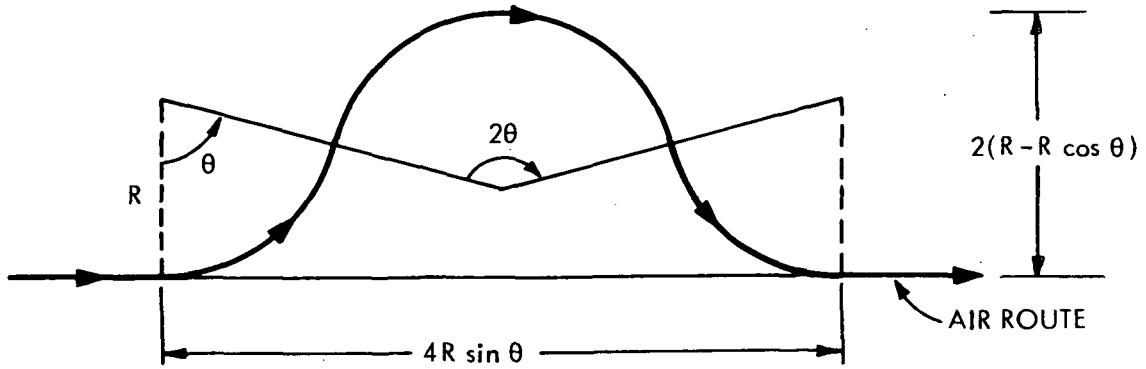


Fig. 3.3 The Oscillation (or θ Delay) Maneuver

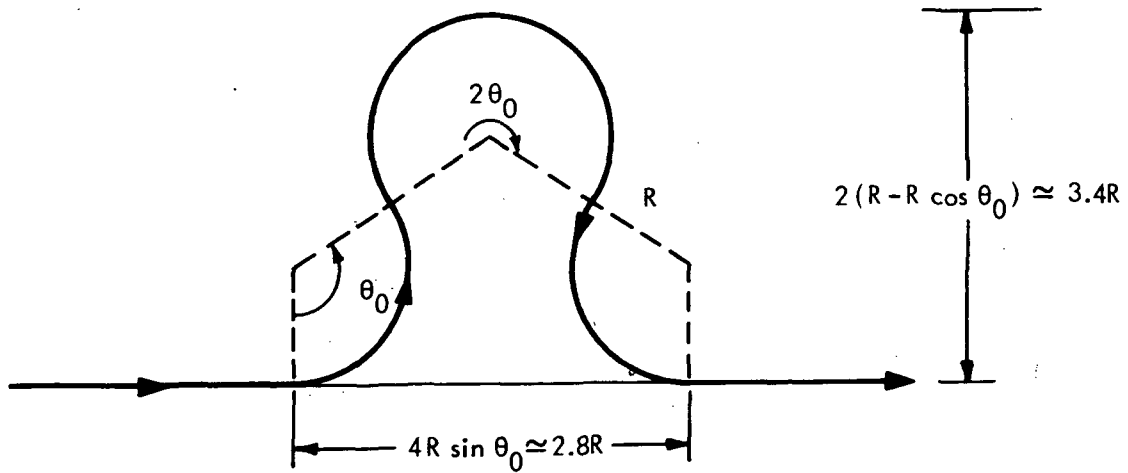


Fig. 3.4 Maximum Oscillation Maneuver

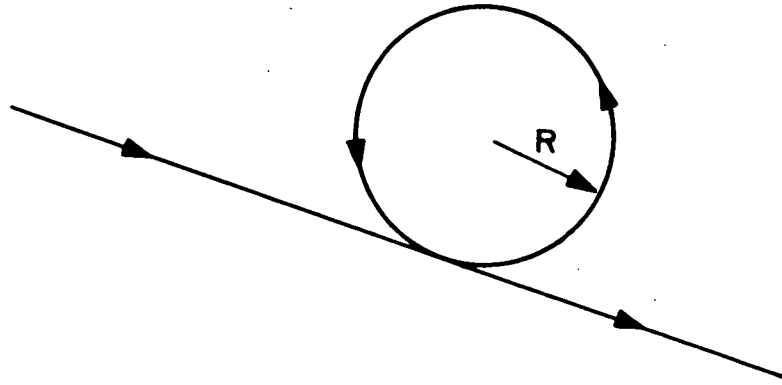


Fig. 3.5 The Circle Maneuver

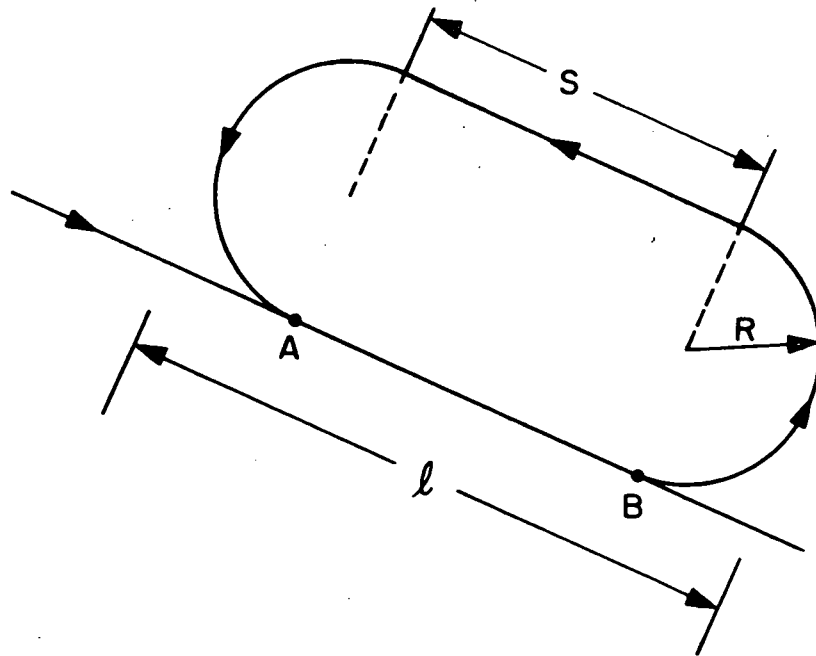


Fig. 3.6 The Fly-around Maneuver

maneuver illustrated in figure 3.5.

c) If $D < t_D \leq 2D$ then the delay maneuver will be the so-called fly-around maneuver, illustrated in figure 3.6. The aircraft turns hard for $D/2$ seconds then flies backwards for $\frac{t_D - D}{2}$ seconds and then turns hard again for $D/2$ seconds. The length l of the "racetrack" pattern is:

$$l = S + 2R = \frac{(t_D - D)v}{2} + 2R \quad (3.21)$$

The maximum l occurs when $t_D = 2D$ and is

$$l_{\max} = \frac{Dv}{2} + 2R = (\pi+2)R \quad (3.22)$$

d) If $2D < t_D \leq 3D$ then since $t_D = D + t_o$, $D < t_o \leq 2D$, the delay maneuver will be a circle maneuver followed by a fly-around maneuver as described in (c). Note that the same delay could have been effected by a single fly-around maneuver where the straight line path would last $\frac{t_D - D}{2}$ seconds. In such cases, however, the length l of the "racetrack" pattern would be:

$$l = S + 2R = \frac{(t_D - D)v}{2} + 2R$$

and would be larger than the maximum l found in 3.22 of part (c).

We asserted earlier that our objective will be to keep the airspace utilized small. Thus although the fly-around maneuver would accomplish the delay in a shorter time, it would waste more airspace. We shall postulate in this report that the "length" of the area of the airspace, required to accomplish a delay, will not exceed the value of $(\pi+2)R$. The reason for this restriction will become more apparent

when we analyze the delay assignment algorithm.

e) If $3D < t_D$ then $t_D = K \cdot 2D + t_1$ ($K = 1, 2, \dots$) where $D < t_1 \leq 3D$. The delay maneuver will then be K fly-around maneuvers of the "maximum racetrack" type, followed by a maneuver as described in part (d). It is seen again that the airspace utilized has "length" t_{\max}^1 .

3.3 Trajectories Inside the IMS

While flying through the IMS the aircraft have to accomplish the following objectives:

- a) Reach the OM with a heading toward the runway.
- b) Decelerate from the entrance speed v to the landing speed v_L , and
- c) Descend from the altitude level they are flying to the altitude of the OM.

All aircraft arrive at the boundary of the IMS headed radially toward the OM. If they continued flying in a straight line, they would reach the OM, but the heading would not be along the positive x axis in general. On the other hand, since only at most one maneuver is allowed at any time, the trajectory that the aircraft will be ordered to follow must have enough straight line parts. The problem is illustrated in figure 3.7 (For the illustrations, the z dependence is dropped. We just remember that descent can occur only in the portions of the trajectory that are straight). In addition to the above constraints the trajectory must intuitively be "close" to the radius of the OM,

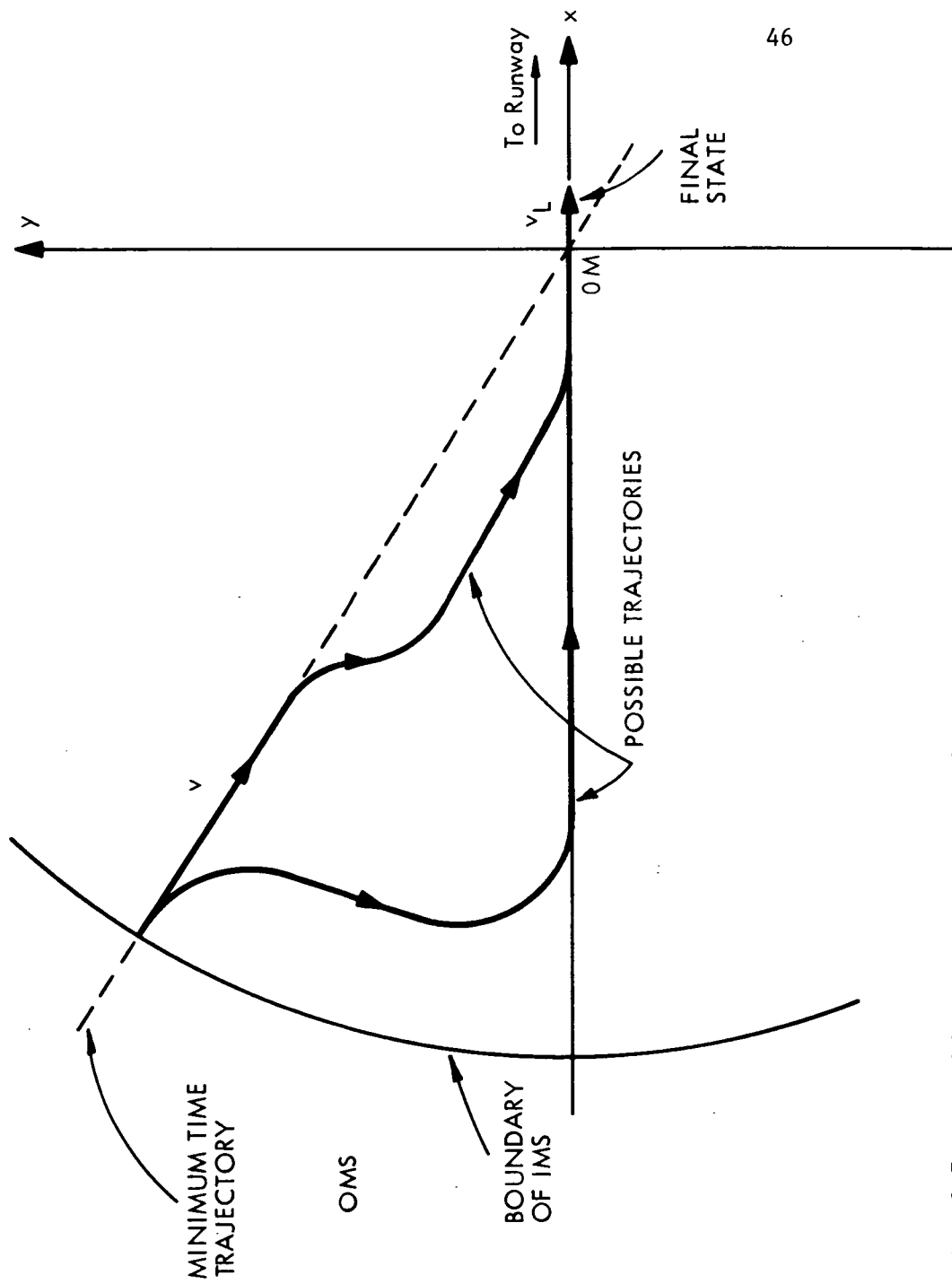


Fig. 3.7 Possible Trajectories to the OM

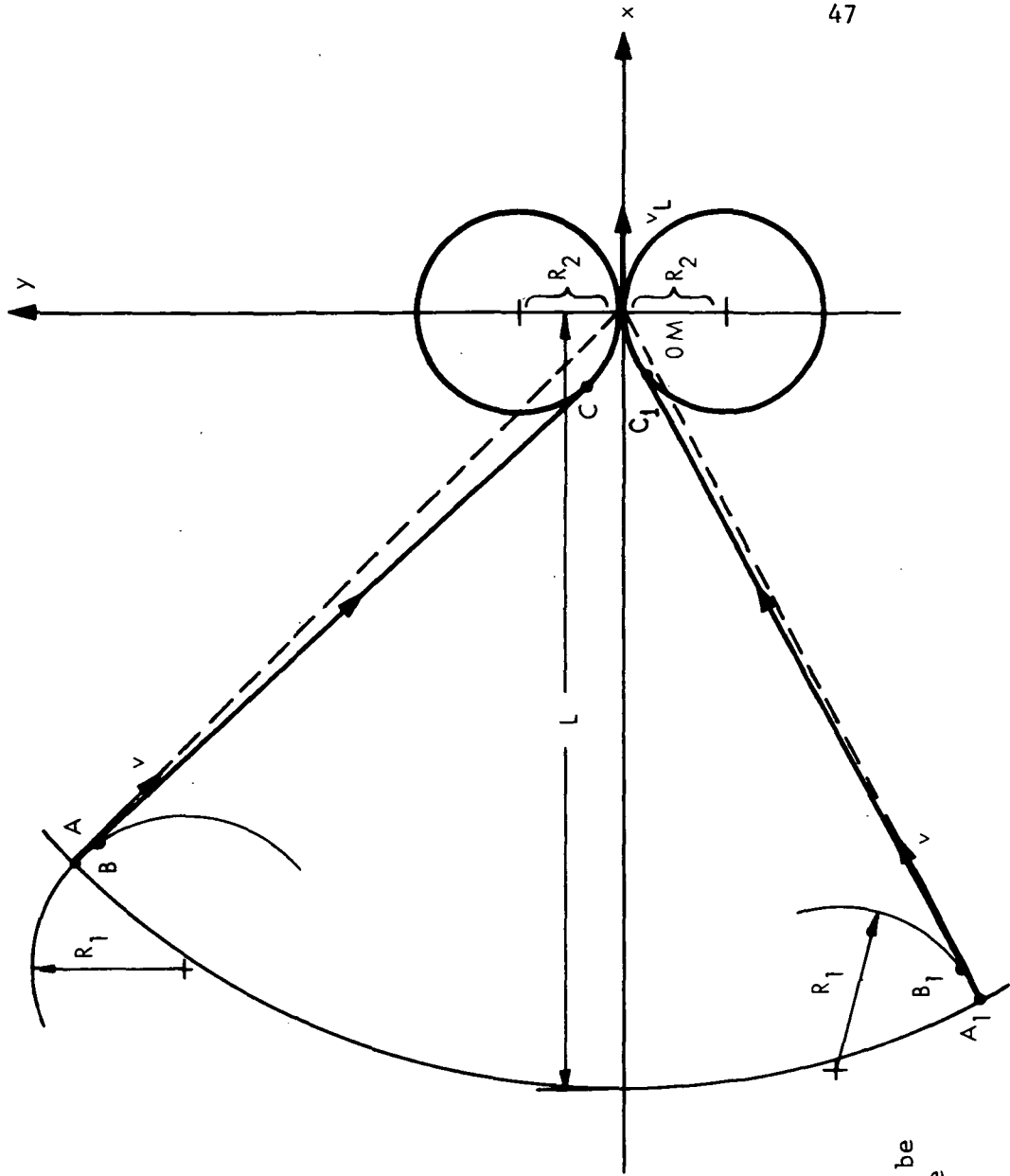


Fig. 3.8 Trajectories to be Followed Inside the IMS

reaching the entrance to the IMS point, in order to minimize interference from aircraft entering from other points of the IMS boundary. Finally all the objectives (a)-(c) must take place in a fixed and prespecified time T_0 (to be determined later).

We tried to formulate an optimal control problem that would seek the best trajectory under the above constraints. The system is nonlinear with many inputs. The traditional cost criteria, "minimum energy" or "minimum fuel", did not give satisfactory answers or gave answers that were singular. It was then decided to postulate a "reasonable" type of trajectory, easy for the pilots and computationally tractable.

The following type of trajectory was the best we could conceive.

1) The aircraft will start turning hard as soon as it enters the IMS.

2) The turn will stop when the heading is along a line which is tangent to the circle of minimum radius R_2 , centered on the y-axis, tangent to the x-axis, and on the same half plane as the entrance point.

3) Then the aircraft just follows this straight line until it reaches the circle of radius R_2 . Subsequently, it turns hard along this circle and ends at the OM with proper heading. While on the straight line the aircraft can decelerate and descend.

The type of trajectory we have in mind is illustrated in figure 3.8. Notice that $R_1 > R_2$. This is so because $v > v_L$, and the

minimum radius is smaller if the speed is lower. The chosen trajectory, e.g., ABC-OM is seen to be very close to the radius A-OM. It is also easily executed by a pilot. What remains now is to calculate the magnitudes of the turns and the length of the straight portion of the trajectory.

Consider figure 3.9. The objective is to find the magnitudes of α and γ and the length CE. The problem will be first solved for the second quadrant. Then symmetry will dictate the results for entrance points along the rest of the boundary of the IMS.

Some thought will point out the fact that the magnitude of the angles $\alpha, \beta, \theta, \epsilon$ and ϕ_0 lie all in the interval $[0, \frac{\pi}{2}]$, for all entrance points in the second quadrant. We shall hereby denote by $\alpha, \beta, \theta, \epsilon$ the magnitudes of the respective angles. From the right triangle BJD we obtain

$$(BD) = [x_0^2 + (y_0 - R_2)^2]^{1/2} \quad (3.23)$$

δ is given by

$$\delta = \frac{\pi}{2} + |\phi_0| - \epsilon \quad (3.24)$$

where ϵ is obtained from triangle BJD by

$$\epsilon = \tan^{-1} \frac{y_0 - R_2}{|x_0|} \quad (3.25)$$

From the triangle ABD we obtain via the law of cosines

$$(AD) = [R_1^2 + (BD)^2 - 2R_1(BD) \cos\delta]^{1/2} \quad (3.26)$$

From the right triangle AGD we obtain

$$\cos\beta = \frac{R_1 + R_2}{(AD)} \rightarrow \beta = \cos^{-1} \frac{R_1 + R_2}{(AD)} \quad (3.27)$$

From the triangle ABD and the law of sines we obtain

$$\frac{\sin(\alpha + \beta)}{(BD)} = \frac{\sin\delta}{(AD)} \quad (3.28)$$

which implies

$$\alpha = -\beta + \sin^{-1}\left[\sin\delta \frac{(BD)}{(AD)}\right] \quad (3.29)$$

From the same triangle and the law of sines it also follows that

$$\frac{\sin\theta}{R_1} = \frac{\sin\delta}{(AD)} \quad (3.30)$$

hence

$$\theta = \sin^{-1}\left[\sin\delta \frac{R_1}{(AD)}\right] \quad (3.31)$$

It is now true that

$$\gamma = \pi - \left(\frac{\pi}{2} - \epsilon\right) - \theta - \beta = \frac{\pi}{2} + \epsilon - \theta - \beta \quad (3.32)$$

$$(CE) = (AG) = (R_1 + R_2)\tan\beta \quad (3.33)$$

All the equations (3.23) - (3.33) are explicit relations and thus computationally easy to implement. It is interesting to note

that if v is not radially directed, the equations are unaffected. The significance of this is that if an aircraft enters the IMS with some error $\Delta\phi$ in its heading ϕ_0 , the equations for the calculation of α and ϵ remain unchanged; thus new values for α, γ and (CE) can be readily found. This observation will be crucial when we discuss error correction.

Let us now discuss the form of equations (3.23) - (3.33) for entrance points in the other quadrants. Figure 3.10 shows a trajectory for the first quadrant. It is easily seen that the only equations that change are (3.24) and (3.32). In both of them ϵ is replaced by $\pi - \epsilon$ so that they look like

$$\delta = \frac{\pi}{2} + |\phi_0| - (\pi - \epsilon) \quad (3.24a)$$

$$\gamma = \frac{\pi}{2} + (\pi - \epsilon) - \theta - \beta \quad (3.32a)$$

All the other equations are unchanged.

For an initial condition (x_0, y_0, ϕ_0) in the bottom half plane the trajectory is symmetrical about the x-axis to the trajectory for the initial condition $(x_0, -y_0, -\phi_0)$. Thus only equations (3.23) - (3.33) are again necessary.

The radius R_2 is specified by the following equation

$$\frac{v_L}{R_2} = \phi_{\max} \quad (3.34)$$

Where $\phi_{\max} = 3^\circ / \text{sec} = \frac{\pi}{60} \text{ rad} / \text{sec}.$

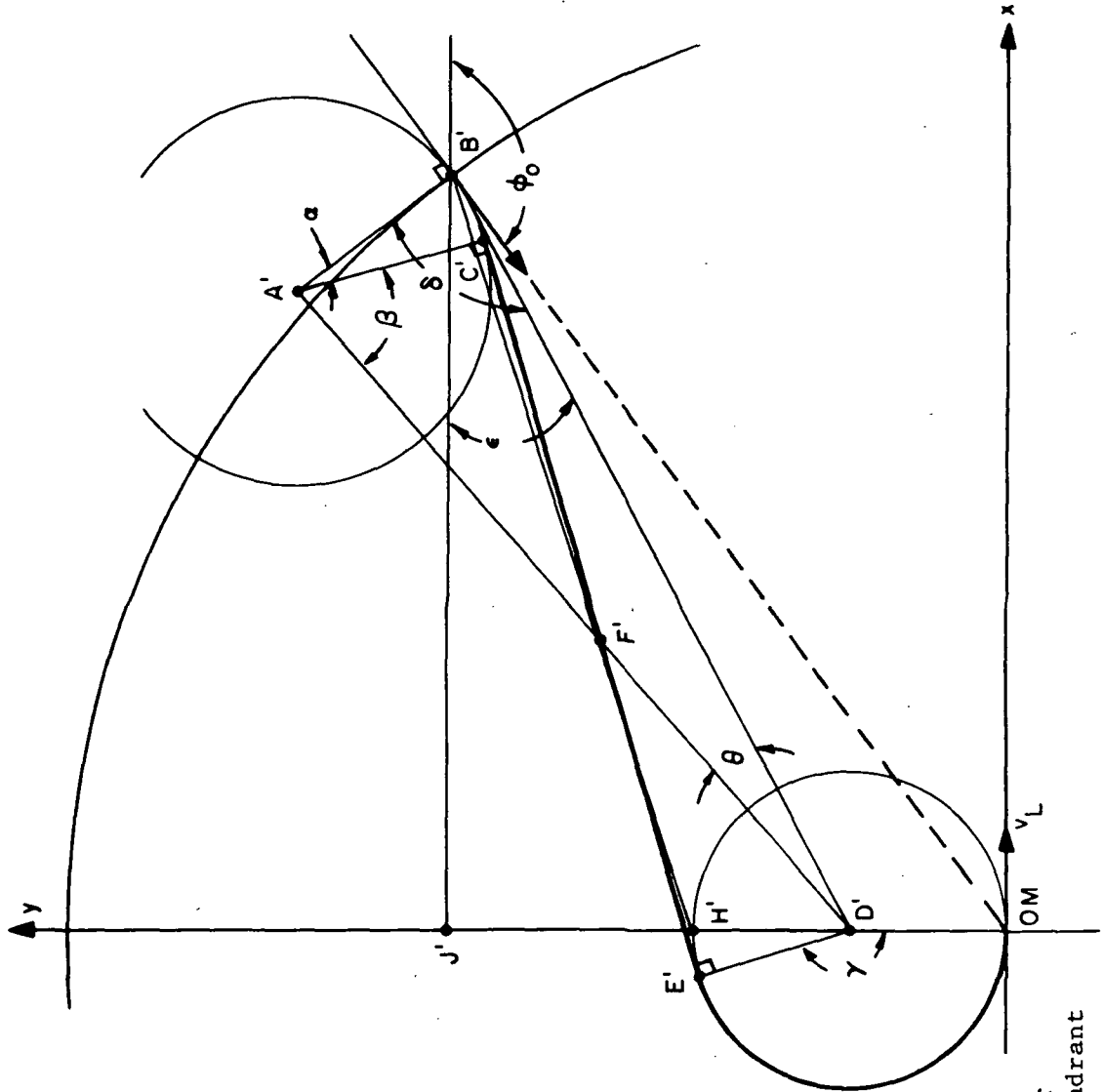


Fig. 3.10 Trajectory for
the First Quadrant

This is so because $100 \leq v_L \leq 150$ Knots and in this speed range the maximum turn rate is specified as $3^\circ/\text{sec}$ and not by the maximum bank angle. The radius R_1 on the other hand is calculated via equation (3.19). The value of v_L will vary with aircraft type and load, thus R_2, α, γ and (CE) must be calculated separately for every aircraft entering the IMS.

Typical values of R_1 and R_2 are shown in Table 3.1.

Table 3.1

Ranges of R_1 and R_2

v	$R_1 = \frac{v^2 \sqrt{3}}{g}$	v_L	$R_2 = \frac{60 v_L}{\pi}$
200 Knots	.99 n.miles	100 Knots	.53 n.miles
220 "	1.19 "	120 "	.636 "
250 "	1.54 "	130 "	.71 "
300 "	2.21 "	150 "	.796 "

It will be seen in Chapter IV that the radius of the IMS will be at least 25 n.miles. Thus the chosen turn-straight-turn trajectories will be very nearly straight lines in view of the small magnitudes of R_1 and R_2 . For the analysis of Chapter IV the turns will be completely neglected since the error involved will be very small.

3.4 Speed and Descent Profiles in the IMS

The time T_0 in which all aircraft should cross the IMS, and the radius L of the IMS will be chosen later. In this section the sets

of speed and descent profiles out of which the nominal ones can be chosen are described, assuming that there is enough time and space to accomplish all the objectives.

Once L and T_0 are specified then for every initial condition (X_0, Y_0, ϕ_0) there is a unique value for each of the angles α and γ and the length CE (ref. figure 3.9). The time that is left to cross the straight portion of the trajectory is:

$$T_{CE} = T_0 - \frac{\alpha R_0}{v} - \frac{\gamma R_0}{v_L} \quad (3.35)$$

We now formalize the problem of finding the profiles.

Consider the aircraft as a point in space with the states $X(t)$, $V(t)$, $Z(t)$ denoting length, speed and altitude respectively.

The state equations are:

$$\dot{X}(t) = V(t) \quad (3.36)$$

$$\dot{V}(t) = u_1(t) \quad (3.37)$$

$$\dot{Z}(t) = u_2(t) \quad (3.38)$$

The problem now is the following. Given that the system represented by the three equations above is at $[X(0), V(0), Z(0)] = [0, v, H]$ at time $t = 0$, find the controls u_1, u_2 restricted by

$$-B \leq u_1(t) \leq 0 \quad (3.39)$$

$$-\lambda \leq u_2(t) \leq 0 \quad (3.40)$$

$$u_1(t) u_2(t) = 0 \quad (3.41)$$

so that the system reaches the state $[(CE), v_L, 0]$ at time T_{CE} .

Here B is the maximum deceleration allowable, assumed to be 1 knot/sec, and λ is the maximum descent rate permissible which was assumed to be 1000 ft/min. The constraint 3.41 merely says that only one maneuver at a time can be performed.

The system can be written as:

$$\underline{Y}(t) = \underline{A} \underline{Y}(t) + \underline{G} \underline{u}(t) \quad (3.42)$$

$$\text{where } \underline{Y}(t) = \begin{bmatrix} X(t) \\ V(t) \\ Z(t) \end{bmatrix} \quad \underline{A} = \begin{bmatrix} 0 & 1 & 0 \\ 0 & 0 & 0 \\ 0 & 0 & 0 \end{bmatrix} \quad \underline{G} = \begin{bmatrix} 0 & 0 \\ 1 & 0 \\ 0 & 1 \end{bmatrix}$$

$$\underline{Y}(0) = \underline{Y}_0 = \begin{bmatrix} 0 \\ v \\ H \end{bmatrix} \quad \underline{Y}(T_{CE}) = \underline{Y}_F = \begin{bmatrix} (CE) \\ v_L \\ 0 \end{bmatrix}$$

Assuming that a solution exists it is given implicitly by the variation of constants formula.

$$\underline{Y}_F = e^{\underline{A}T_{CE}} \underline{Y}_0 + e^{\underline{A}T_{CE}} \int_0^{T_{CE}} e^{-\underline{A}\tau} \underline{G} \underline{u}(\tau) d\tau \quad (3.43)$$

$$\text{or} \quad \int_0^{T_{CE}} e^{-\underline{A}\tau} \underline{G} \underline{u}(\tau) d\tau = e^{-\underline{A}T_{CE}} \underline{Y}_F - \underline{Y}_0 \quad (3.44)$$

$$\text{with } e^{\underline{A}t} = \begin{bmatrix} 1 & t & 0 \\ 0 & 1 & 0 \\ 0 & 0 & 1 \end{bmatrix}$$

so (3.44) can be written

$$\int_0^{T_{CE}} \begin{bmatrix} 1 & -\tau & 0 \\ 0 & 1 & 0 \\ 0 & 0 & 1 \end{bmatrix} \begin{bmatrix} 0 & 0 \\ 1 & 0 \\ 0 & 1 \end{bmatrix} \begin{bmatrix} u_1(\tau) \\ u_2(\tau) \end{bmatrix} d\tau = \begin{bmatrix} 1 & -T_{CE} & 0 \\ 0 & 1 & 0 \\ 0 & 0 & 1 \end{bmatrix} \begin{bmatrix} (CE) \\ v_L \\ 0 \end{bmatrix} - \begin{bmatrix} 0 \\ v \\ H \end{bmatrix}$$

We thus obtain the three equations:

$$\int_0^{T_{CE}} (-\tau) u_1(\tau) d\tau = (CE) - T_{CE} v_L \quad (3.45)$$

$$\int_0^{T_{CE}} u_1(\tau) d\tau = v_L - v \quad (3.46)$$

$$\int_0^{T_{CE}} u_2(\tau) d\tau = -H \quad (3.47)$$

Equation 3.45 can be written as:

$$\int_0^{T_{CE}} [v_L - \tau u_1(\tau)] d\tau = (CE) \quad (3.45a)$$

Equation (3.45a) only says that the integral under the curve $v(t)$ is the distance travelled (CE), while equations 3.46 and 3.47 are self explanatory. Along with the constraints on u_1 and u_2 (3.45)-(3.47) have infinite solutions, in general. Figure 3.11 illustrates some possible profiles. Notice that the area under all speed profiles is the same, and that no descent is occurring while deceleration is taking place.

We attempted to formulate an optimization problem which if solved would yield a "best" profile. It was found that the traditional "minimum energy" or "minimum fuel" types of cost criteria did not yield satisfactory answers. For example the "minimum energy criterion" yielded controls that changed continuously with time, a situation clearly undesirable from the pilot's viewpoint. It will be seen later, when the radius L of the IMS and the time T_0 are chosen, that a particular kind of speed profile will be postulated for each aircraft, such that it satisfies equations (3.45)-(3.47), and furthermore, solves the velocity mix problem (to be defined in the next chapter).

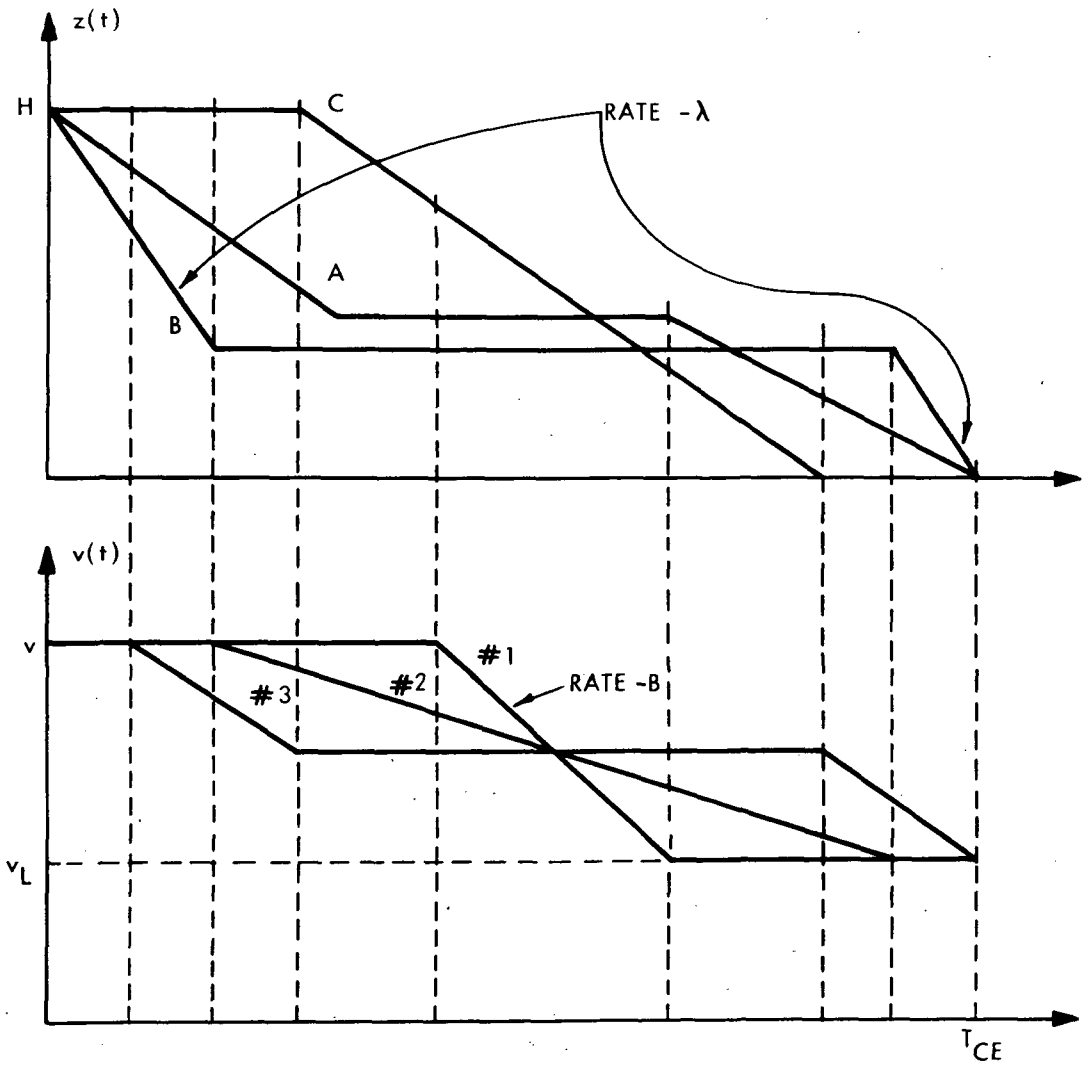


Fig. 3.11 Descent and Speed Profiles in the IMS. A,B,C Correspond to #'s 1,2,3 Respectively

CHAPTER IV
SYSTEM GEOMETRY

The previous chapter analyzed the kinds of trajectories that the aircraft will follow while inside the NTA. In this chapter consideration will be given to the magnitude of the three regions in which the NTA airspace is divided. The philosophy will be to try to pick each region, namely the IMS the OMS and the buffer zone, as small as possible. Thus the NTA will be as small as possible. Consequently, at any time the average number of aircraft inside the NTA, which is proportioned to the radius of the NTA (see Simpson p. 77), will be small, and the ground computer will not be required to keep track of too many airplanes simultaneously.

In section 4.1 the smallest possible radius L of the IMS and the smallest time T_0 will be found. Remember that T_0 is such that aircraft of all altitude levels and any landing speed can cross L and reach the OM, having accomplished all their objectives, in this common for all time interval. In section 4.2 it will be seen that because of the velocity mix problem the actual IMS radius cannot be chosen equal to its minimum value found in 4.1. Then it will be shown that by increasing L appropriately the velocity mix problem can be solved. In section 4.3 consideration will be given to the question "how close can one pick successive altitude levels, and how many alti-

tude levels are necessary?" In the final section 4.3 the magnitudes of the OMS and the buffer zone will be picked, after consideration is given to the functions that take place while the aircraft flies in these regions.

4.1 Minimum T_0 and Minimum Radius of the IMS

In this section we present the concepts that are necessary to choose the smallest IMS radius, and the smallest time T_0 .

The particular turn-straight-turn type of trajectories inside the IMS chosen in Chapter III are not so important in the analysis. What is important, is the fact that the aircraft must decelerate and descend. Thus, in order to be able to evaluate quantities of interest explicitly we shall assume throughout this section that the aircraft do not execute any turns but head straight for the OM, along the radius of the IMS ending at the entrance point. It was seen in Chapter III that the actual trajectories are close to being radial. So we expect that the errors involved will be small. It will be seen that the results can be modified slightly to account for the turn-straight-turn trajectories of the aircraft in the IMS.

4.1.1 The Minimum Time T_0

T_0 must be picked in such a way that every aircraft, no matter what the speed v , with which it enters the IMS, is and no matter what its landing speed v_L is, should have enough time to decelerate to its landing speed and descend some altitude H_v . In this

way T_o could be chosen as the common for all aircraft time to cross the IMS.

Consider an aircraft entering the IMS with speed v (i.e., from a particular altitude level located H_v feet above the level of the OM) and with landing speed v_L . Then the smallest time in which it can accomplish the two objectives stated above is:

$$t_o = \frac{H_v}{\lambda} + \frac{v - v_L}{B} \quad (4.1)$$

where

a) λ is the maximum descent rate and,

b) B is the maximum deceleration.

Given that $v \in [V_1, V_2]$ ($V_1 = 200$ Knots, $V_2 = 300$ Knots), $v_L \in [V_{L1}, V_{L2}]$ ($V_{L1} = 100$ Knots, $V_{L2} = 150$ Knots) and that the highest altitude level will carry traffic at V_2 it is easily seen that the maximum value of t_o will occur when $H_v = H_{V2}$, $v = V_2$, $v_L = V_{L1}$.

$$T_{o1} = \frac{H_{V2}}{\lambda} + \frac{V_2 - V_{L1}}{B} \quad (4.2)$$

Thus in the worst case design we are considering, T_o must be at least as large as T_{o1} .

$$T_o \geq T_{o1} \quad (4.3)$$

A typical value of T_{o1} for $H_{V2} = 6000$ feet $\lambda = 1000$ ft/min. $B = 1$ Knot/sec. is $T_{o1} = 9.33$ minutes.

Suppose now that L , the radius of the IMS, has been given. For an aircraft characterized by (v, v_L) there is a smallest time t^* in

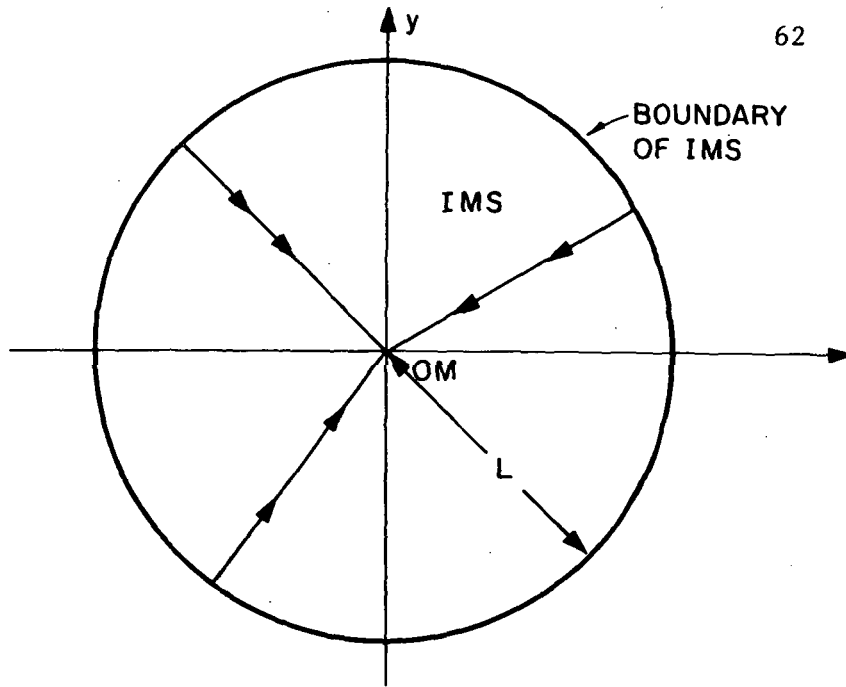


Fig. 4.1 Trajectories Inside IMS for the Analysis in Chapter IV

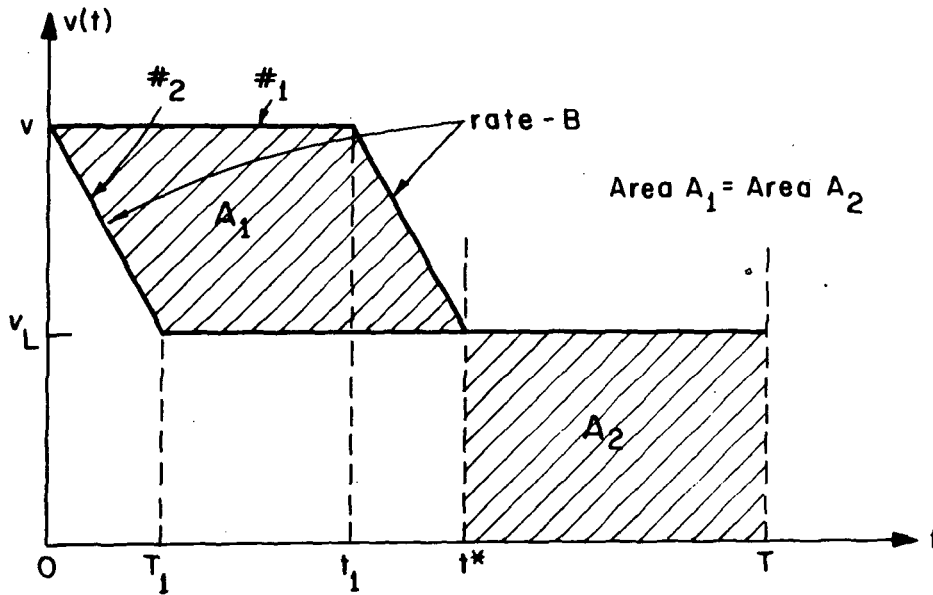


Fig. 4.2 Extremal Speed Profiles for Fixed L

which it can traverse L . This is accomplished if the aircraft flies with speed v most of the way and decelerates at rate $-B$ at the very end. The speed profile is pictured in figure 4.2 (#1). We find t^* from the following two equations.

$$v - B(t^* - t_1) = v_L \quad (4.4)$$

$$v t_1 + \int_{t_1}^{t^*} [v - B(\tau - t_1)] d\tau = L \quad (4.5)$$

From these we can solve for t^* .

$$t^* = t^*(v, v_L) = \frac{L}{v} + \frac{(v - v_L)^2}{2B v} \quad (4.6)$$

Similarly there is a largest time T in which L can be traversed. This is found if the aircraft decelerates with the maximum rate B immediately after it enters the IMS, and continues thereafter with speed v_L (see fig. 4.2, profile #2). T is found from the following two equations.

$$\int_0^{T_1} (v - B\tau) d\tau + v_L(T - T_1) = L \quad (4.7a)$$

$$v - BT_1 = v_L \quad (4.7)$$

From which we find

$$T = T(v, v_L) = \frac{L}{v_L} - \frac{(v - v_L)^2}{2B v_L} \quad (4.8)$$

It should be clear that

$$T(v, v_L) > t^*(v, v_L) \quad (4.9)$$

Let us now try to find the maximum value of $t^*(v, v_L)$ and the minimum value of $T(v, v_L)$ for $v \in [V_1, V_2]$, $v_L \in [V_{L1}, V_{L2}]$. From eq. (4.6) it is seen that t^* as a function of v_L is a convex parabola with vertex (minimum) at $v_L = v$. As a function of v , t^* is the sum of a straight line, a constant, and a hyperbola. It has a minimum at $v^2 = v_L^2 + 2BL$.

From eq. (4.8) it is seen that T as a function of v_L is the sum of a straight line, a constant and a hyperbola. It is monotonically decreasing for $0 < v_L$, $v^2 < 2BL$. As a function of v , T is a concave parabola with vertex (maximum) at $v = v_L$. The assertion that T is a monotonically decreasing function of v_L in the intervals stated is based on the fact that $2BL > v^2$ for $v \in [V_1, V_2]$. For a first "very rough" estimate of L of about 20 n.miles (average speed of 120 Knots for $T_0 = 10$ minutes) it is seen that $2BL = 2 \times 1 \frac{\text{Knot}}{\text{Sec}} \times 20 \text{ n.miles} = (40) \times (60)^2 (\text{Knots})^2$, so that $\sqrt{2BL} > 360$ Knots and the inequality $v^2 < 2BL$ holds for $v \in [V_1, V_2]$ (actually L will be found larger than this "first estimate").

In figure 4.3 we plot $t^*(v, v_L)$ and $T(v, v_L)$. It is easily seen from the discussion above, also illustrated in figure 4.3, that the maximum value of t^* occurs at the point (V_1, V_{L1}) while the minimum value of T occurs at (V_2, V_{L2}) , i.e.,

$$t^*_{\max}(v, v_L) = t^*(V_1, V_{L1}) \quad (4.10)$$

$$T_{\min}(v, v_L) = T(V_2, V_{L2}) \quad (4.11)$$

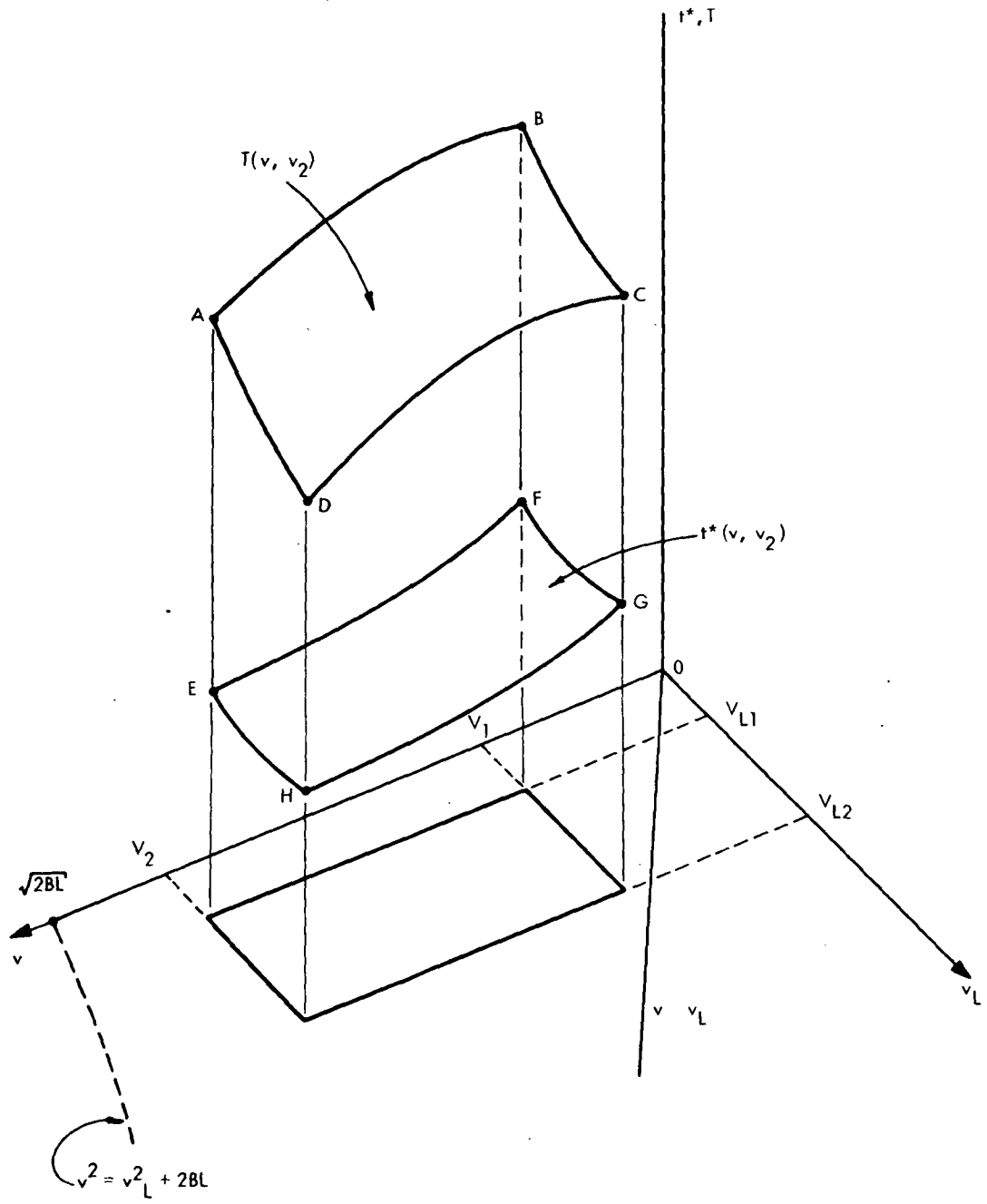


Fig. 4.3 $t^*(v, v_L)$ and $T(v, v_L)$

The reason for which we wanted to find T_{\min} and t_{\max}^* now becomes clear. If L is chosen in such a way that $T_{\min} \geq t_{\max}^*$, then if T_{O_2} is picked in the interval $[t_{\max}^*, T_{\min}]$ it is seen that any aircraft, no matter what its entrance speed and landing speed is, can traverse the length L in time T_{O_2} . The only objective that has been accomplished during the time T_{O_2} is that the aircraft has decelerated (the equations for t^* and T do not include altitude). Thus the condition:

$$T_{\min}(v, v_L) \geq t_{\max}^*(v, v_L)$$

$$v \in [V_1, V_2], v_L \in [v_{L1}, v_{L2}] \quad (4.12)$$

is a necessary and sufficient condition that a T_{O_2} can be found, such that all aircraft can traverse a distance L in T_{O_2} and decelerate.

Let us find the minimum L for which (4.12) holds. Considering (4.10) and (4.11), (4.12) becomes:

$$\frac{L}{v_{L2}} - \frac{(v_2 - v_{L2})^2}{2B v_{L2}} \geq \frac{L}{v_1} + \frac{(v_1 - v_{L1})^2}{2B v_1} \quad (4.13)$$

thus

$$\frac{L_{\min}}{v_{L2}} - \frac{(v_2 - v_{L2})^2}{2B v_{L2}} = \frac{L_{\min}}{v_1} + \frac{(v_1 - v_{L1})^2}{2B v_1}$$

which yields

$$L_{\min} = \frac{(v_1 - v_{L1})^2 v_{L2}}{2B(v_1 - v_{L2})} + \frac{(v_2 - v_{L2})^2 v_1}{2B(v_1 - v_{L2})} \quad (4.14)$$

For $V_1 = 200$ Knots, $V_2 = 300$ Knots, $V_{L1} = 100$ Knots, $V_{L2} = 200$ Knots and $B = 1$ Knot/sec, we find $L_{\min} = 16.7$ n.miles

$$(4.15)$$

Equation (4.14) denotes that if $L \geq L_{\min}$ then there will always exist a T_{O2} .

If $L = L_{\min}$ then $T_{\min} = t^*_{\max} = T_{O2}$. This T_{O2} and the T_{O1} found in (4.2) are the two critical numbers that go into finding T_O . Since T_O must be greater than or equal to both of these numbers, so that the constraints of descent by H_V and deceleration to the landing speed can be met by all pairs of (v, v_L) , the smallest value of T_O is the maximum of the two numbers T_{O1} and T_{O2}

$$T_{O\min} = \max (T_{O1}, T_{O2}) \quad (4.16)$$

The value of T_{O2} can be found by either (4.10) or (4.11) with $L = L_{\min}$. We find

$$T_{O2} \approx 5.43 \text{ minutes} \quad (4.17)$$

It is thus seen that the limiter in the choice of T_O will be T_{O1} unless H_{V2} is picked very small. Thus let us pick

$$T_O = T_{O\min} = T_{O1} > T_{O2} \quad (4.18)$$

If the same analysis is performed for the turn-straight-turn type of IMS trajectories, the results are almost the same. The first effect is that both of the surfaces $T(v, v_L)$ and $t^*(v, v_L)$ shift slightly upward (not by the same amount for all (v, v_L) pairs). The upward shift occurs because for a given IMS radius L , the path to

be traveled is no longer a straight line but a longer path, consisting of both circles and straight lines (see fig. 3.9).

The value of T_o (cf. eq. (4.2)) also becomes larger, because part of the trajectory to the OM consists of circles, thus leaving a straight line portion which is, in general smaller than L (see fig. 3.9). The increases in T_{o_1} and T_{o_2} are about 10%. Thus if the value of $T_{o_{min}}$ found in (4.16) is increased by 10%, and if the actual T_o is chosen greater than or equal to this new $T_{o_{min}}$, then all aircraft can reach the OM with correct heading, in time T_o .

4.1.2. The Minimum Radius L

Now that T_o is fixed consideration to the value of the minimum L will be given. First, we rewrite equations (4.6) and (4.8) with t^* and T replaced by T_o .

$$T_o = \frac{L}{v} + \frac{(v - v_L)^2}{2Bv} \quad (4.19)$$

$$T_o = \frac{\ell}{v_L} - \frac{(v - v_L)^2}{2Bv_L} \quad (4.20)$$

Now we solve (4.19) and (4.20) for ℓ and L .

$$L = L(v, v_L) = T_o v - \frac{(v - v_L)^2}{2B} \quad (4.21)$$

$$\ell = \ell(v, v_L) = T_o v_L + \frac{(v - v_L)^2}{2B} \quad (4.22)$$

What equations (4.21) and (4.22) imply is that if the aircraft has some time T_o at its disposal then the maximum distance it

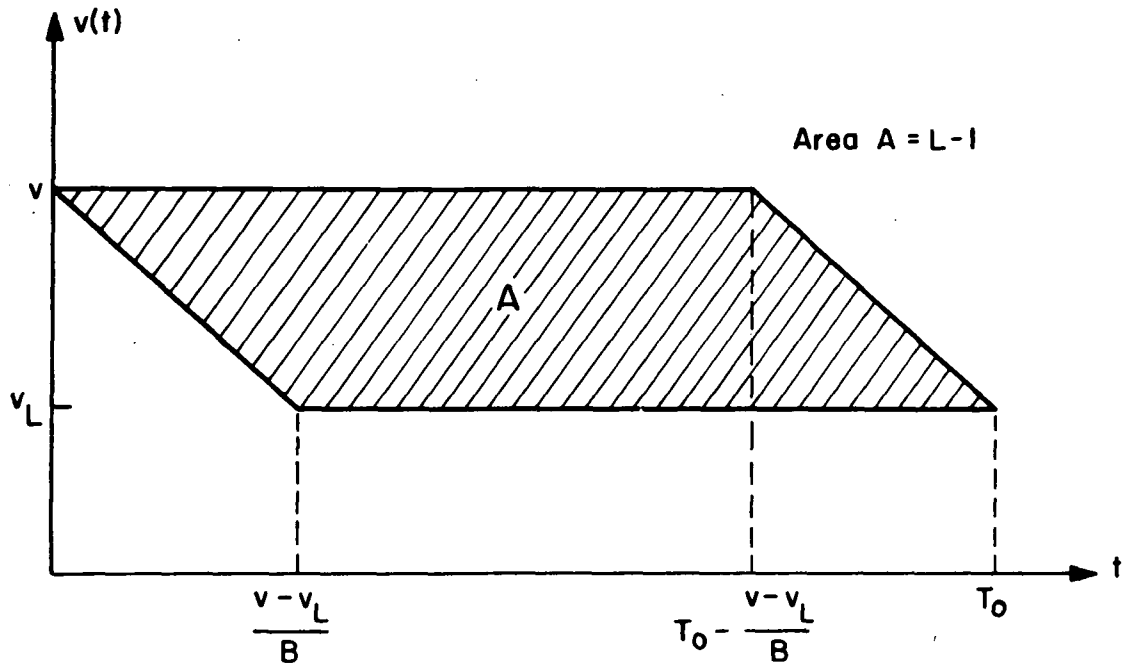


Fig. 4.4 Extremal Speed Profiles for Fixed T_0

can travel is L and the minimum is ℓ . In the former case the deceleration is delayed until the end, while in the latter it is initiated at time zero (see figure 4.4). We now look for extrema of $L(v, v_L)$ and $\ell(v, v_L)$ in the range $v \in [V_1, V_2]$ and $v_L \in [V_{L1}, V_{L2}]$.

The extrema can be found because both ℓ and L are parabolas as functions of v and v_L . Figure 4.6 illustrates the nature of the curves $\ell(v, v_L)$ and $L(v, v_L)$. The minimum value of L is seen to be at the point (V_1, V_{L1}) , while the maximum value of ℓ is at (V_2, V_{L2}) . If we consider the intersections of a plane $v = \text{constant}$ with the surfaces $L(v, v_L)$ and $\ell(v, v_L)$ (see figure 4.6), then the minimum value of the segment ML occurs at M , and the maximum value of the segment JK occurs at K . The reason for which we consider these intersections is that we would like to find the smallest radius of the IMS for each altitude level (which as we saw is characterized by the speed v all aircraft flying on it must have).

What we would like to examine now is whether the point M is always higher than the point K (of fig. 4.6) for any value of $v \in [V_1, V_2]$. If it is, then it is easy to see that given v (i.e., the particular altitude level) the smallest possible radius of the boundary of the IMS is the value of $\ell(v, v_L)$ at the point K . This is so because any aircraft with entering speed v (fixed) and landing speed $v_L \in [V_{L1}, V_{L2}]$ will have enough distance to travel in time T_0 and accomplish its objectives.

We now state as a theorem and prove an even stronger result.

Theorem: Suppose that we pick the radius of the IMS (same

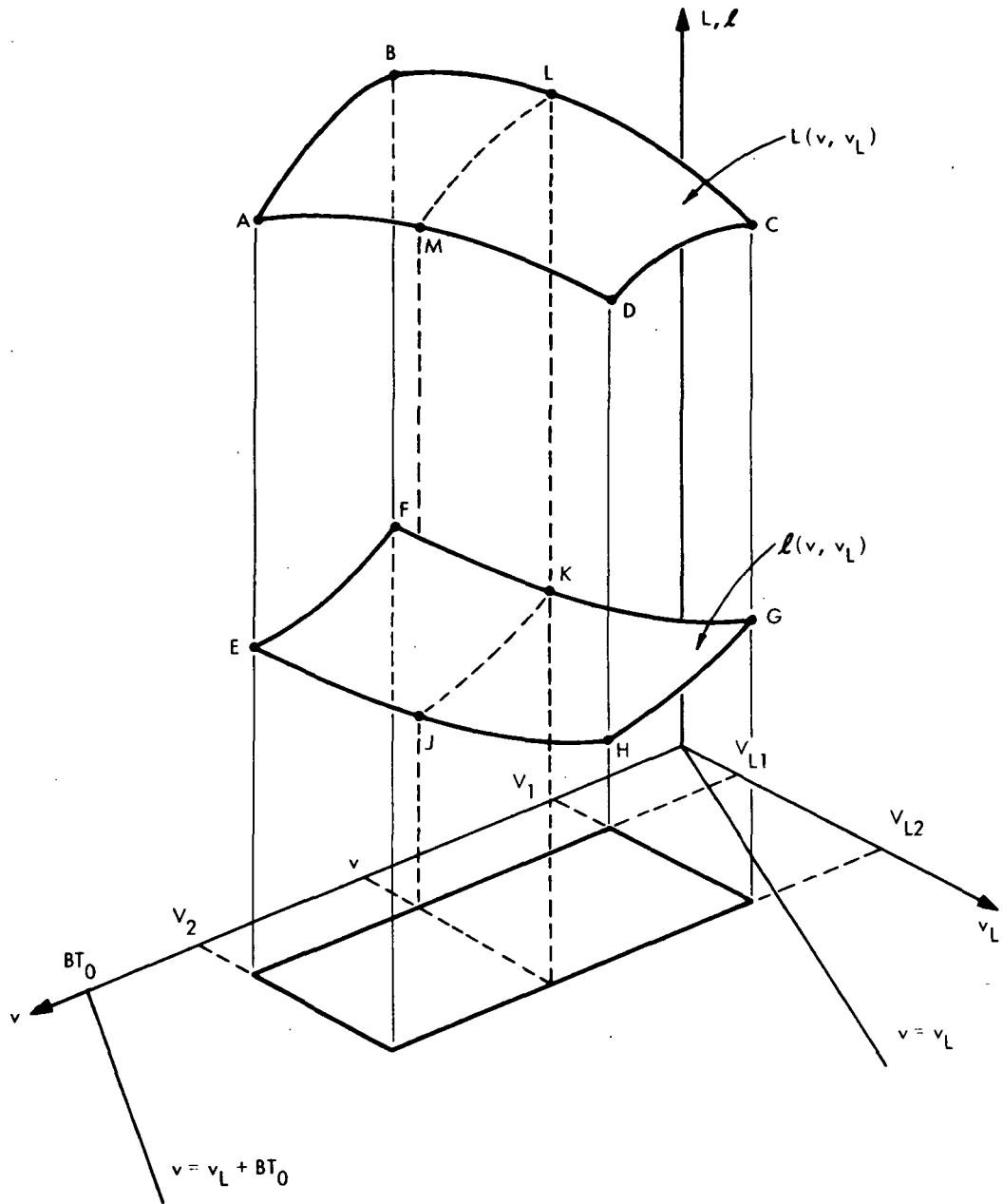


Fig. 4.6 $L(v, v_L)$ and $l(v, v_L)$; Fixed T_0 .

For all altitude levels) such that $T_o = T_{\min} = T(V_2, V_{L2})$ (cf. section 4.1.1). If $T_{\min} \geq t_{\max}^*$, it follows that $L(V_1, V_{L1}) \geq \ell(V_2, V_{L2})$.

Proof: We saw in section 4.1.1 that the value of T_o for the particular problem at hand is bound to be governed by the altitude H_{V2} rather than by the value of T_{o2} . In other words T_o will in general be greater than T_{o2} . Suppose, nevertheless, that we "raise" the surfaces ABCD and EFGH of figure 4.3 by increasing L , so that $T_{\min} = T(V_2, V_{L2}) = T_o$. Since L is increased above the critical value L_{\min} found in (4.15), the "gap" between T_{\min} and t_{\max}^* is increased and thus the condition $T_{\min} \geq t_{\max}^*$ is satisfied.

From the equality

$$T(V_2, V_{L2}) = T_o \quad (4.23)$$

and equation (4.8) we obtain

$$\frac{L_o}{V_{L2}} - \frac{(V_2 - V_{L2})}{2BV_{L2}} = T_o$$

which yields

$$L_o = T_o V_{L2} + \frac{(V_2 - V_{L2})}{2B} \quad (4.24)$$

We also have that $T_{\min} \geq t_{\max}^*$ or

$$\frac{L_o}{V_{L2}} - \frac{(V_2 - V_{L2})}{2BV_L} \geq \frac{L_o}{V_1} + \frac{(V_1 - V_{L1})}{2BV} \quad (4.25)$$

If we substitute in (4.25) the value of L_o found in (4.24)

we obtain

$$T_o + \frac{(V_2 - V_{L2})^2}{2BV_{L2}} - \frac{(V_2 - V_{L2})^2}{2BV_{L2}} \geq \frac{T_o V_{L2}}{V_1} + \frac{(V_2 - V_{L2})^2}{2BV_1} + \frac{(V_1 - V_{L1})^2}{2BV_1} \quad (4.26)$$

or

$$T_o V_1 - \frac{(V_1 - V_{L1})^2}{2B} \geq T_o V_{L2} + \frac{(V_1 - V_{L2})^2}{2B} \quad (4.27)$$

which is exactly

$$L(V_1, V_{L1}) = L_{\min} \geq \ell(V_2, V_{L2}) = \ell_{\max} \quad (4.28)$$

Q.E.D.

What the theorem above indicates is that all we need to do, in order to guarantee that the surface ABCD of figure 4.6 is above the highest point of the surface EFGH of the same figure, is to pick $T_o \geq T_{o2}$ (T_{o2} was defined in 4.1.1). Since we have guaranteed that $T_o \geq T_{o2}$ via (4.16) the existence of a minimum value of the IMS radius is ensured.

As was indicated in a previous paragraph of this section, the minimum values for the radii of the circles where the different altitude levels meet the IMS, can be found along the line segment FG of figure 4.6. In other words given v (i.e., given the altitude level) the smallest value of L_v , the radius of the IMS for this level, is the value $\ell(v, V_{L2})$.

Some typical values of $\ell(v, V_{L2})$ are shown in Table 4.1

TABLE 4.1

Typical Values of $\ell(v, V_{L2})$

T_o	v	V_{L2}	(v, V_{L2})
10 min.	200 Knots	150 Knots	25.35 n.miles
" "	220 "	" "	25.68 "
" "	250 "	" "	26.39 "
" "	280 "	" "	27.36 "
" "	300 "	" "	28.26 "

The fact that the IMS trajectories are not straight lines does not affect the analysis of this section at all. The reason is that, once T_o is chosen via the analysis of section 4.1.1, we are ensured that all aircraft no matter where they enter the IMS, will have enough time to reach the OM and accomplish their "objectives". Thus in order to find L , we only need to work with the simplest of the turn-straight-turn trajectories. These occur when the aircraft enter the IMS of the point $(x, y) = (-L, 0)$, and they are straight lines.

4.2 Determination of the Actual IMS Radii

In this section we ask the question whether the minimum T_o and minimum L found in the previous section guarantee safe separation between aircraft. It will be seen that they do not. Then it will be seen that by holding T_o the same and increasing somewhat the value of L safe separation can be guaranteed for successive aircraft.

4.2.1. The Velocity Mix Problem

Consider one altitude level characterized by speed $v \in [V_1, V_2]$ and located H_v above the level of the OM. Suppose that T_0 has been chosen by equation 4.16, and the radius L_v of the circular boundary, where this altitude level meets the IMS, is equal to $\ell(v, V_{L2})$.

Consider an aircraft that enters the IMS from this altitude level. Suppose that it is supposed to land with speed V_{L2} . It is given time T_0 to descend by H_v and decelerate to its landing speed. It is seen that due to the way the radius L_v was chosen ($L_v = \ell(v, V_{L2})$), this particular aircraft has no flexibility at all with respect to the speed profile. In other words as soon as it enters the IMS, it must decelerate to its landing speed V_{L2} as fast as it can, and then continue flying for time $T_0 - \frac{v - V_{L2}}{B}$ at speed V_{L2} . It will then have reached the OM.

On the other hand, if the entering aircraft is to land with V_{L1} then, the latest time it can start decelerating is τ seconds after its entrance to the IMS (cf. fig. 4.7). Thus it is seen that for this aircraft there is more flexibility in choosing $V(t)$, its speed profile. We would not like to have to discriminate against heavier aircraft (which have higher v_L). Also we would like to have the speed profile known to ground for tracking purposes.

Thus we shall postulate that the speed profile of any aircraft inside the IMS is such that the deceleration is delayed until the very end. Namely the aircraft proceeds for time τ with speed v ,

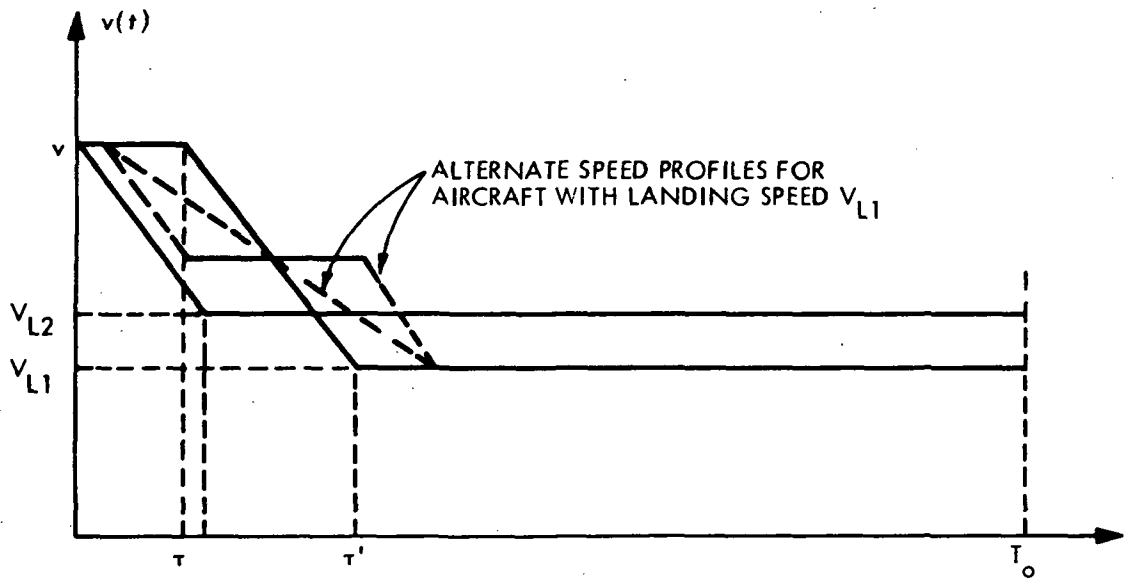


Fig. 4.7 Speed Profiles for Entrance Speed $v \in [V_1, V_2]$ and Extreme Landing Speeds

then decelerates with rate B to the landing speed and continues flying at v_L for the rest of the time. The time τ is found by the following two equations

$$v - B(\tau' - \tau) = v_L \quad (4.29)$$

$$L_v = \int_0^{T_0} v(t) dt$$

which implies

$$\ell(v, v_{L2}) = v\tau + \int_{\tau}^{\tau'} [v - B(t - \tau)] dt + (T_0 - \tau')v_L \quad (4.30)$$

Solving for τ we obtain

$$\tau = \frac{\ell(v, v_{L2})}{v - v_L} - \frac{v_L T_0}{v - v_L} - \frac{v - v_L}{2B} \quad (4.31)$$

Thus given $L_v = \ell(v, v_{L2})$ and T_0 the speed profile in the IMS of every aircraft entering from the altitude level H_v is known via (4.31).

Typical values of τ are shown in Table 4.2. on the following page.

Consider now the minimum separation standards over the OM and on the runway, between successive aircraft. Let the minimum runway time separation between two successive landing aircraft be t_0 , and the minimum longitudinal separation over the OM be s_0 . Let the landing speed of the first and second aircraft to cross the OM be v_{ℓ_1} and v_{ℓ_2} respectively.

If $v_{\ell_1} > v_{\ell_2}$ the aircraft will be moving apart from each

TABLE 4.2
 Typical Values of τ ($T_o = 10$ min)

v	(v, V_L)	v_L	τ
200 Knots	25.35 n.miles	150 Knots	0 min.
" "	" "	120 "	3.33 "
" "	" "	100 "	4.37 "
250 "	26.39 "	150 "	0 "
" "	" "	120 "	2.12 "
" "	" "	100 "	2.65 "
300 "	28.26 "	150 "	0 "
" "	" "	120 "	1.30 "
" "	" "	100 "	1.81 "

other along the glide path, so the shortest time t_s the second can be scheduled after the first is

$$t_s = \frac{s_o}{v_{\ell 2}} \quad (4.32)$$

If, on the other hand, $v_{\ell 1} < v_{\ell 2}$ then the second one will be closing in behind the first aircraft and thus the time t_s would be

$$t'_s = t_o + s \left(\frac{1}{v_{\ell 1}} - \frac{1}{v_{\ell 2}} \right) \quad (4.33)$$

where s is the distance of the OM from the runway threshold (see also Bloomstein² and Odoni³ for more extensive discussion).

For $t_o \sim 1$ minute, $s_o \sim 2.5$ n.miles, and $v_L \in [V_{L1}, V_{L2}]$, we obtain values of t_s of the order of 1 minute.

After this short diversion, let us go back to the speed

profiles. Assume that two aircraft enter successively the IMS, from the same altitude level, at approximately the same point of the circular boundary of the IMS. Thus, for all practical purposes one is "behind" the other. Assume that they enter the IMS t_s seconds apart (this was the reason for the diversion above). We distinguish two cases:

$$a) \quad v_{\ell 1} \leq v_{\ell 2}$$

In this case figure 4.8 shows the two speed profiles for arbitrary $v_{\ell 1}$ and $v_{\ell 2}$ satisfying $v_{\ell 1} < v_{\ell 2}$. The initial longitudinal separation between the two aircraft is the area ABCD (t_s represents the time the second aircraft enters the IMS after the entrance of the first). This separation will decrease by the area EFGHJK by the time the first aircraft reaches the OM. Thus the smallest longitudinal separation in the IMS between the two aircraft will occur over the OM which is desirable. This because the aircraft have been scheduled t_s seconds apart, which in terms of landing speeds means safe separation.

It is not hard to see that for all possible values of t_s , as long as $v_{\ell 1} \leq v_{\ell 2}$, the minimum longitudinal separation will occur over the OM. Furthermore, it does not matter what the descent profile of each aircraft is, because they will never be violating the horizontal separation standards.

$$b) \quad v_{\ell 1} > v_{\ell 2}$$

For this case figure 4.9 shows two typical speed profiles.

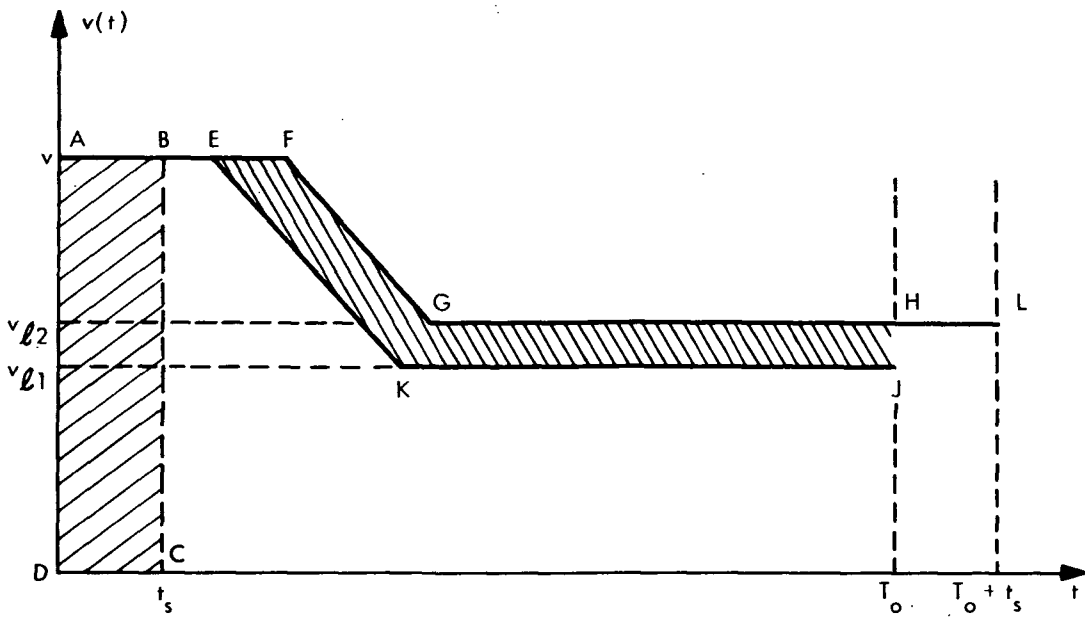


Fig. 4.8 Speed Profiles of Successive Aircraft if $v_{l1} < v_{l2}$

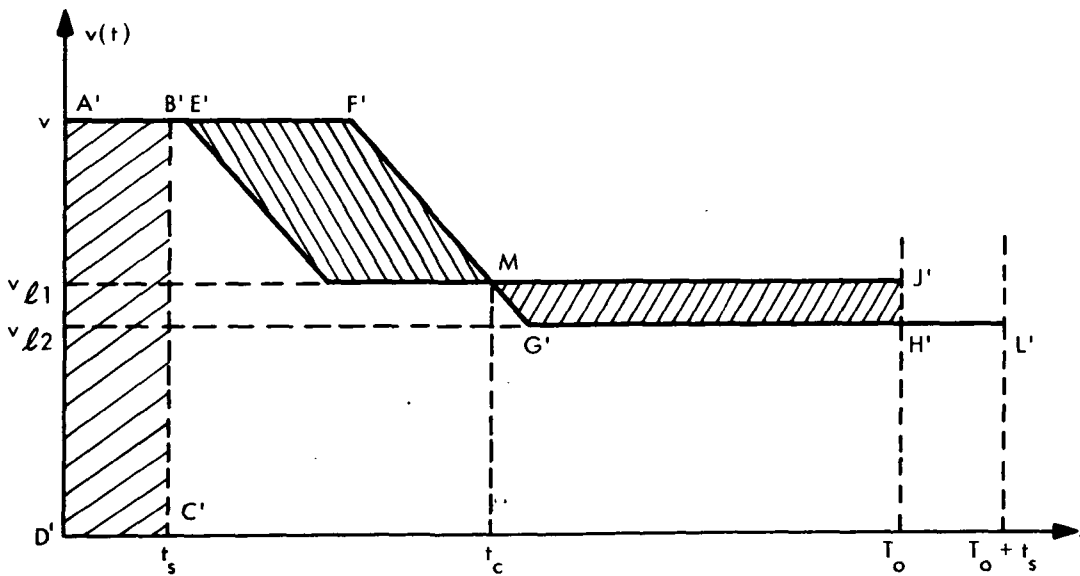


Fig. 4.9 Speed Profiles of Successive Aircraft if $v_{l1} > v_{l2}$

The initial separation is the area $A'B'C'C'$. As time progresses the horizontal separation decreases by the area $E'F'MK'$ and then, surprisingly, it increases again by the area $MG'H'J'$. It is thus seen that the minimum longitudinal separation between the two aircraft occurs at some time $t_c < T_o$. If $t_s = \frac{S_o}{v_{\ell 2}}$ then the separation at time T_o is scheduled to be S_o . However, as it was just seen, at time t_c the separation will be smaller than S_o . Since S_o will usually be equal to the minimum safe longitudinal separation (about 2.5 n.miles) it is seen that the aircraft will be dangerously close at some point t_c . As a matter of fact it can be easily demonstrated, by plugging in some values for v , $v_{\ell 1}$ and $v_{\ell 2}$, that the separation at time t_c can even be negative! In other words the aircraft that is to land second can supercede the first one but then it has to decelerate to its landing speed which is smaller than $v_{\ell 1}$. Thus since $v_{\ell 1} > v_{\ell 2}$ the first one will "catch up" with it and pass it again developing a separation equal to s_o over the OM.

The situation just illustrated above is exactly what we shall hereby call the mix problem. One might suggest that the problem arises because of the particular way the speed profiles were chosen. However, consideration of the top altitude level (speed $v = V_2$) readily reveals that the mix problem exists there no matter what the speed profiles are, and is serious (negative separations).

The next question is whether by using altitude we can prescribe descent profiles such that whenever minimum horizontal separation standards are violated, the altitude separation is large enough to guarantee

safety. Instead of presenting generalized arguments a specific example will be given.

Consider the top altitude level at altitude H_{V_2} above the OM. From equation (4.16) and the discussion of section 4.1.1 it was seen that in general for reasonable altitudes (eg. $H_{V_2} > 5000$ ft) T_o will be equal to $\frac{H_{V_2}}{\lambda} + \frac{V_2 - V_{L1}}{B}$. Let this be the case. Consider two successive aircraft, the first with landing speed equal to V_{L2} and the second with landing speed V_{L1} . Let $t_s = \frac{S_o}{V_{L1}} = \frac{2.5 \text{ n.miles}}{100 \text{ Knots}} = 1.5 \text{ min.}$ Figure 4.10 illustrates the speed profiles for the two aircraft. The values for the different points in time are picked from table 4.2 and the nature of the particular speed profiles postulated.

It is seen that $t_c = 5.8$ minutes. Looking at the descent profile (fig. 4.11) for the second aircraft it is seen that it is fixed, because $T_o = \frac{H_{V_2}}{\lambda} + \frac{V_2 - V_{L1}}{B}$ and this aircraft needs $\frac{V_2 - V_{L1}}{B}$ minutes to decelerate, so it must spend all the remaining time descending. On the other hand the first aircraft needs only $\frac{V_2 - V_{L2}}{B}$ minutes to descend so it has $\frac{V_{L2} - V_{L1}}{B} = \frac{5}{6}$ minutes to play with respect to the descent profile. The area abcd of fig. 4.11 is the region in which the descent profile of the the first aircraft must lie.

Given this flexibility for aircraft #1 there is a time $t \in [t_1, t_2]$ when the two aircraft will be on the same level. Considering the particular values of t_1 and t_2 it is seen that the best altitude profile for the first aircraft would be along the line ad. Then the longitudinal separation at time t_1 would be larger than at time t_2 .

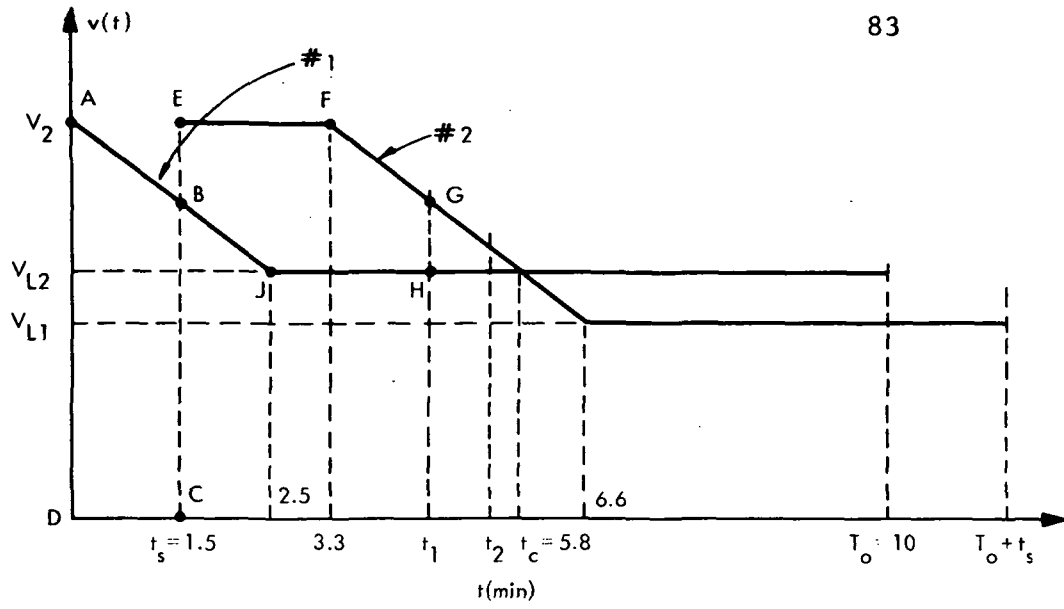


Fig. 4.10 Speed Profiles for Extreme Cases. Aircraft Enter the IMS From Top Altitude Level

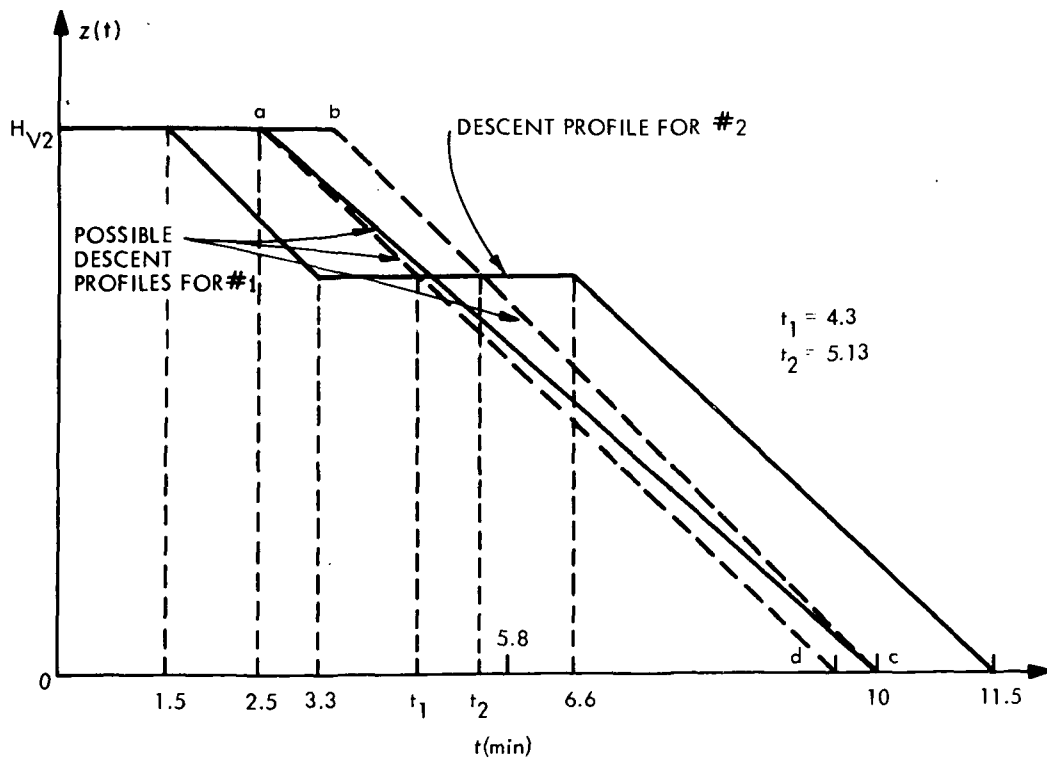


Fig. 4.11 Descent Profiles for the Extreme Cases in the Top Altitude Level

The longitudinal separation, however, at time t_1 is from figure 4.10 equal to

$$d_{\text{hor}} = \text{Area (ABCD)} - \text{Area (EFGHJB)} \quad (4.34)$$

which with the values involved is found to be $d_{\text{hor}} = .36$ n.miles!!

Thus at time t aircraft #2 is intolerably close to #1.

This example demonstrated that the values of T_o and L_v picked in section 4.1 do not guarantee safe separation between successive aircraft in the IMS.

4.2.2 Solution of the Velocity Mix Problem for One Altitude Level

Since the velocity mix problem described above cannot be resolved either by prescribing different speed profiles or by ordering strict descent profiles, we try to increase T_o and L_v .

Consider figures 4.6 and 4.9. If T_o is increased somewhat and L_v is picked at the intersection of the plane $v = \text{constant}$ and the line FG (cf. fig. 4.6), which will have moved upward, the speed profiles of fig. 4.9 will change but the critical time T_c will not go closer to T_o (see fig. 4.12). So the problem is not alleviated.

A solution is now proposed. It was previously seen that the mix problem arose because the aircraft had to start decelerating at an early time. We now propose to increase L_v , while keeping T_o the same, in such a way that the deceleration will occur at the very end. We cannot pick an arbitrary value of L_v . Looking at figure 4.6 it is seen that the value of $L(v, v_L)$ at the point M is such that all

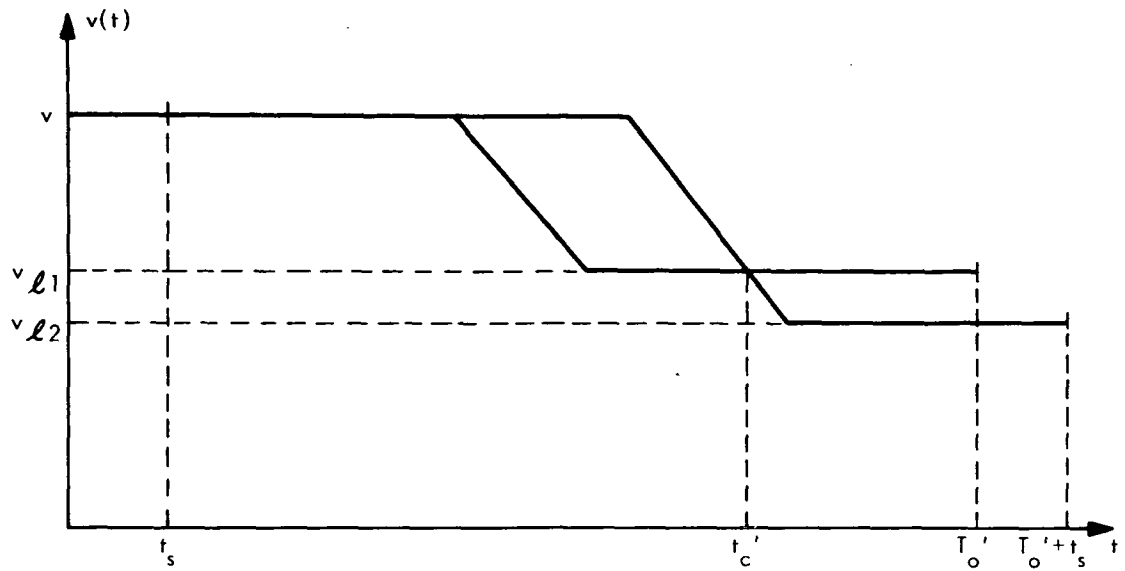


Fig. 4.12 Effect of Increasing Both T_o and L_v on the Mix Problem

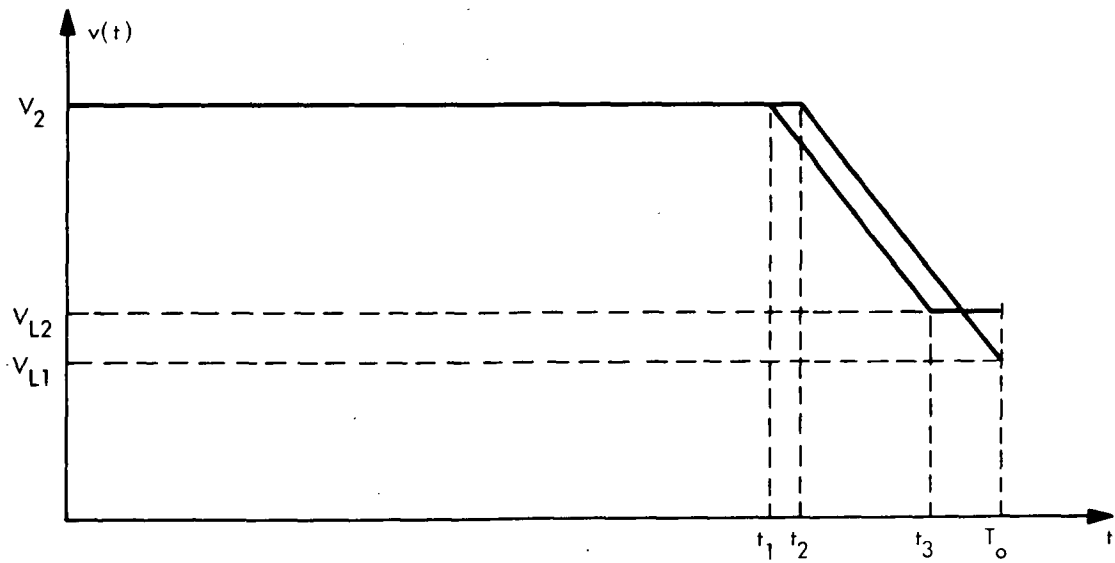


Fig. 4.13 Effect of Increasing Only L_v , on the Speed Profiles For One Altitude Level

aircraft have enough "room" to accomplish the "objectives" in time T_o . However, this value of L_v has the additional feature that the speed profiles will be such that the deceleration for all aircraft will occur very close to the end of time T_o .

Let us examine the speed profiles for the altitude level V_2 (for numerical convenience). What we are interested in is the values of the time points t_1 and t_2 , (cf. fig. 4.13). Since $L_{V_2} = L(V_2, V_{L1})$ (see fig. 4.6) it is seen that the aircraft with landing speed V_{L1} will have a speed profile such that

$$T_o - t_2 = \frac{V_2 - V_{L1}}{B} \quad (4.35)$$

For $T_o = 10$ min, t_2 is 6.67 min.

For the aircraft that lands with landing speed V_{L1} , the latest time t_1 when it should start the deceleration is found via the following equation (cf. fig. 4.13)

$$\int_0^{T_o} v(t) dt = L(V_2, V_{L1}) \quad (4.36)$$

or

$$(V_2 - V_{L2})t_1 + T_o V_{L2} + \frac{(V_2 - V_{L2})^2}{2B} = T_o V_2 - \frac{(V_2 - V_{L1})^2}{2B} \quad (4.37)$$

solving for t_1 we obtain

$$t_1 = T_o - \frac{V_2 - V_{L2}}{B} - \frac{(V_2 - V_{L1})^2}{2B(V_2 - V_{L2})} \quad (4.38)$$

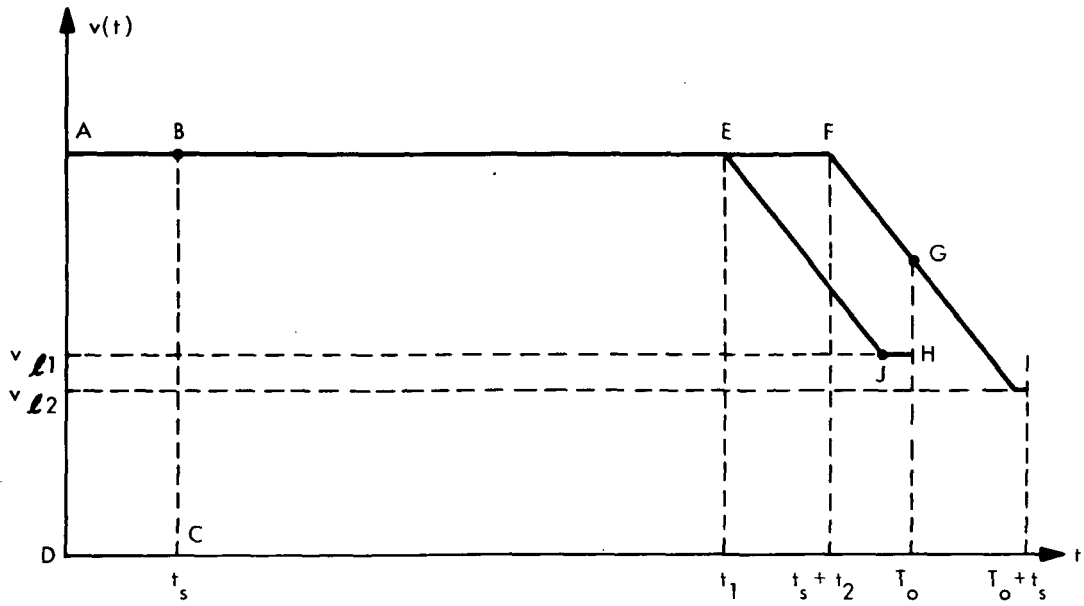


Fig. 4.14 Alleviation of the Mix Problem

For $T_0 = 10$ min. $t_1 = 6.54$ min. Comparing t_1 and t_2 it is seen that they differ by only .13 min. The same situation arises if a lower v is chosen.

Let us now see what the significance of the above result is. We saw in the previous section that the mix problem arose when the landing speed of the second of two successive aircraft was smaller than the landing speed of the first. Consider the same situation now. From figure 4.14, it is seen that the initial longitudinal separation is the area (ABCD). This separation remains the same throughout the flight except when both aircraft are close to the OM. It is seen that since $t_1 \approx t_2$ the smallest longitudinal distance between the two aircraft will occur over the OM which is what we had aimed for.

Another interesting feature is that since the longitudinal separation remains safe, it does not matter what the altitude separation is. Thus the pilot is given full freedom to choose his descent profile, as long as he descends to the level of the OM in time T_0 .

Typical values of $L(v, V_{L1})$ for different values of v are shown in table 4.3. For smaller values of T_0 it is seen that L_v is smaller. Since T_0 is at least 5.5 min (cf. eq. 4.17), it is seen that the altitude of the highest altitude level will be what will govern the choice of T_0 via eq. (4.2). The choice of H_{V2} will be left open in this thesis to be picked by the designer of an actual ATC system, based on the concepts presented here.

TABLE 4.3
 Typical Values of $L(v, V_{L1})$

T_o	v	$L(v, V_{L1})$
10 min.	200 Knots	31.91 n.miles
"	230 "	35.96 "
"	270 "	41.00 "
"	300 "	44.45 "
8 min.	200 "	25.31 "
"	230 "	28.31 "
"	270 "	32.00 "
"	300 "	34.45 "

4.2.3 Conclusions

In this section we found that if the smallest radius of the circular boundary of the IMS, for any altitude level, is chosen according to the method of section 4.2.2, then every aircraft entering the IMS from that particular altitude level, no matter what speed it lands with, can reach the OM in time T_o , fixed by equation (4.16). Safe separation between successive aircraft is guaranteed by the choice of the radius L_v . Finally, the speed profile is fixed for every aircraft, while the descent profile is left for the pilot to decide.

4.3 Selection of Position of Altitude Levels

In the previous section, it was seen that safe separation was guaranteed if the successive aircraft entering the IMS had previously flown on the same altitude level. No mention was made of successive aircraft entering from different altitude levels. In this section, this new problem is examined. It will be seen that by choosing the altitude levels appropriately, conflicts will be avoided.

Since $L_v = L(v, v_{L1})$, if we are told that one altitude level is to carry traffic at speed v , we can immediately determine the minimum radius of the IMS for this level via the formula

$$L_v = T_{ov} - \frac{(v - v_{L1})^2}{2B} \quad (4.39)$$

It is understood that if $v_k > v_{k+1}$ then $Hv_k > Hv_{k+1}$, i.e., higher altitude levels will handle higher speed traffic.

Now consider two altitude levels H_{v_a} and H_{v_b} . Assume that $v_a > v_b$ so that $Hv_a > Hv_b$. Because of equation (4.39) it is true that $Lv_a > Lv_b$. We would like to consider successive aircraft entering the IMS from these two altitude levels. We distinguish two cases.

- a) First aircraft enters the IMS from H_{v_b} and second enters from H_{v_a} .

In this case, no matter what the landing speeds of the two aircraft are, and no matter what their descent profile is, there will be no conflict whatsoever. This is because the minimum longitudinal separation between the two aircraft in the IMS will occur over the OM. Figure 4.15 illustrates the point.

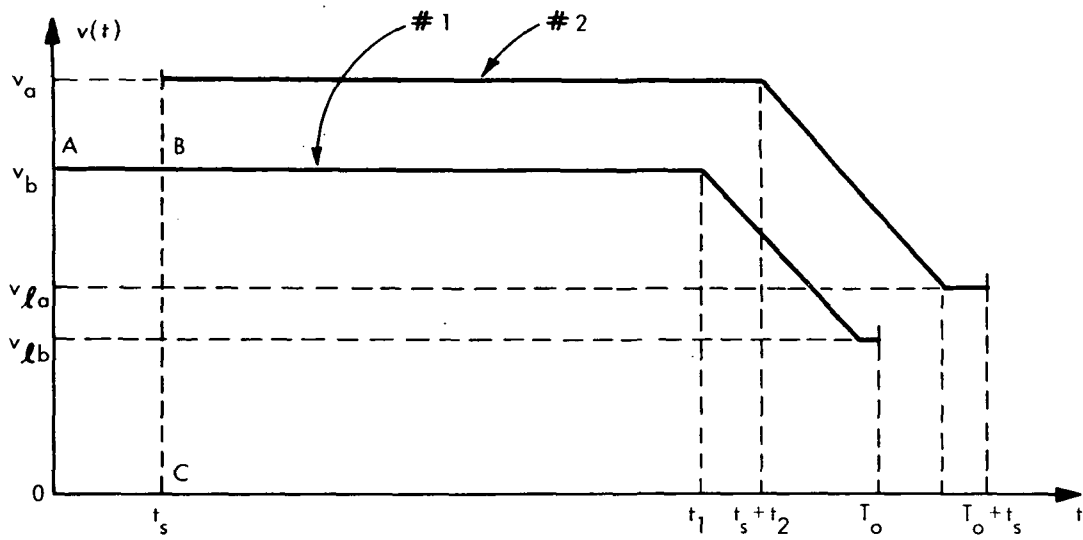


Fig. 4.15. Speed Profiles for Successive Aircraft Entering the IMS From Different Altitude Levels

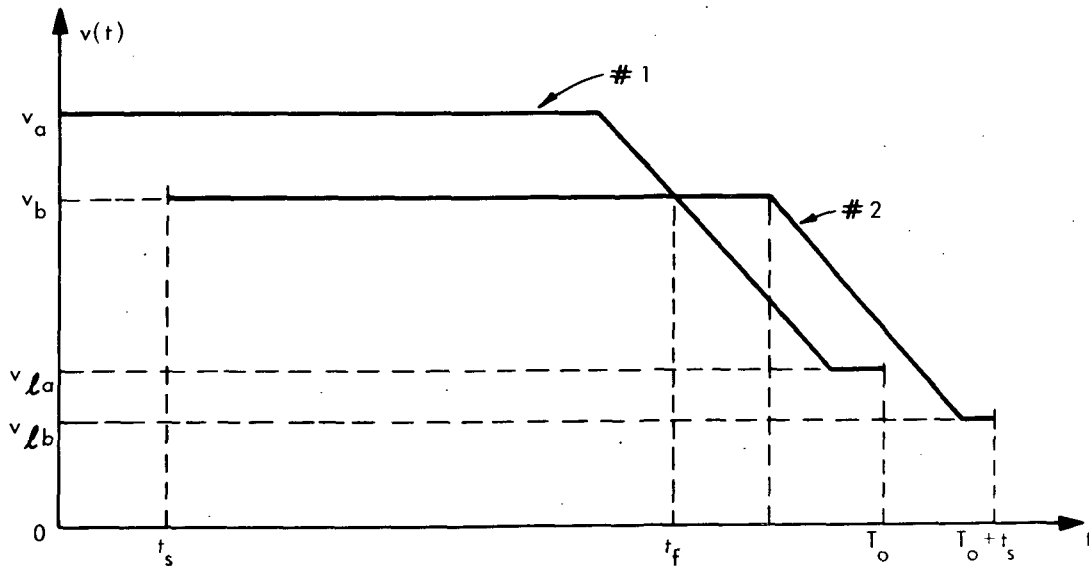


Fig. 4.16. Same Speed Profiles as in Fig. 4.15 with Entrance Order Reversed

The deeper reasons for this convenient result are embedded into the choices for the speed profiles and the lengths Lv_a and Lv_b . The initial longitudinal separation between the two aircraft is

$$d(0) = v_b t_s + (Lv_a - Lv_b) \quad (4.40)$$

The second aircraft is faster, and will be closing in behind the first one. However, Lv_a and Lv_b have been chosen so that the aircraft decelerations will occur close to the OM. That is why there is no longitudinal conflict.

- b) First aircraft enters the IMS from Hv_a and second enters from Hv_b .

In this case there is a problem of altitude separation. Figure 4.16 illustrates two typical speed profiles. The initial separation is

$$d(0) = v_a t_s - (Lv_a - Lv_b) \quad (4.41)$$

In general $d(0)$ given in (4.41) can be positive negative or zero, reflecting the fact that $Lv_a - Lv_b$ varies over a wide range with v_a and v_b (cf. table 4.3). Thus, if the altitude separation between the levels a and b is not large, then the danger of a near miss exists. We now present a method of choosing Hv so that no conflict will occur.

The case will be examined for $t_s = 1$ min. From the analysis of section 4.2.1 the above chosen t_s seems to be the smallest scheduled temporal separation between successive aircraft.

Assume that the highest altitude level is to carry traffic at speed $V_2 = 300$ knots. We would like to find the quantity $H_{V_2} - H_v$ where v is the speed of the next lower level.

First we examine the following problem. Given v the speed for the lower altitude level, and that the second aircraft enters the IMS from H_v t_s minutes after the first aircraft has entered the IMS from H_{V_2} , find the time t_{sf} after the entrance of the second aircraft, such that the longitudinal separation $d(t_{sf})$ between the two is safe (which will be assumed 2.5 n. miles), and the first aircraft is ahead. Since the minimum radius of the IMS is different for each altitude level, and depends on the speed each level "carries", we expect that for different values of v (i.e., different IMS radii), the initial longitudinal separation between the two successive aircraft can vary considerably depending on the difference $V_2 - v = \Delta v$.

We distinguish three cases

i) $d(0) \geq 2.5$ n. miles

From (4.41) we obtain

$$d(0) = V_2 t_s - (L_{V_2} - L_v) \quad (4.42)$$

or

$$d(0) = V_2 t_s - \left[\left(T_0 V_2 - \frac{(V_2 - v_{L1})^2}{2B} \right) - \left(T_0 v - \frac{(v - v_{L1})^2}{2B} \right) \right]$$

(4.43)

From (4.43), given T_0 , we can calculate the smallest v for which $d(0) \geq 2.5$ n. miles. Let us assume from now on that $T_0 = 10$ min. Then if we define

$\Delta v = V_2 - v$ we find that for $\Delta v \leq 26$ knots $d(0)$ is greater than or equal to 2.5 n. miles so that we don't have to worry about t_{sf} .

In other words, if the altitude level that lies below the top one "carries" traffic at a speed that is not much smaller than V_2 , then successive aircraft, entering the IMS from these levels, will never be dangerously close inside the IMS, no matter what the vertical distance between the two levels is.

$$\text{ii) } 0 \leq d(0) < 2.5 \text{ n. miles.}$$

In this case the first aircraft is ahead but not by enough. If the speed difference is Δv , t_{sf} is found by

$$t_{sf} = \frac{2.5 - d(0)}{\Delta v} \quad (4.44)$$

The condition $d(0) < 2.5$ indicates that $\Delta v > 26$ knots. The condition $d(0) \geq 0$ sets an upper bound on Δv via

$$t_s V_2 \geq T_o V_2 - \left[\frac{(V_2 - V_{L1})^2}{2B} \right] - \left[T_o v - \frac{(v - V_{L1})^2}{2B} \right] \quad (4.45)$$

from which we find that $\Delta v \leq 42$ knots.

What the above results signify is the following. If the next to the top altitude level "carries" traffic with speed v such that $26 \leq \Delta v = V_2 - v \leq 42$ knots, then at the time the second aircraft enters the IMS from its own altitude level, the first one is already ahead. However, it is ahead by a distance smaller than d_{min} , so some time t_{sf} elapses until safe longitudinal separation is established.

iii) $d(0) < 0$

This situation might occur if $\Delta v > 42$ knots. Then t_{sf} can be found by

$$t_{sf} = \frac{2.5-d(0)}{\Delta v}$$

The overall conclusions are that if the speed v is in the interval $[274,300]$ knots, then there is nothing to worry about with regard to conflicts. If $v \in [258,274]$ knots then some altitude separation between the aircraft at the time of entrance of the second one of them, must make up for violation of the longitudinal separation standard. If $v \in [200,258]$ then the same statement of the previous sentence holds with the addition that the altitude separation must exist for a longer period of time, because t_{sf} is now longer.

We are now equipped with the tools to make a decision about the magnitude of H_v . The philosophy is the following. The designer of the altitude levels is free to pick v . Once v is picked, then the following procedure is used to find H_v .

If $v \in [274,300]$ knots then the value of the smallest $H_{V_2} - H_v$ is constrained only by FAA standards of vertical separation. The present standards call for 1000 feet of minimum crossing altitude separation between aircraft. So if $v \in [274,300]$ knots the second altitude level can be just 1000 feet below the top one.

If $200 < v < 274$ knots then t_{sf} is calculated from eq. (4.44) and $H_{V_2} - H_v$ is chosen so that at time $t_s + t_{sf}$ the first aircraft, assuming that during all this time it is descending at the maximum rate

of λ , has reached the altitude level H_v (see fig. 4.17)

Analytically, this becomes

$$(t_s + t_{sf})\lambda = H_{V_2} - H_v \quad (4.46)$$

Typical values of $H_{V_2} - H_v$ are shown in table 4.4.

TABLE 4.4

Typical values of $H_{V_2} - H_v$

$t_s = 1$ min., $\lambda = 1000$ ft/min, $T_o = 10$ min.

v	t_{sf}	$H_{V_2} - H_v$
270 knots	1.9 min.	2900 feet
230 knots	5.15 min.	6150 feet
200 knots	6.0 min.	7000 feet

The above discussion and especially table 4.4 give a general rule of thumb for the choice of H_v . The rule is that the smaller Δv is chosen, the smaller one can pick $\Delta H = H_{V_2} - H_v$. To pick the third altitude level (if there is a desire to do so) just replace in the above procedure the value of V_2 by the speed of the second altitude level and repeat the steps. Thus the altitude levels can be chosen one after the

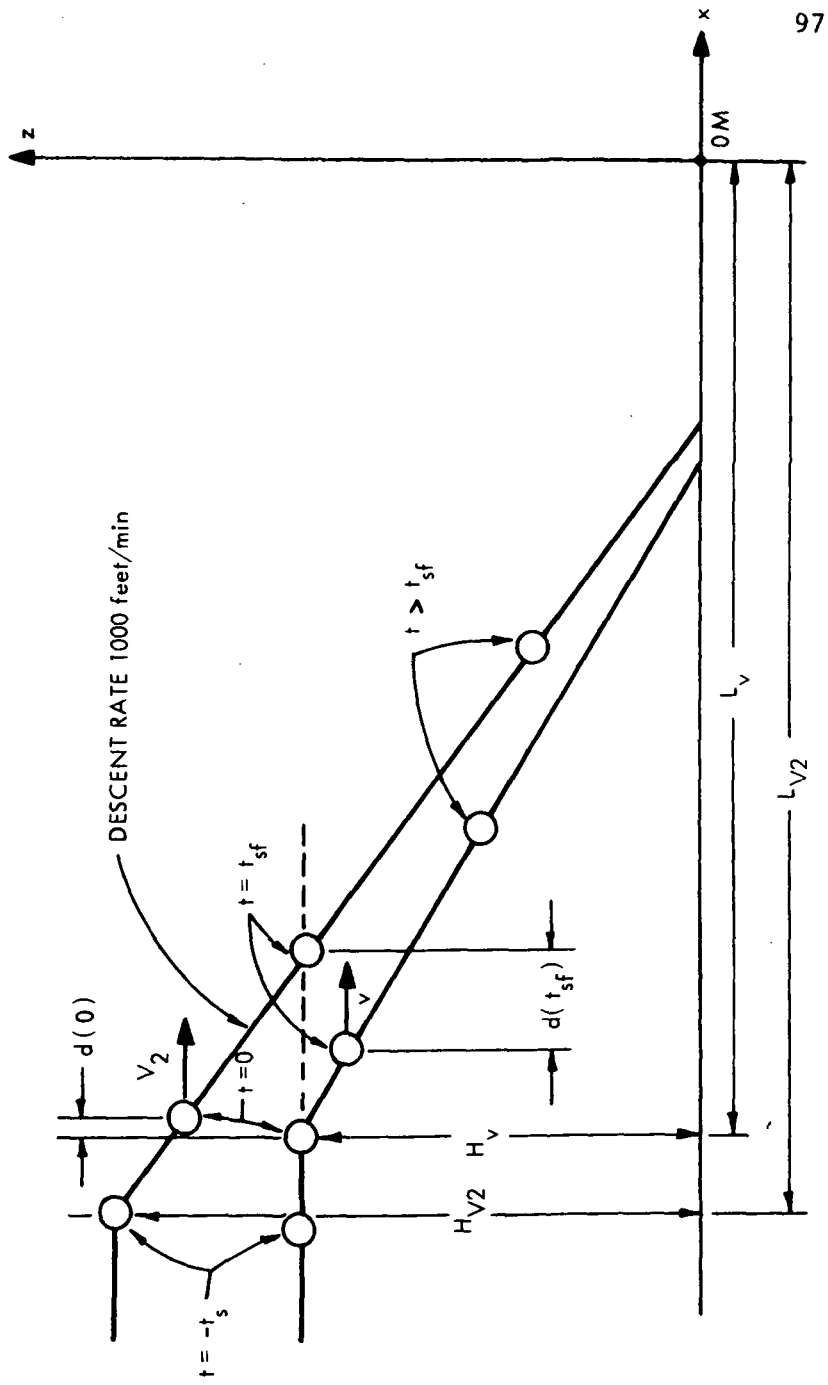


Fig. 4.17 Progress of Successive Aircraft Entering IMS from Adjacent Altitude Levels

other. It is seen again that with the procedure chosen the altitude levels will be located in such a way that no conflict will ever occur in the IMS. Finally we remark that there is nothing sacred about V_2 being the speed of the top altitude level. It could very well be some other one, but the concepts and the procedures would remain unchanged.

4.4 Length of OMS and Buffer Zone

So far in this chapter the IMS and the positions of the altitude levels were defined precisely. What remains to be considered is the length of the OMS and that of the BZ. In this section these lengths are picked for each altitude level in a way that suits the specific functions the OMS and the BZ are designed for.

4.4.1 The Traffic "Source Points"

In Chapter II it was mentioned that the delay maneuver, if any, of each aircraft will be initiated at some point along the straight portion of the minimum time trajectory. In Chapter III the different delay maneuvers were described. It was seen (cf. fig. 3.4) that the furthest an aircraft ever deviates from its straight trajectory, is when it executes the maximum oscillation maneuver. Then the excursion from the straight line is approximately $3.4 R$, where R is the minimum turn radius for the particular altitude level.

It is apparent that near misses should be avoided in the OMS. The most likely time a conflict might occur is when an aircraft is

executing a delay maneuver and another one's minimum time trajectory intersects or passes near the delay path.

We shall avoid this difficulty with two conventions. The first is that traffic is not to enter the NTA from any point of its circular boundary, but only from a number of points, to be called "Source Points", distributed on the boundary of the NTA.

The second convention is that delay maneuvers will not be initiated at any arbitrary point of the straight portion of the minimum time trajectory, but at points specified by the delay assignment algorithm, to be described in the next chapter. Here we shall only pick the source points.

Consider figure 4.18. The trajectories AEGO and BFHO represent the "worst" minimum time trajectories that can occur. We would like to arrange the distance (AB) between the source points A and B, so that the minimum distance between the two trajectories, which is (GH), is equal to $3.4 R + d_{\min}$. The reason for this particular value is the following. All aircraft whenever delayed, will be required to execute their delay maneuvers only on one side of their trajectory. Thus the closest we would like two trajectories to be is d_{\min} plus the maximum excursion from the straight line which was found in fig. 3.4 to be $3.4 R$.

The equations applicable are

$$(AB) = 2R_N \sin (\phi + \omega) \quad (4.47)$$

$$\sin \phi = \frac{R}{R_N - R} \quad (4.48)$$

$$\sin \omega = \frac{(GII)}{2L} = \frac{3.4R+d_{\min}}{2L} \quad (4.49)$$

A typical approximate value for (AB) for $v = 250$ knots, $d_{\min} = 2.5$ miles, $L \approx 39$ n. miles, $R_N \approx 70$ n. miles is $(AB) \approx 16.9$ n. miles or $\text{arc}(AB) \approx 17$ n. miles.

Thus if the traffic source points are chosen every 17 n.miles along the boundary of this NTA, it is guaranteed that no matter what the heading of the entering aircraft is and no matter what their delay maneuvers are, no violation of minimum separation standards will occur between aircraft entering the OMS from different source points.

In figure 4.19 a possible configuration for the fixed air routes that end at a source point is shown. These air routes are outside the NTA and will be of no concern to us. The convention of traffic source points will greatly simplify the delay assignment algorithm, described later.

4.4.2 The Length of the OMS

While inside the OMS each aircraft will be traversing all or part of the straight line portion of its minimum time trajectory. At some point of this straight trajectory it will be required to leave the nominal path and execute a delay maneuver.

The concept of "delay slots" is now introduced. This idea will help the delay assignment algorithm, and will contribute significantly in the maintenance of safe separations between successive aircraft.

A delay slot (fig. 4.20) will be defined to be a section of the pie shaped area defined by two source points and the OM, bounded by two circular arcs cocentric with the boundaries of the NTA and the IMS. If R_1 , R_2 are the radii of the outer and inner arcs respectively then

$$\ell = R_1 - R_2 = (\pi+2)R + d_{\min}. \quad (4.50)$$

The particular value of $R_1 - R_2$ chosen in (4.50) is such that there exists "room" in the delay slot for execution of any kind of delay maneuver. Since from eq. (3.22) the maximum "length" of a delay pattern is $(\pi+2)R$, and since we would like to keep delay patterns, executed inside longitudinally adjacent slots, at least d_{\min} apart, equation (4.50) follows.

Typical values for $R_1 - R_2$ are shown in table 4.5.

TABLE 4.5

Typical Delay Slot Lengths

v	R	$\ell = R_1 - R_2$
200 knots	.99 n. miles	7.64 n. miles
220 knots	1.19 n. miles	8.62 n. miles
250 knots	1.54 n. miles	9.41 n. miles
280 knots	1.75 n. miles	11.5 n. miles
300 knots	2.21 n. miles	13.87 n. miles

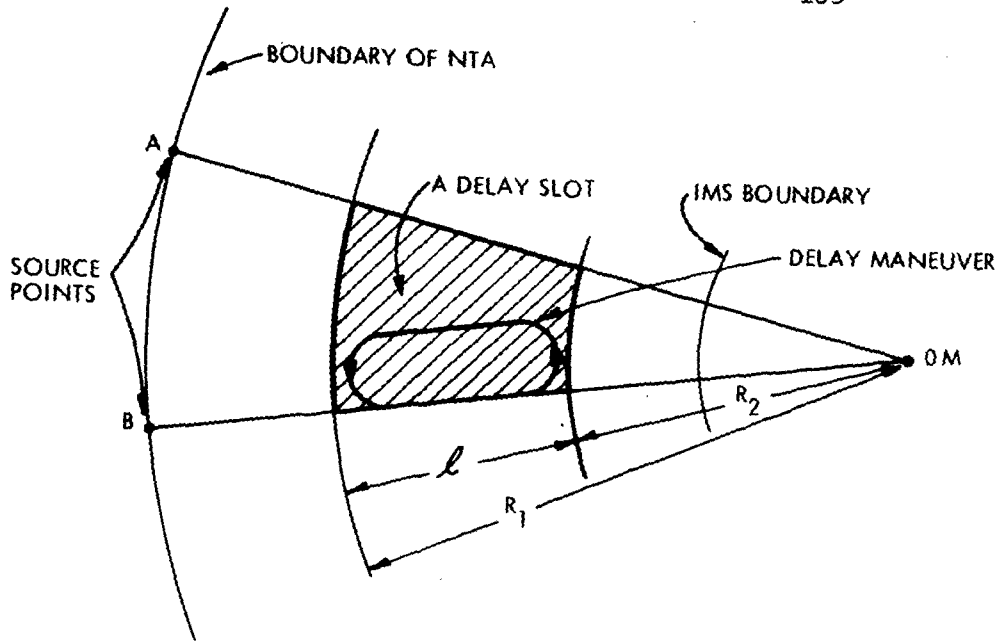


Fig. 4.20 Illustration of a Delay Slot

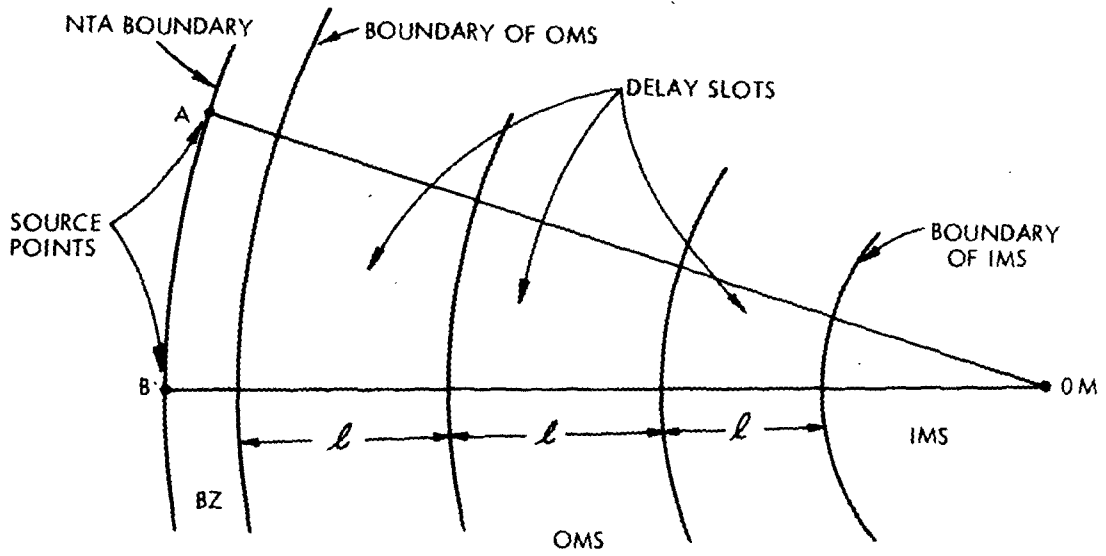


Fig. 4.21 Choice of the Length of OMS

Now the length of the OMS is chosen so that it can accommodate an integer multiple of delay slots (cf. fig. 4.21). The greater the number of slots that can be accommodated longitudinally inside the OMS is, the larger the number of aircraft that can be delayed simultaneously in separate slots (the details of the delaying process will be presented in Chapter IV). On the other hand, the longer the OMS is, the larger the NTA will be.

As an example consider an altitude level that carries traffic at 250 knots. Suppose that the length of the OMS is chosen to be two slots. From table 4.5 the length of the OMS is about 19 n. miles. From table 4.3 ($T_o = 10$ min) the radius of the IMS for this plane is about 39 n.miles. The length of the BZ will be shortly found to be of the order of 10 n.miles. Thus $R_n \approx 19 + 39 + 10 = 68$ n.miles. The length of the boundary of the NTA will thus be $2 R_n \approx 428$ n.miles. Consequently the boundary can accommodate at most $428/17 \approx 25$ source points. Since two delay slots are allowed for each source point, it is seen that at most fifty aircraft can be executing delay maneuvers simultaneously!

4.4.3 The Length of the Buffer Zone

The only thing that remains to be considered now, before it becomes clear how the NTA airspace is divided, is the length of the BZ.

As was mentioned in Chapter II the length of the BZ will be chosen in such a way, that an aircraft leaving this zone will have been scheduled, namely its expected time of arrival (ETA) will be known, and the amount of delay, if any, also known precisely. Thus, before we

consider the length of the BZ we shall consider the circumstances under which an aircraft entering the NTA some time after another, can still be scheduled to land ahead of the first one.

The concepts presented here will be thoroughly discussed when we describe the scheduling algorithm. Since, however, the geometry and the algorithms are closely related we must know some of the structure of the algorithms before the reasons for the choice of the particular geometry are understood.

Consider one altitude level. For aircraft entering the NTA at this particular level, a first-come-first-serve scheduling rule will be adopted. He who enters first, in other words, no matter what his entrance heading is, will land first.

Suppose an aircraft enters the NTA from one altitude level H_v . Suppose that the next aircraft to enter the NTA does so at a lower altitude level H_{v_1} ($v_1 < v$). The radius of the boundary of the NTA will be assumed to be the same for all altitude levels, contrary to the fact that the radii of the IMS and the OMS might not all be the same. This fact, coupled with the fact that $L_{v_1} < L_v$ (the radii of the IMS), shows that the minimum time trajectory of the aircraft at H_{v_1} will be longer than the trajectory of the first aircraft at H_v . Since $v_1 < v$, it is seen that the slower aircraft will travel a longer path, thus its ETA will be almost always greater than the ETA of the first aircraft.

This heuristic argument may not be very convincing; it will be presented more accurately later. However, the point to be made is

that the landing order of an aircraft flying at one altitude level, cannot be changed by an aircraft that enters the NTA subsequently and at a lower level. If, on the other hand, the aircraft to enter the NTA next, does so from a higher level, there is a chance that its ETA will be much smaller than the ETA of the first aircraft. So, although the aircraft on top entered second, it can still be scheduled ahead of an aircraft already inside the NTA.

Consider the top altitude level characterized by v . An aircraft entering the NTA at this level will be assigned landing order immediately. Since the aircraft flies on the top level, the policy will be that this order is final, i.e., it cannot be changed by an aircraft entering the NTA subsequently. Thus, the BZ can be very small. As a matter of fact, the only thing that limits the smallness of this BZ is the fact that there should be enough room so that an aircraft entering the NTA at the top level with any heading will enter the OMS only while it flies the straight portion of its minimum time trajectory.

The limiting situation is shown in figure 4.22. In this case

$$L_{BZ} = (AD) = R + (BD) = R + (BO) - (DO) = R + (BO) - (CO)$$

so

$$L_{BZ} = R + [R^2 + (L_{OMS} + L_v)^2]^{1/2} - L_{OMS} - L_v \quad (4.51)$$

The expression in (4.51) is in terms of the L_{OMS} and L_v which have already been chosen. Typical minimum values of L_{BZ} are

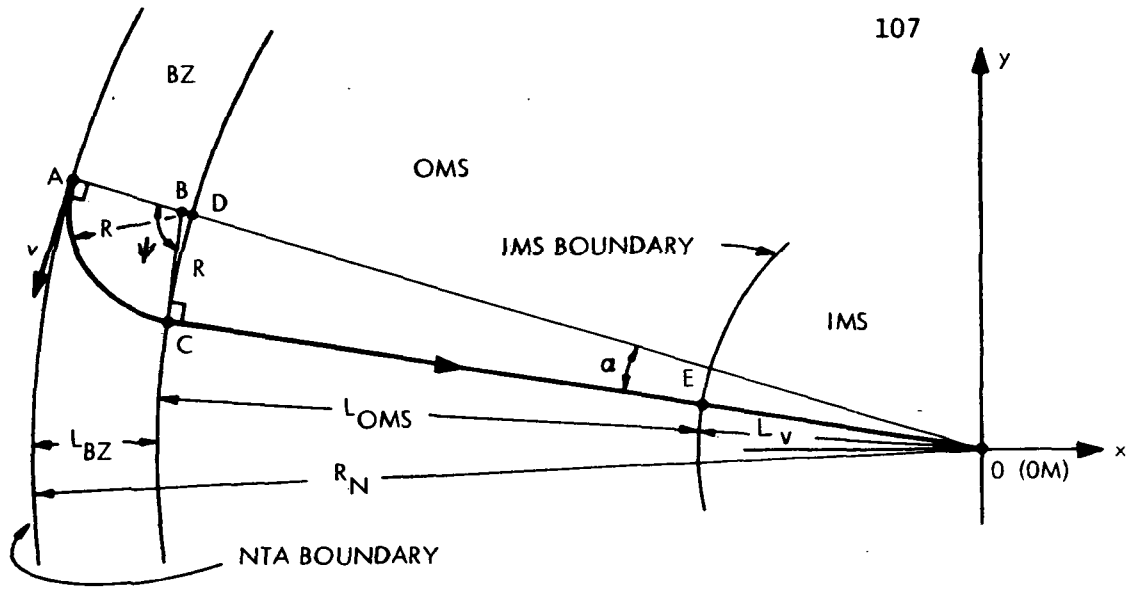


Fig. 4.22 Buffer Zone for Top Altitude Level

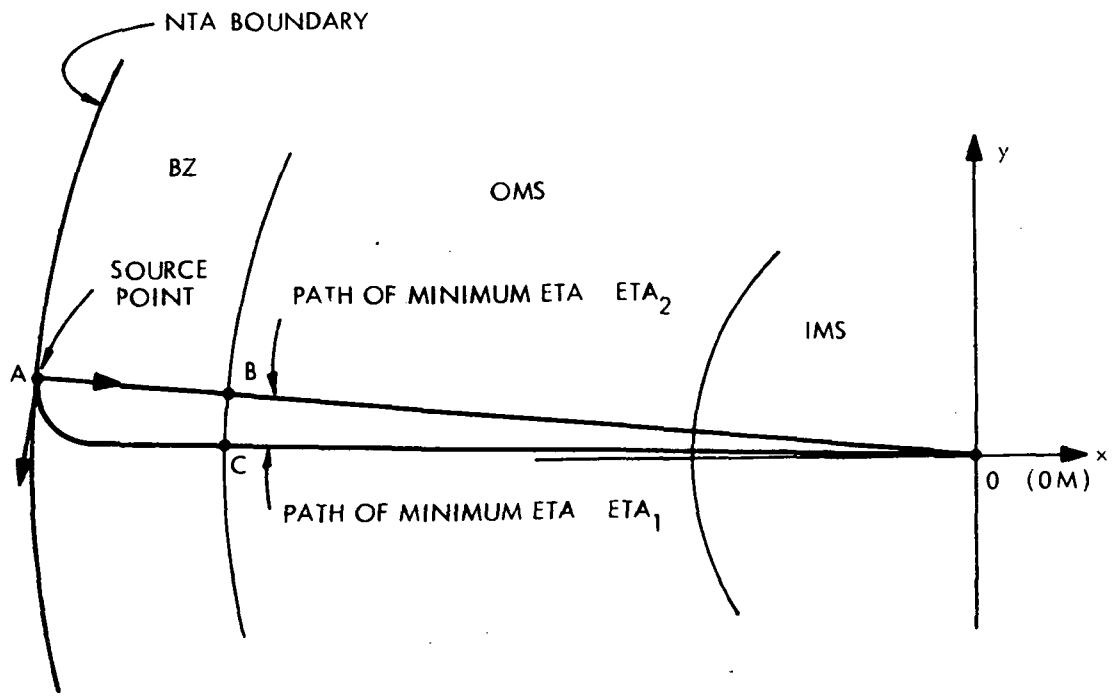


Fig. 4.23 Buffer Zone for a Lower Level

shown in table 4.6. Thus, if for example, the top altitude level is chosen to carry speed $v = 270$ knots, then, if we would like to have two delay slots in the OMS, the smallest possible radius of the NTA is, by table 4.6, 65.1 n. miles.

TABLE 4.6

Typical Minimum BZ Lengths for Top Altitude Level

v	R	L_{OMS} (2 Delay Slots)	L_v	L_{BZ}	NTA
200 knots	.99 n.m.	15.38 n.m.	31.91 n.m.	1 n.m.	48.3 n.m.
230 knots	1.30 n.m.	18.0 n.m.	35.96 n.m.	1.40 n.m.	55.4 n.m.
250 knots	1.54 n.m.	18.8 n.m.	39.0 n.m.	1.84 n.m.	59.64n.m.
270 knots	1.90 n.m.	22.0 n.m.	41.0 n.m.	2.10 n.m.	65.1 n.m.
300 knots	2.21 n.m.	27.75 n.m.	44.45 n.m.	2.55 n.m.	74.8 n.m.

Let us consider now the choice of the smallest BZ length for a lower level. Since the upper level has been defined completely, and since the NTA radius will be the same for all levels, the length $R_N - L_v$ is known for the lower altitude level.

Consider an aircraft entering this lower level at time $t = 0$, with heading tangential to the boundary of the NTA. Let immediately thereafter a second aircraft enter the NTA at the top level with radial heading. The ETA's of the two aircraft are found as follows:

$$ETA_2 = \frac{(R_N - L_{v_{top}})}{v_{top}} \quad (4.52)$$

From figure 4.22 we have

$$ETA_1 = \frac{\text{length (ACE)}}{v_{low}} \quad (4.53)$$

or

$$ETA_1 = \frac{1}{v_{low}} \left\{ \left(\frac{\pi}{2} + \sin^{-1} \frac{R_{low}}{R_N - R_{low}} \right) R_{low} + \sqrt{R_N^2 - 2R_{low}R_N} - L_{v_{low}} \right\} \quad (4.54)$$

Some thought should show that $ETA_1 > ETA_2$. So, the first to enter the NTA aircraft has ETA that is higher than the ETA of the aircraft that entered second. This is so because the second aircraft entered the NTA at a higher level and thus has speed at least as large as the speed of the first aircraft. Furthermore, the second aircraft has to travel a smaller distance till the IMS boundary.

The rule that will be adopted later for scheduling is that for a situation as described above it will not be always true that the aircraft with smaller ETA will land first. The only time the second aircraft will be allowed to land first will be when

$$ETA_1 - ETA_2 > \Delta t \quad (4.55)$$

where Δt is about 1 min. In other words, the second aircraft can supercede the first as long as by doing so it does not oblige the slower aircraft to execute a delay maneuver. The motivation and more discussion about this idea will be presented in chapter V.

What is of interest here is to find what is the maximum value of $ETA_1 - ETA_2$. The extreme situation is described by equations (4.52) and (4.53). We obtain $(ETA_1 - ETA_2)_{max} =$

$$= \frac{1}{v_{low}} \left\{ \left(\frac{\pi}{2} + \sin^{-1} \frac{R_{low}}{R_N - R_{low}} \right) R_{low} + \sqrt{R_N^2 - 2R_{low}R_N - L_{v_{low}}} \right\} - \frac{(R_N - L_{v_{top}})}{v_{top}} \quad (4.56)$$

Typical values of this quantity are shown in table 4.7.

TABLE 4.7

Typical Values of $(ETA_1 - ETA_2)_{max}$

v_{top}	v_{low}	R_N	R_{low}	$L_{v_{top}}$	$L_{v_{low}}$	$(ETA_1 - ETA_2)_{max}$
300 knots	270 knots	74.8n.m.	1.90n.m.	44.45n.m.	41.0n.m.	1.60 min.
300 knots	250 knots	74.8n.m.	1.54n.m.	44.45n.m.	39.0n.m.	2.74 min.
300 knots	230 knots	74.8n.m.	1.30n.m.	44.45n.m.	35.96nm.	4.00 min.
270 knots	250 knots	65.1n.m.	1.54n.m.	41.0n.m.	39.0n.m.	1.10 min.
270 knots	230 knots	65.1n.m.	1.30n.m.	41.0n.m.	35.96nm.	2.22 min.
270 knots	200 knots	65.1n.m.	.99n.m.	41.0n.m.	31.91nm.	4.67 min.

We are still not ready to find the minimum value of the BZ. First, let us evaluate $(ETA_1 - ETA_2)_{max}$ as given in equation (4.56) but for two aircraft in the same level. In other words, we calculate the maximum spread of ETA's for one level. We obtain

$$\begin{aligned} \Delta ETA_{v_{low}} &= (ETA_1 - ETA_2)_{\max(\text{same level})} = \\ &= \frac{1}{v_{low}} \left\{ \left(\frac{\pi}{2} + \sin^{-1} \frac{R_{low}}{R_N - R_{low}} \right) R_{low} + \sqrt{R_N^2 - 2R_{low}R_N - R_N} \right\} \quad (4.57) \end{aligned}$$

Typical values are shown in table 4.8. See figure 4.23 for definition of minimum and maximum ETA's for one level.

TABLE 4.8
Typical Values of $\Delta ETA_{v_{low}}$

v_{low}	R_N	$\Delta ETA_{v_{low}}$
300 knots	74.8 n. miles	.24 min.
270 knots	65.1 n. miles	.22 min.
250 knots	59.6 n. miles	.25 min.
200 knots	48.3 n. miles	.18 min.

The rule for choice of the minimum length of the BZ is

- 1) First find $(ETA_1 - ETA_2)_{\max} = \Delta ETA$ from equation (4.56).
- 2) Compare ΔETA to the quantity Δt of equation (4.55)
- 3) If $\Delta ETA \leq \Delta t$ then pick the minimum L_{BZ} for the lower level, the same exact way L_{BZ} for the top level was picked.
- 4) If $\Delta ETA > \Delta t$ but $\Delta ETA \leq \Delta t + \Delta ETA_{v_{low}}$ then pick $L_{BZ(\min)}$ exactly as in part 3).

- 5) If $\Delta\text{ETA} > \Delta t + \Delta\text{ETA}_{v_{\text{low}}}$ then pick $L_{\text{BZ}(\text{min})}$ by the equation

$$L_{\text{BZ}(\text{min})} = v_{\text{low}} (\Delta\text{ETA} - \Delta t - \Delta\text{ETA}_{v_{\text{low}}}) \quad (4.58)$$

This rule which might seem fuzzy now will become clearer after Chapter V. It is only a formal way of defining the BZ radius, so that there is no chance that an aircraft can lose its landing order after it has crossed the BZ.

The L_{BZ} found above was the minimum acceptable L_{BZ} . The number of delay slots for the OMS of the lower level can be picked now as follows. Given the R_N chosen for the top level pick N the number of delay slots for the lower level by the formula

$$N = \left[\frac{R_N - L_v - L_{\text{BZ}v}}{\lambda} \right] \quad (4.59)$$

where λ is given by eq. (4.49) and the brackets denote the "largest integer" function.

4.5 Conclusions

In this Chapter, the NTA airspace was described. The particular levels and radii involved were not chosen uniquely. Rather, tools were given with which a designer who is facing additional constraints for a particular airport, e.g., weather patterns, temperature variation throughout the year, etc., can choose the geometry of the NTA.

Once the concepts are understood the tradeoffs between different quantities become clear. For example, it is advantageous to have the top altitude level carry traffic of low speed because then the NTA can be chosen smaller. Also it is advantageous to design successive altitude levels to carry similar speeds, because then one can place these altitude levels very close together and still avoid violations of separation standards.

CHAPTER V
THE SYSTEM ALGORITHM

In this chapter we describe in detail the decision making algorithm of the proposed ATC system. The function of this ground-based facility is to assign to every aircraft that enters the NTA a precise flight plan. If the pilot follows the directions of the computer, he is ensured that during his approach to the airport he will encounter no conflicts from other traffic.

In section 5.1 the algorithm is described in block form. We also describe the functions the pilot executes while under the control of the ground computer. Subsequently, in section 5.2 the subroutines of the system algorithm are described in detail. Finally, in section 5.3 an informal discussion of the system's computational requirements is presented.

5.1 Functional Description of the Algorithm.

The ATC system described in this thesis uses the computer as the major decision element. In figure 5.1 the operations that occur while the pilot flies through the NTA are shown.

As soon as the pilot enters the NTA he radioes to ground the aircraft identification, his position, heading, time of entrance, speed v and landing speed v_L .

The computer accepts this information and establishes a "space" in memory where all calculations will be done. The machine then copies in that space the decision algorithm shown in figure 5.1. There are many of these working spaces in memory and each one "handles" one aircraft. The memory space becomes available after the aircraft enters the IMS and has started executing its IMS trajectory.

For the communication between the parts of the memory where different aircraft are handled we assume that there exists a table in memory to be called memory information table (MIT). This table contains all the geometrical constants of the NTA airspace and in addition keeps all the information about an aircraft that is of use when the need to serve a subsequent arrival arises. Figure 5.2 indicates a possible format of the table, which will always be in memory and will be updated when new aircraft enter the NTA or when some are close to the OM and thus out of the jurisdiction of the computer.

The algorithm now assigns to the newly entered aircraft an identification symbol. Next the number of aircraft still in the buffer zones of all altitude levels is determined and updated by one, to account for the new arrival. In order for the computer to know how many aircraft are in the BZ the pilots radio to ground the time they leave the BZ.

Next step is to automatically determine the expected time of arrival (ETA) of the aircraft to the OM, as well as the type of the minimum time trajectory (MTT) to be followed until the IMS

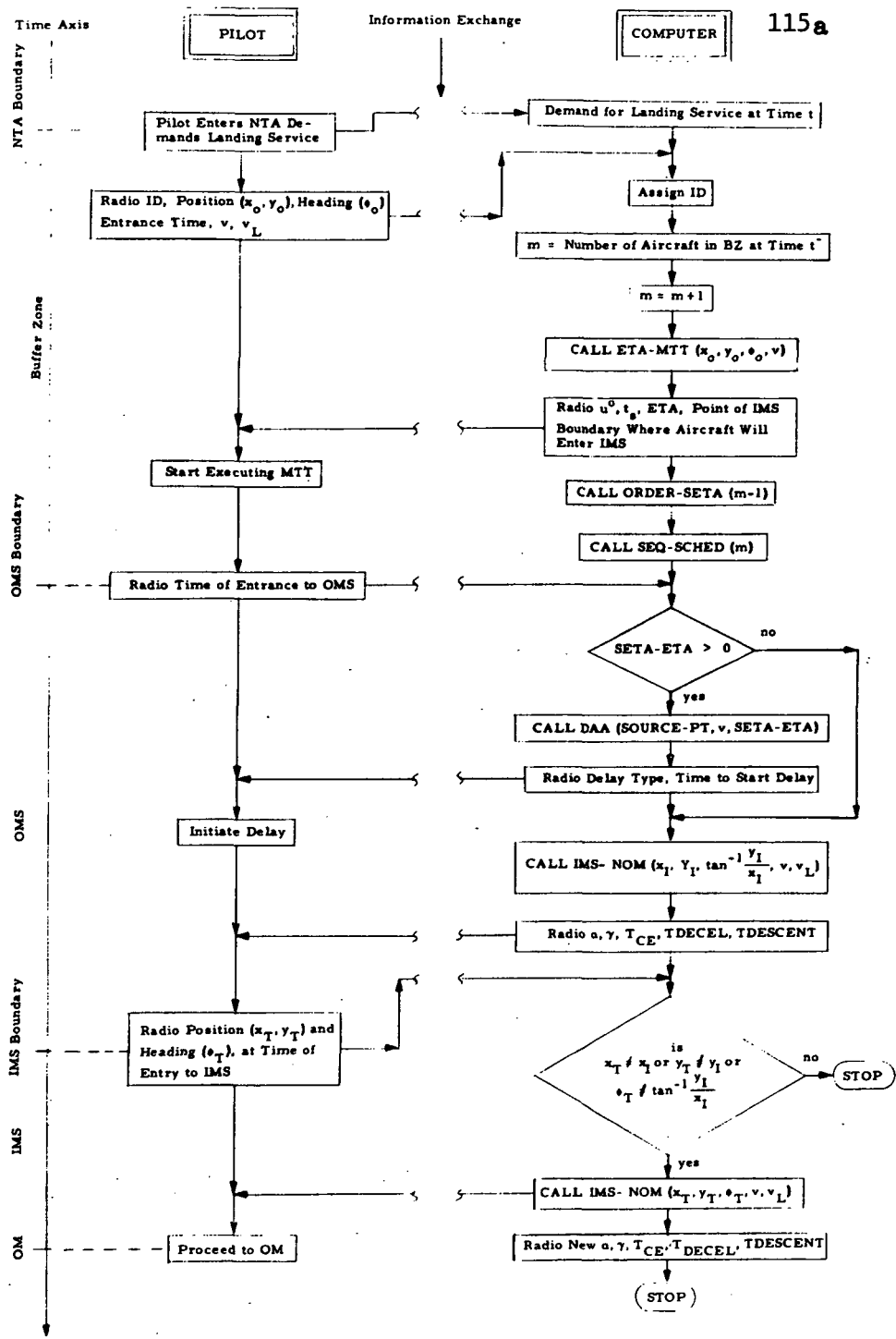


Fig. 5.1 The Man-Machine ATC System

System Constants
Table of Altitude Levels, Associated Speeds and Altitudes of Each One
Table of Co-ordinates of Traffic Source Points
Table of Radii of IMS, OMS and BZ for Each Level
Table of Number of Delay Slots in OMS of Each Level
T_o = Time to Cross IMS (Same for All Aircraft)
B = Maximum Deceleration Rate
λ = Maximum Descent Rate
$A = g/\sqrt{3}$ (g = accel. of gravity) = Maximum Value of Turn Rate in OMS
d_{min}
t_o = Minimum Runway Temporal Separation of Two Successive Landings
Δt_{tl} = Minimum Time Gap between Two Successive Arrivals, Large Enough for a Take-off to Take Place between the Landings
t_{tl} = Minimum Temporal Separation between a Landing Followed by a Take-off ($t_{tl} \leq \frac{\Delta t_{tl}}{2}$)

Aircraft ID	Source Point	Altitude Level	v	v_L	ETA
	Point of Entrance to IMS	SETA	Delay Type	Time to Start Delay	
	Angles of Turn-Straight-Turn IMS Trajectory				Speed Profile in IMS
	Time to Leave BZ				
Aircraft ID					

Fig. 5.2 Memory Information Table (MIT)

boundary. The system algorithm here calls the subroutine ETA-MTT which returns the control law u^o , as well as the switch time t_s , ETA, and the point of the IMS boundary where the MTT leads. This information is transmitted to the pilot who starts executing the maneuver.

The next function of the main algorithm is to sequence and schedule the aircraft. The first step of this process is to arrange the scheduled expected times of arrival (SETA's) of the $m-1$ aircraft already inside the BZ. This is done by calling the subroutine ORDER-SETA which arranges that $SETA(ID(1)) < SETA(ID(2)) \dots < SETA(ID(m-1))$.

The SETA of the new aircraft is now found by calling the subroutine SEQ-SCHED. This subroutine compares the ETA of the new aircraft with the ETA's (not SETA's) of all other aircraft and according to a rule, to be described shortly, arranges the landing order of the new aircraft and computes its SETA. The SETA's of the other aircraft might be changed in the process.

Once the aircraft enters the OMS its SETA cannot be changed. If $SETA > ETA$ then the aircraft must be delayed while inside the OMS. The delay assignment algorithm (DAA) is then called. This subroutine calls at first the subroutine DELAY-TYPE which returns the type of delay maneuver to be performed. Then the DAA assigns to the new aircraft a delay slot where the delay maneuver will be performed, and computes the exact time when the aircraft should leave the straight flight and go into the delay path. The type of delay maneuver and the time to start it are radioed to the pilot.

The flight plan so far calculated, calls for arrival at the IMS boundary at time $SETA - T_0$. The point at which the aircraft is supposed to enter the IMS is also known. With this information the subroutine IMS-NOM is called to calculate the magnitudes of the turns in the turn-straight-turn trajectory, which will be followed inside the IMS (see Chapter III). The same routine calculates the speed profile of the aircraft inside the IMS. This speed profile is such that the deceleration is delayed until the very end, as discussed in Chapter IV. In addition, the latest time to start descending is also calculated by the same routine.

The magnitudes of the angles, the time of the straight flight T_{CE} , the time to start decelerating T_{DECEL} , as well as the latest time to start the descent are transmitted to the pilot, while he still flies inside the OMS.

As soon as the pilot enters the IMS he again radioes to ground his position and heading. If these are different from the ones, from which IMS-NOM derived the flight plan for the IMS, then this same subroutine is called again to provide new values of the turn angles, T_{CE} , T_{DECEL} and $T_{DESCENT}$.

After the transmission of this last information, automatic control stops. Thus the space in computer memory, which was reserved for calculations associated with the aircraft that just entered the IMS, can be erased and made available for the calculation of the flight plan of a new arrival to the NTA.

5.2 System Subroutines

In this section the subroutines that the system algorithm calls are described in detail. The order of presentation is same as the order they appear in fig. 5.1.

5.2.1 The Subroutine ETA-MTT

The flow chart for this routine is shown in fig. 5.3. The inputs are the position (x_0, y_0), heading (ϕ_0), and speed (v) of the aircraft at the time it enters the NTA.

The subroutine calculates the control law u^0 , ETA, t_g , and point at which the MTT crosses the IMS boundary, via equation (3.9)-(3.17) which are repeated in the flow chart.

5.2.2 The Subroutine ORDER-SETA

The flow chart for this subroutine is shown in fig. 5.4. The input to this routine is a number of aircraft. We assume that in essence the subroutine accepts as input the ID's of a certain number of aircraft, and arranges their SETA's in increasing order of magnitude. Thus, after the subroutine completes its cycle, the "first" aircraft is the one with smallest SETA.

5.2.3 The Subroutine SEQ-SCHED

This subroutine is an important one. It does the sequencing and scheduling for each new arrival. Its flow chart is shown in fig. 5.5.

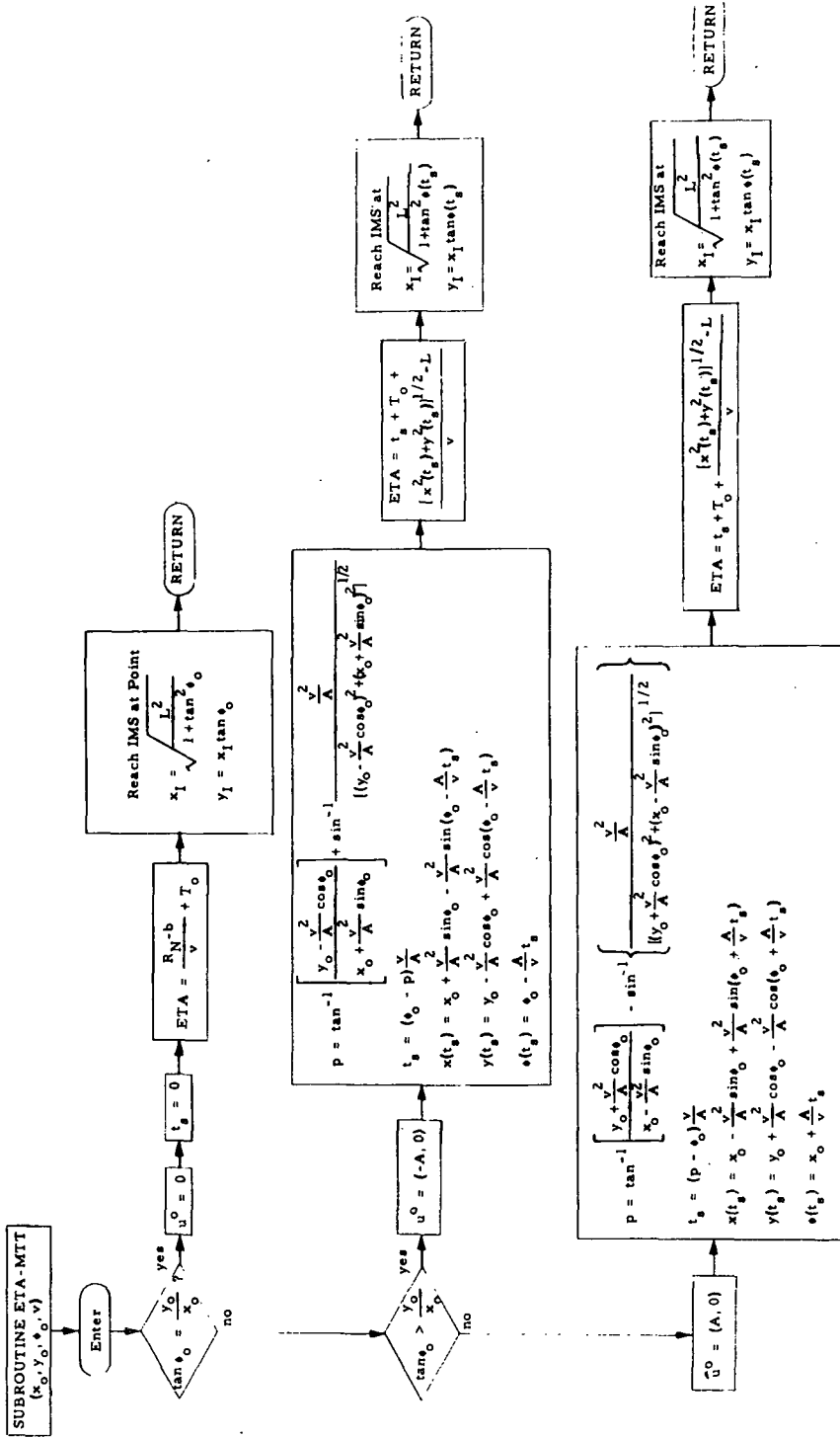


Fig. 5.3 Flow Chart for Subroutine ETA-MTT

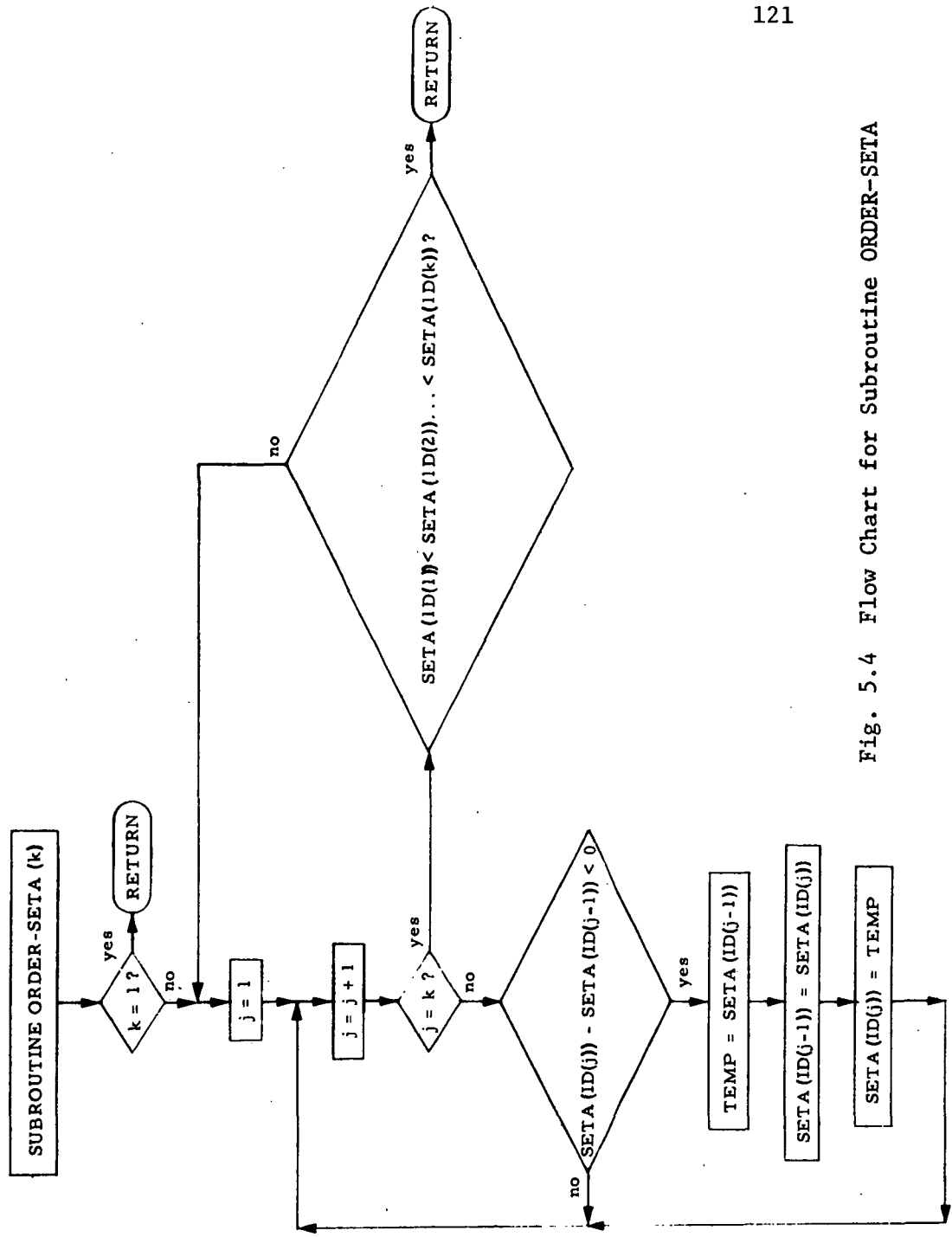
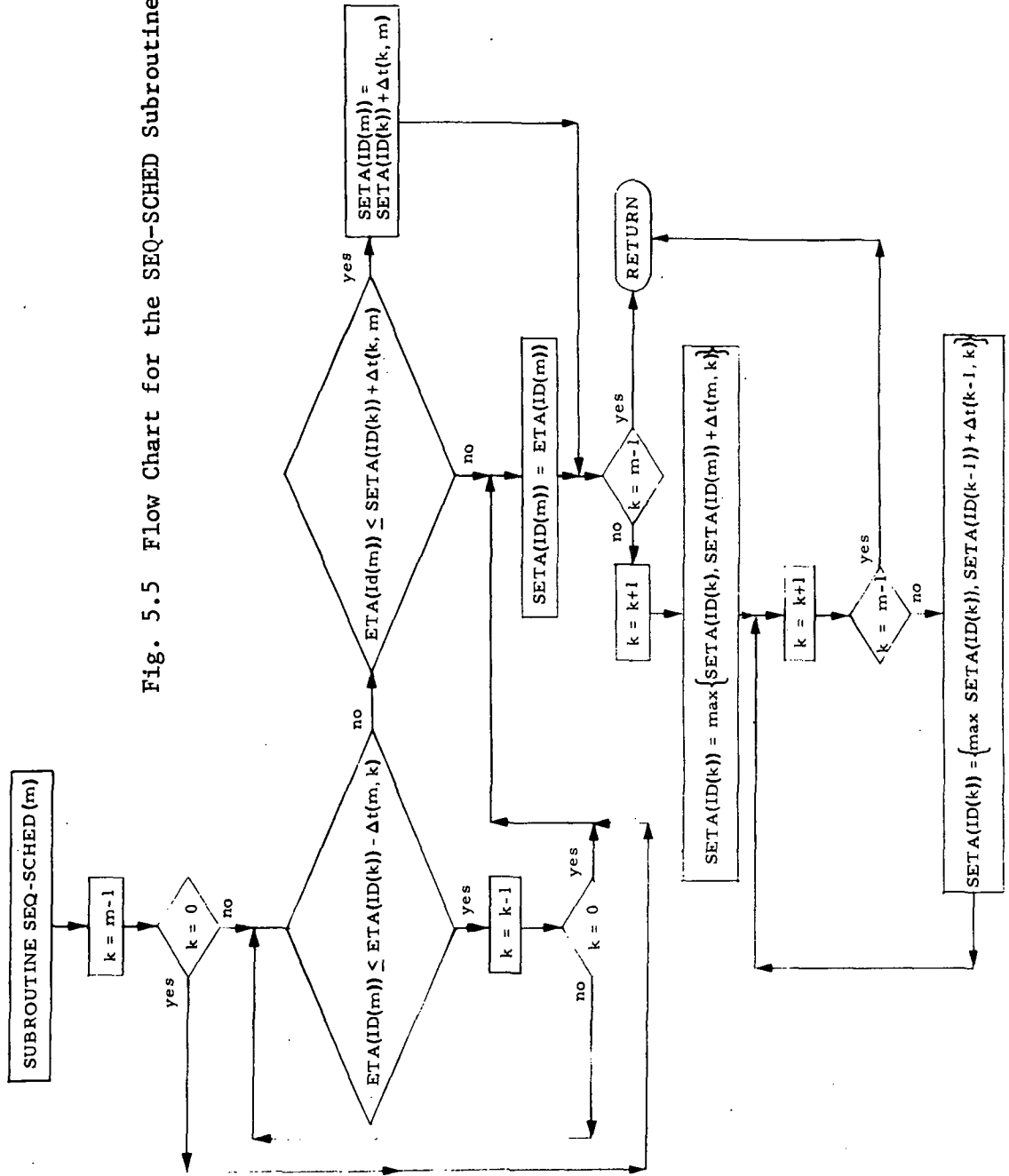
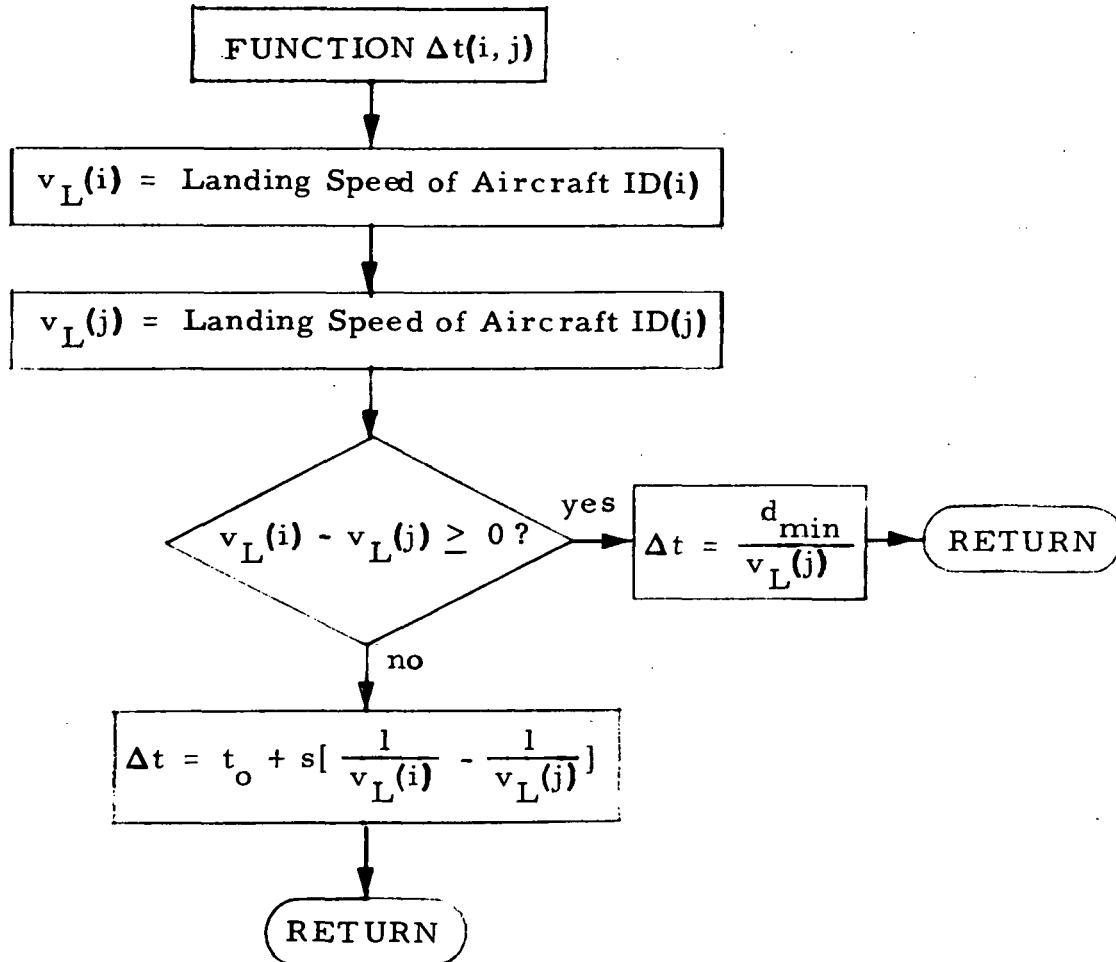


Fig. 5.4 Flow Chart for Subroutine ORDER-SETA

Fig. 5.5 Flow Chart for the SEQ-SCHED Subroutine



Fig. 5.6 Flow Chart for the Function Δt

The inputs are the ID's for the aircraft that are inside the BZ. The task is to assign a SETA to the last aircraft.

The rule by which landing order is assigned is not according to increasing ETA. As was seen in section 4.4.3, in order that an aircraft, with entry order to the NTA, larger than the entry order of another aircraft, be assigned smaller landing order, it is necessary that $ETA(ID(m)) < ETA(ID(m-n))$, where m and $m-n$ denote entry order. However, the above condition is not sufficient.

The sufficient condition is found as follows.

a) Calculate the minimum allowable temporal separation over the OM, between the m 'th and $m-n$ 'th aircraft, via equation (4.32) or (4.33) depending on whether $v_L(m) \geq v_L(m-n)$ or $v_L(m) < v_L(m-n)$ respectively. Call this time $\Delta t(m,m-n)$ (The flow chart for the exact calculation of Δt is shown in figure 5.6)

b) If $ETA(ID(m)) \leq ETA(ID(m-n)) - \Delta t(m,m-n)$ then allow the m 'th aircraft to supersede the $m-n$ 'th one in landing order.

c) If $ETA(ID(m)) > ETA(ID(m-n)) - \Delta t(m,m-n)$ then the m 'th aircraft will land after the $(m-n)$ 'th.

The motivation behind such a rule is that the NTA geometry is such that aircraft flying the higher altitude levels, tend to have smaller ETA's. This is so because they fly at higher speeds, and have to travel smaller distances to reach the IMS. If strict ordering of ETA's was the sequencing rule, there would be a tendency by pilots to crowd the top levels, where they would get fast service. The rule just stated tries to alleviate this problem.

Now that sequencing is finished the SEQ-SCHED subroutine schedules the new aircraft, namely computes its SETA as follows:

a) If the new aircraft has not superceded any other one in landing order, then its SETA will be either Δt seconds greater than the SETA of the aircraft scheduled to land just before the new one, or equal to its ETA. The decision depends on how large the ETA of the new aircraft is, as shown in fig. 5.5.

b) If the new aircraft has superceded in landing order some aircraft then its SETA is assigned as in part (a). However, now there might be a need to reschedule the aircraft that have been surpassed.

The rescheduling rule is

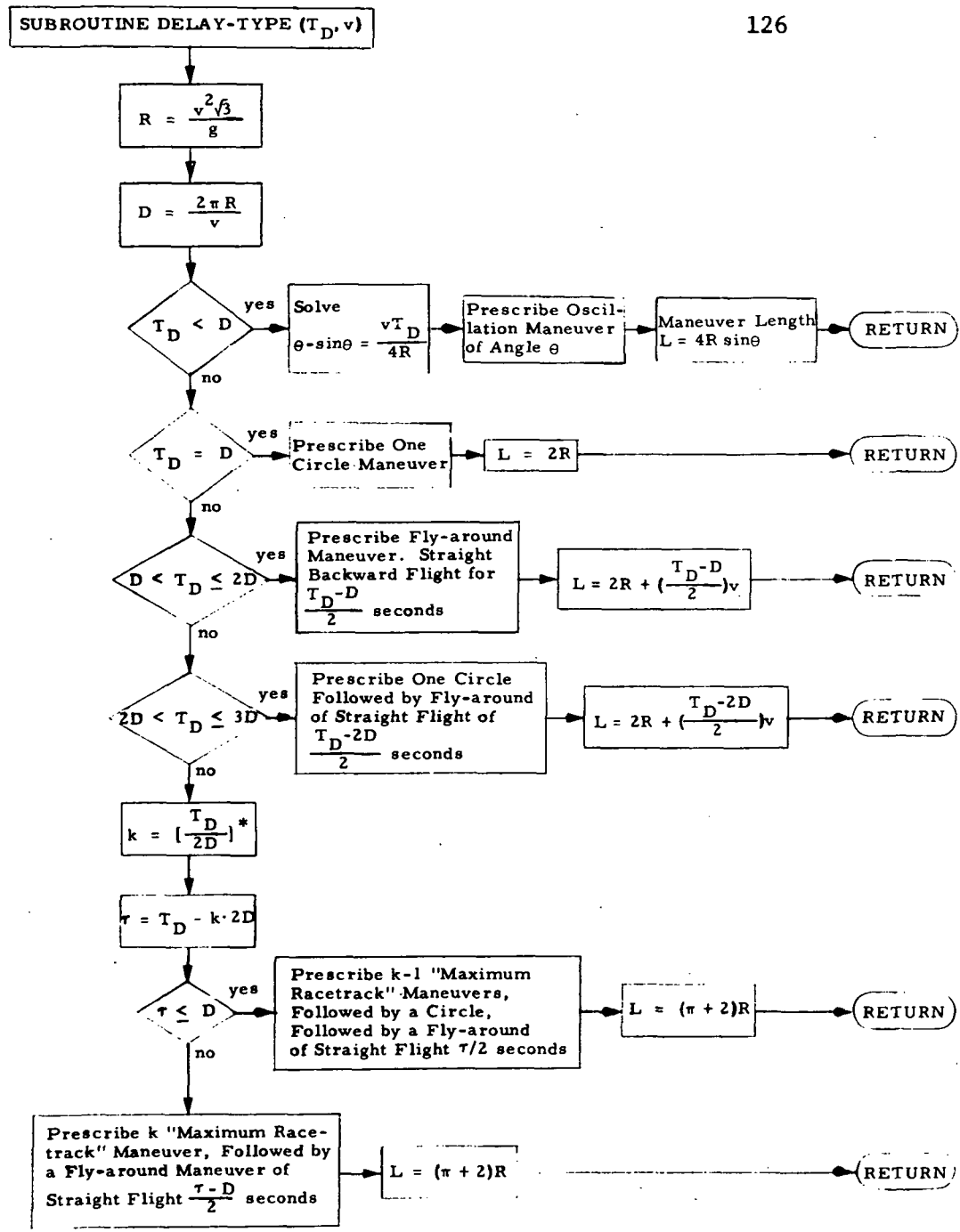
$$\text{SETA}(\text{ID}(k)) = \max \left\{ \text{SETA}(\text{ID}(k)), \text{SETA}(\text{ID}(k-1)) + \Delta t(k-1, k) \right\} \quad (5.1)$$

This rule merely says that if the SETA's of the aircraft that must be rescheduled are close to each other, then these SETA's will be increased, otherwise they will remain unchanged.

5.2.4 The Subroutine DELAY-TYPE

Before we describe the delay assignment algorithm (DAA) we shall describe the subroutine DELAY-TYPE...

The flow chart for DELAY-TYPE is shown in fig. 5.7. The routine accepts as inputs the time T_D , by which the aircraft is to be delayed, and its speed v . Then it calculates, via the rules described in section 3.2, the type of maneuver which will effect the desired delay, and the length of the delay maneuver (see fig. 5.10)



* $\lfloor \frac{T_D}{2D} \rfloor$ denotes the "largest integer" function.

Fig. 5.7 Flow Chart for the Subroutine DELAY-TYPE

5.2.5 The Subroutine DAA

This is another important subroutine. Its purpose is to define a point during the time the aircraft is flying inside the OMS, namely in a straight line, at which the aircraft can start its delay maneuver, if any.

The reason for which a systematic delay assignment procedure is defined is that the holding stacks are eliminated from our system. Consequently, the aircraft must be delayed somewhere else. If we do not define precisely a delaying procedure then there is a chance that two aircraft which enter the NTA from the same source point come very close together while they are performing delay maneuvers. This is possible because if there is no interference from other aircraft, the delay maneuver can be initiated at any point of the straight part of the trajectory. Thus, the first pilot might start delaying at some point while the other pilot might want to wait until he is closer to the OM to initiate his delay. The situation is pictured in figure 5.9.

The delay assignment algorithm (DAA) mainly consists of assigning to each aircraft that has to perform a delay maneuver, a delay slot in which to do it. Furthermore, the kind of delay maneuver is dictated, and the latest time the aircraft can start on its delay path and still finish inside the delay slot, is prescribed. Let us go through the procedure in detail (see fig. 5.8)

The routine accepts as inputs the source point from which the aircraft entered the NTA, the speed v of the particular altitude level, and the amount of delay that the aircraft has been assigned

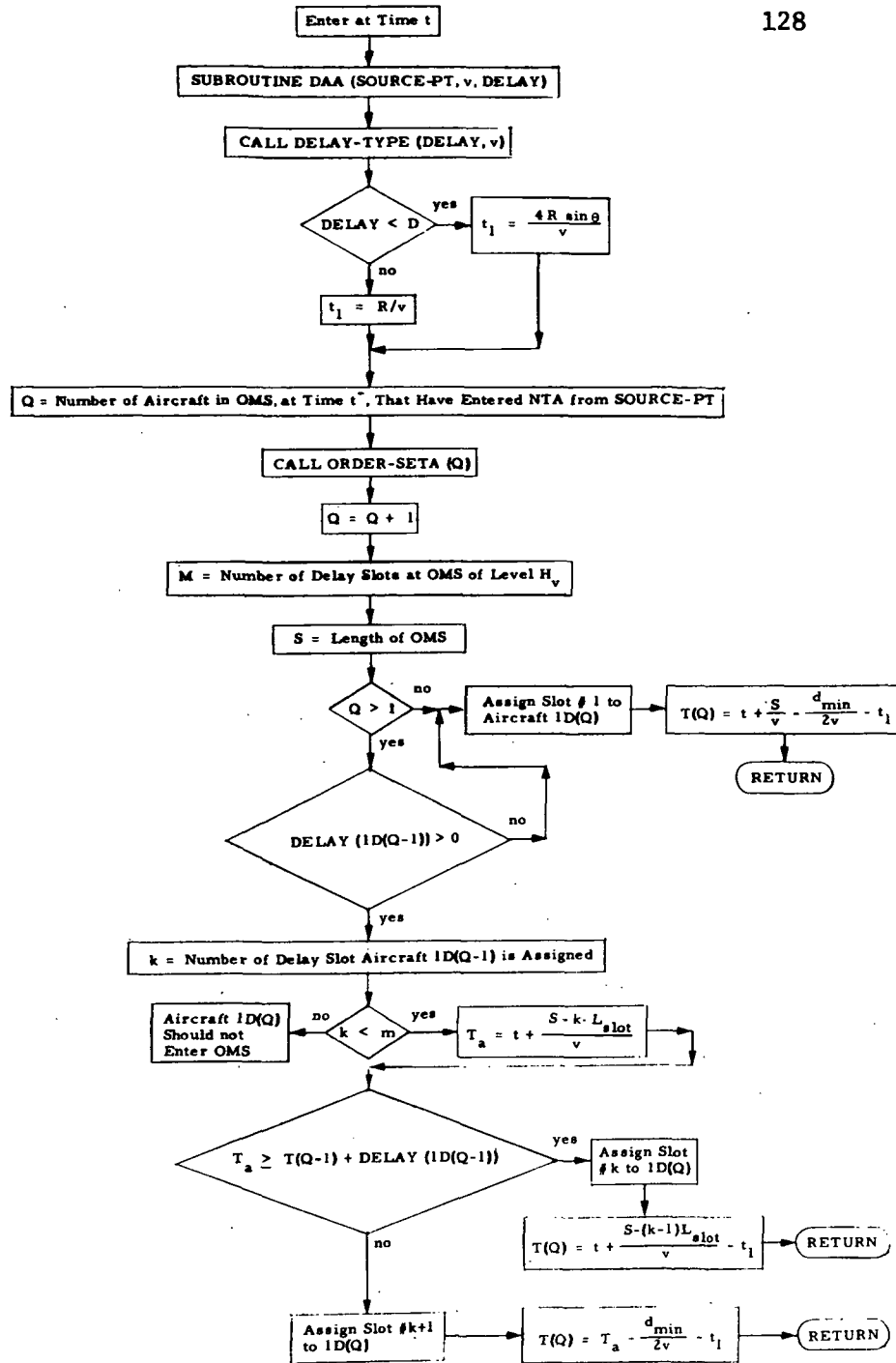


Fig. 5.8 Flow Chart for the Subroutine DAA

by the SEQ-SCHED subroutine.

At first the subroutine DELAY-TYPE is called and thus the kind of delay maneuver is "learned."

If no other aircraft that have entered the NTA at the same source point are presently in the OMS, then the DAA assigns to the aircraft under consideration, the delay slot that is closest to the IMS (the first one). It subsequently computes the latest time $T(Q)$ the aircraft should start its delay maneuver, so that the whole delay path is safely inside the delay slot. The point is illustrated in figure 5.11. The time $T(Q)$, as well as the delay maneuver are returned to the main program (whence they are radioed to the pilot).

If there is another aircraft ahead of the one considered, the DAA questions whether the aircraft ahead is to be delayed. If not then the present aircraft is assigned to the first slot as prescribed above. If yes then the DAA calculates the time T_a it will take the new aircraft to reach the beginning of the delay slot, where the aircraft ahead is performing or about to perform its delay maneuver. Then T_a is compared to the time $T(Q-1) + \text{DELAY}(\text{ID}(Q-1))$ by which the aircraft ahead will have completed its delay. If T_a is larger then the new aircraft will reach the slot of the previous aircraft after the latter has completed its delay maneuver, so the new aircraft can be assigned to that delay slot. If T_a is smaller then the new aircraft is assigned to the next closest to the OM slot.

The DAA in other words allows each aircraft to use a delay slot and be "undisturbed" while it is executing the delay maneuver

The only point that deserves further discussion is the block labelled "Aircraft ID(Q) should not enter OMS". The significance of this block is that it signals that all the delay slots are "occupied". In such a case no more aircraft should be delivered to the source point thus flagged.

Since there are many source points at each altitude level, and many levels, it should be clear that saturation is highly unlikely. However, it is possible.

The only way to alleviate the problem is by metering, namely feeding every source point from the air routes outside the NTA, with a limited number of aircraft per hour. This number would depend on the number of slots and average delay per aircraft. Notice that if no aircraft is delayed or if the delays are very small, a traffic source point can accommodate as many aircraft as it is fed, the limit being dictated by the safe separation standards.

5.2.6 The Subroutine IMS-NOM

This subroutine accepts as inputs some position coordinates (x,y) , a heading (ϕ) and the speeds v and v_L with which the aircraft enters the IMS and lands respectively. The task is to compute the magnitudes of the turns α and γ (cf fig. 3.9) and the length of the straight path (CE) of the turn-straight-turn trajectory that is to be followed inside the IMS. Also the subroutine is to compute the point in time TDECEL at which the aircraft should start decelerating and the latest time TDESCENT at which the pilot can start descending. These last

two points are illustrated in figures 5.13 and 5.14.

The flow chart for the subroutine is shown in figure 5.12. The calculation of α , γ and (CE) is done according to equations (3.23)-(3.33) of section 3.3. Subsequently the computer calculates the time that is available to the aircraft to travel the straight part (CE) of the LMS trajectory via

$$T_{CE} = T_0 - \frac{\alpha R_1}{v} - \frac{\gamma R_2}{v_L} \quad (\text{cf. eq. (3.35)})$$

The nominal speed profile for the straight path is now calculated via the equation

$$(v - v_L) t_1 + T_{CE} v_L + \frac{(v - v_L)^2}{2B} = (\text{CE}) \quad (5.2)$$

(also cf. eq. (4.37)) from which we obtain

$$t_1 = \frac{(\text{CE})}{v - v_L} - \frac{T_{CE} v_L}{v - v_L} - \frac{(v - v_L)^2}{2B} \quad (5.3)$$

Thus the real time at which the aircraft should start decelerating is

$$T_{DECEL} = \text{SETA} - T_0 + \frac{\alpha R_1}{v} + t_1 \quad (5.4)$$

The time $\text{SETA} - T_0 + \frac{\alpha R_1}{v}$ is the real time at which the aircraft is scheduled to start on the straight part of the LMS trajectory.

This type of speed profile, illustrated in figure 5.13, delays the deceleration until the very end. In this way as was analyzed in Chapter IV conflicts are avoided.

Next, the subroutine computes the latest time $T_{DESCENT}$ the

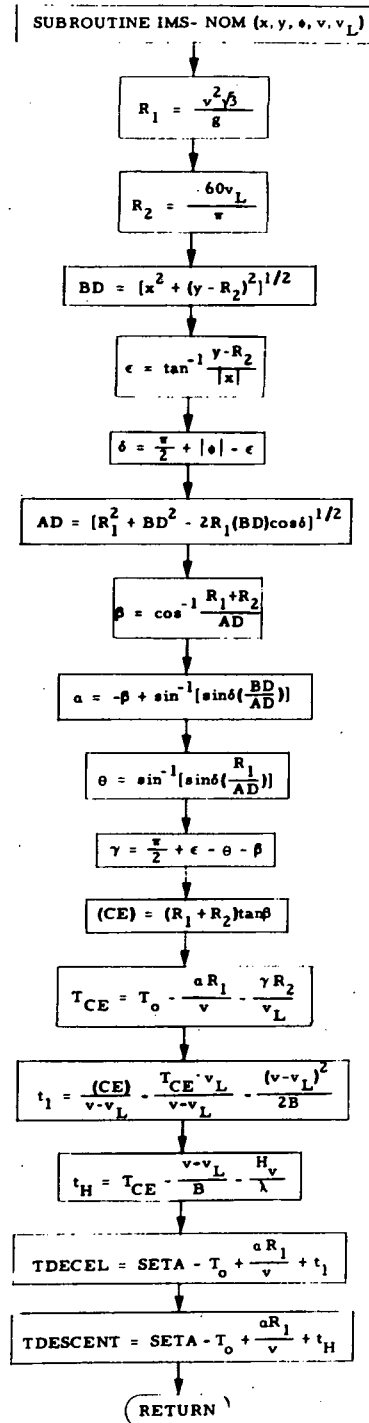


Fig. 5.12 Flow Chart for Subroutine IMS-NOM

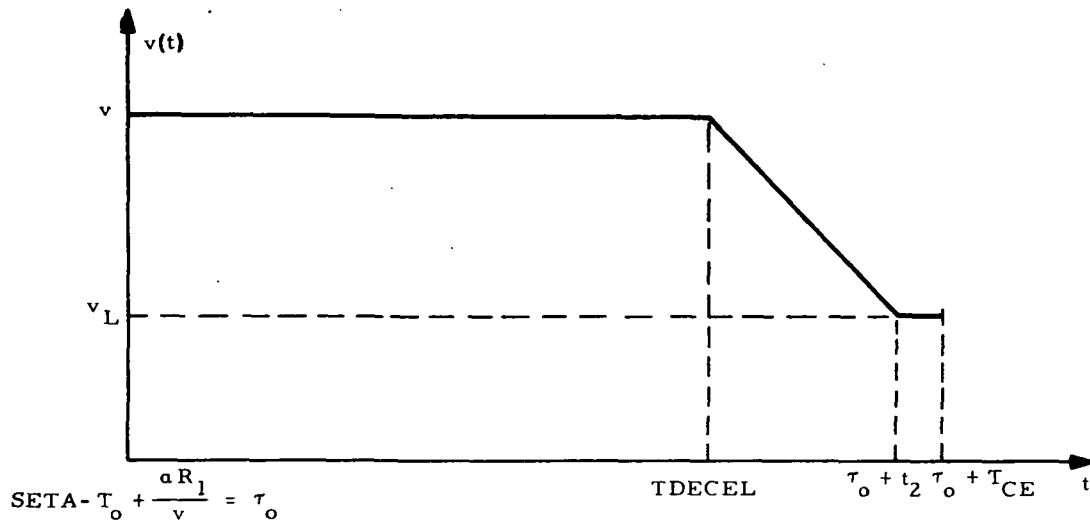


Fig. 5.13 Nominal Speed Profile Along the Straight Part (CE) of the IMS Trajectory

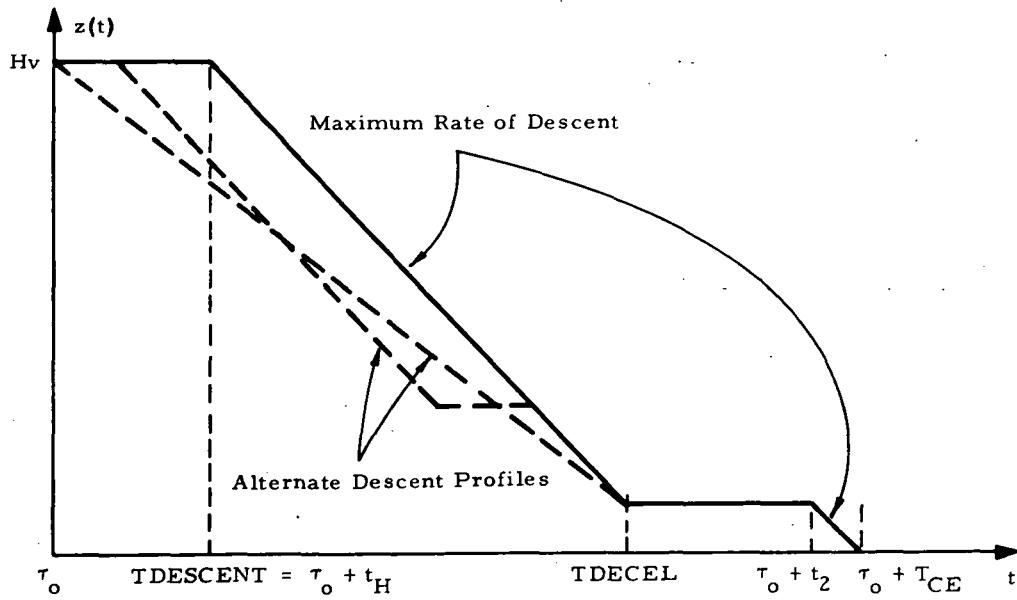


Fig. 5.14 Latest Time to Start Descent in the IMS

aircraft should start descending, if it is to reach the level of the OM within the specified time limits, without descending with rate greater than 1000 ft/min. At first the amount t_H of "flexibility" for descent is calculated via

$$t_H = T_{CE} - \frac{v - v_L}{B} - \frac{H}{\lambda} \quad (5.5)$$

What t_H signifies, is that the pilot does not have to start descending at TDESCENT. He has the option to start descending as early as TDESCENT - t_H . In figure 5.14 some alternate acceptable descent profiles are illustrated.

TDESCENT can now be calculated via

$$TDESCENT = (SETA - T_o + \frac{\alpha R_1}{v}) + t_H \quad (5.6)$$

5.2.7 The Subroutine SCHED-TAKEOFF

This subroutine whose flow chart is illustrated in fig. 5.15 does not appear anywhere in the flow chart for the ATC landing monitor of fig. 5.1. The reason is that this routine is independent of the algorithm for landing, although it uses some of the same subroutines. It has nevertheless, access to the MIT of fig. 5.2.

This subroutine is called when there is demand for a take-off at time t' . It calculates the earliest time that clearance can be given for take-off. This time is called ETTO (for Expected Time of Take-Off).

Since the SETA's of the aircraft that are already inside the OMS and IMS cannot be changed, the first task of SCHED-TAKEOFF is to

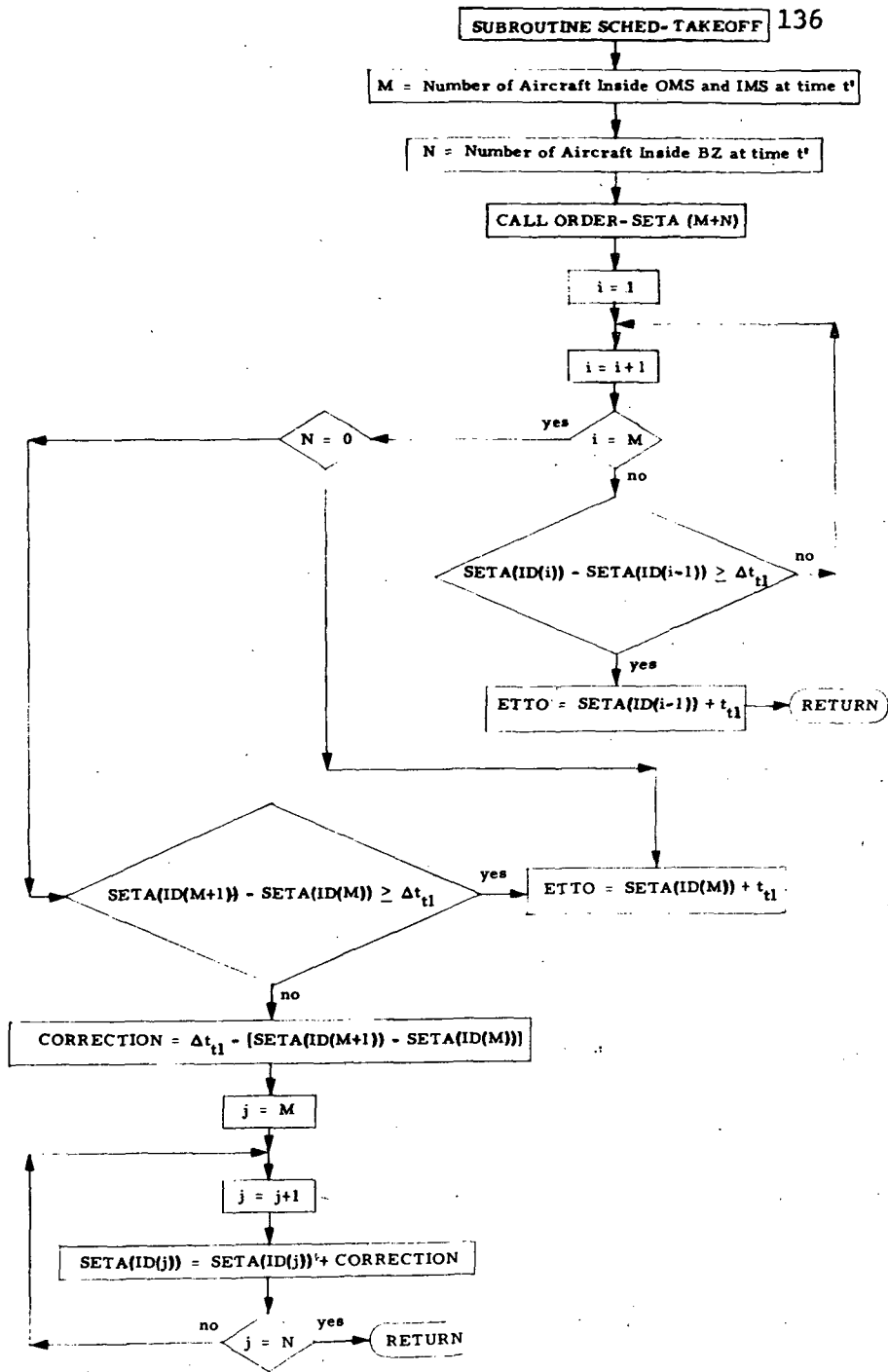


Fig. 5.15 Flow Chart for the Subroutine SCHED-TAKEOFF

decide whether there is a large enough gap $\Delta t_{t\ell}$ between two of these successive SETA's, so that the take-off can be released during that gap. If there is, then the take-off is scheduled for $t_{t\ell}$ seconds after the first one of the successive landings. The values of $\Delta t_{t\ell}$ and $t_{t\ell}$ are kept in MIT (cf. fig. 5.2).

If there is no large enough gap between SETA's of aircraft already in the OMS and the IMS, then the subroutine looks at the gap between the smallest SETA of those aircraft still in the BZ, and the largest SETA among those aircraft still in the OMS and IMS. If this gap is large enough the take-off is scheduled there. If not, then the take-off is still scheduled in that gap. However, now the SETA of the aircraft in the BZ must be augmented to allow enough temporal separation between the take-off and its landing. The SETA's of the rest of the aircraft in the BZ are then adjusted if necessary to account for the correction of the smallest SETA.

5.3 System Computational Requirements

This section is meant to be an informal discussion rather than an evaluation of the computational requirements of the proposed system.

It was seen that the minimum NTA size appropriate for this system is of the order of 50-70 n.miles. The radius of the IMS would be roughly half of the NTA radius. The system algorithm assumes control of the aircraft as soon as they enter the NTA and "keeps track" of them until they reach the IMS, when the final automatic correction instructions are given. The flight through the BZ and the OMS to-

gether, for a nondelayed aircraft, lasts for about 5-10 minutes depending on NTA size.

The ground computer should have enough memory to perform on line all the necessary computations, for all the aircraft that are inside the BZ and the OMS. The average number of aircraft inside the BZ and OMS over a 5-10 minute period can be found given the average arrival rate of aircraft to the NTA, and the mean delay for each aircraft. It should be of the order of 10 aircraft. Thus, the memory should be large enough to accommodate the system calculations for at least 10 aircraft simultaneously. Since the computations to be performed for each aircraft are few, it seems that the computers that could be the control elements of a system such as here, already exist.

The speed with which calculations should be made is not a very important factor. This is so because the calculations for each aircraft are rather straightforward. Furthermore, most of the time interval between transmission of data from the aircraft to ground, and reception of control instructions from on board equipment, will be spent by communications procedures. These can consume much time especially when the transmissions are to cover large distances.

All said, it seems to us that hardware is not a problem with the proposed system.

CHAPTER VI

CONCLUSIONS

The ATC system proposed in this thesis is deterministic.

The geometry and the particular algorithms were chosen with the objective to provide each aircraft with a flight plan inside the NTA, which if followed closely is guaranteed to alleviate all violations of separation standards. The key ideas on which the design is based, are the following:

a) The aircraft on their way to the OM are not required to check past any specific points (called outer fixes in the present ATC jargon). They can enter the IMS through any point of a circular boundary. The fact that aircraft enter the NTA only through a discrete number of traffic source points, does not restrict the entry points to the IMS to a discrete number. This is so because aircraft can enter the NTA with any heading, and different headings call for different minimum time nominal trajectories, namely different points of intersection with the IMS boundary. This makes the system more flexible.

b) All aircraft that enter the NTA should fly along minimum time type of trajectories, at constant speed, while they are outside the IMS. This convention facilitates sequencing and scheduling.

c) All aircraft are required to travel the IMS in the same time T_0 . This is crucial to the development of the whole system. It

simplifies sequencing and scheduling, and allows the computer to calculate nominal trajectories in the IMS far in advance.

d) While in the OMS aircraft can fly on any one of a discrete number of horizontal altitude levels. The vertical distance between successive levels can be chosen so that no conflicts occur in the IMS, where all traffic is merging toward one point.

e) A buffer zone is defined far from the OM. Most of the computations associated with each aircraft are done while they are flying in the BZ. Thus control starts early, and the traffic pattern around the airport can be arranged far in advance.

f) Traffic can enter the NTA from any of a discrete number of traffic source points. They are chosen so that no violations of separation standards occur in the OMS, under worst conditions.

g) Delay slots are defined for each source point, large enough that any type of delay path can "fit" safely inside a slot. The number of slots can be chosen such that the delaying capacity of the OMS can exceed the capacities of the present holding stacks.

It has been said that a deterministic ATC system is impractical. This thesis attempted to demonstrate that, with appropriate air-space segregation, a deterministic system can operate in the NTA. The stochastic nature of traffic does not affect the system operation, because the latter is designed to accept and handle all aircraft that enter the NTA one by one.

It is felt that most of the present ATC system inadequacies occur in periods of congestion. It was our effort to design the new

system so that it is insensitive to heavy traffic loads. This was accomplished by aiming at a worst case design.

It can be seen that with slight modifications the present ATC system can be adapted to the proposed scheme. The present geometry of the NTA's at different FAA airports is not very much different than a "one altitude level" type of geometry, fitting the proposed system. Actually it was seen that the minimum NTA radii envisioned here are of the same order of magnitude as the present NTA radii at different airports. Furthermore, the location of the IMS boundary for one altitude level is roughly at the same distance from the OM as the present delay fixes.

No mention of the function of the air traffic controller was made throughout the analysis. It should not be concluded that his job is eliminated. On the contrary his function becomes essential in the safe operation of the proposed system. Notice that nothing was mentioned about keeping track of deviations of the aircraft from the nominal trajectories. Here is where the controller would fit in a realistic system designed around this report's concepts. He can act as the "feedback correction element" in a closed loop fashion as illustrated in figure 6.1. His job would be simplified if the computer displayed on the controller's radar screen the open loop type of aircraft nominal trajectories determined automatically. Furthermore, the controller would be called on to resolve emergency situations and other adverse conditions which are extremely hard to build into any automated ATC system.

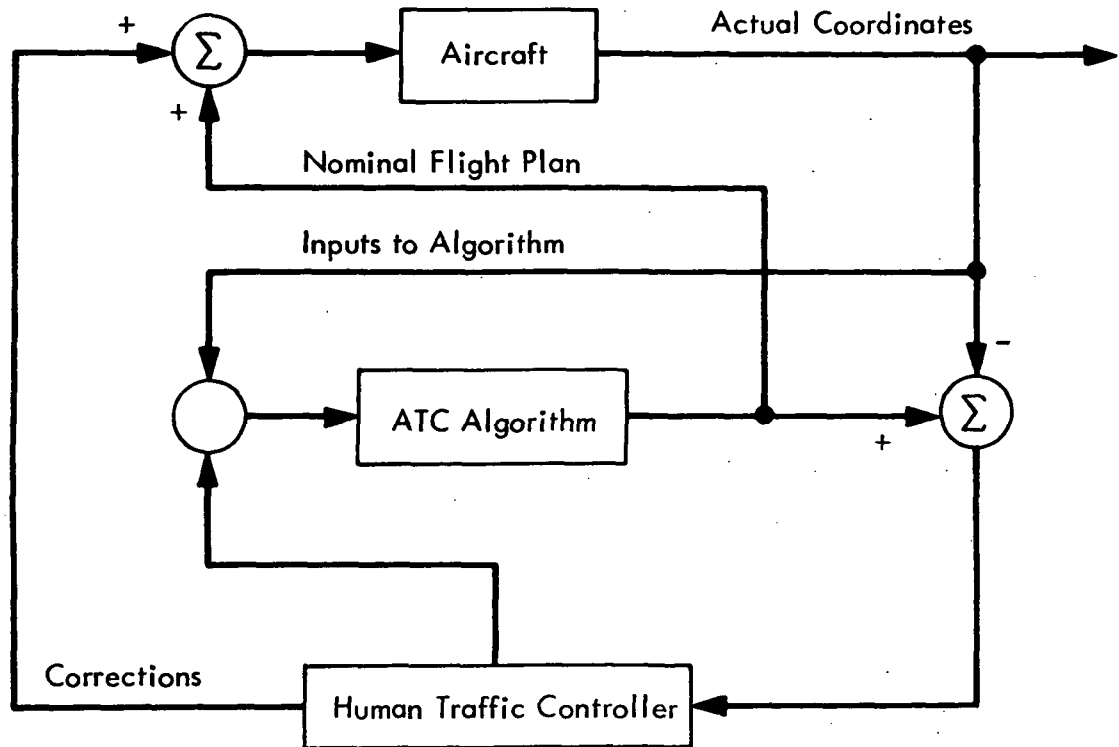


Fig. 6.1 Function of Human Controller in the Proposed System

Finally, it is our feeling that a real time simulation of the proposed system with realistic traffic situations, is required to determine the proposed system's effectiveness and its weak points in comparison with the present ATC system.

CHAPTER VII
IDEAS FOR FURTHER RESEARCH

The proposed system was designed under certain assumptions. Lifting these assumptions offers possibilities for further research.

We propose that further research in this area be in two general directions. First, to evaluate accurately the effectiveness of the proposed system under fewer assumptions. Second, to envision new deterministic systems, perhaps more complicated, based on some of the concepts of this thesis, and such that they automate more ATC functions, like missed approaches, emergency scheduling, etc. We now propose more specific areas for future investigation in ATC.

1) Take-off Routing. - Take-off scheduling was included in the system algorithm described in this thesis. However, no mention was made of how the takeoffs will be directed out of the NTA. It seems that the proposed system is equipped to handle this problem automatically.

The geometry would not be altered at all. A solution would be to change few traffic source points to "traffic exit points". Since the source points are picked far apart from each other it would not be too hard to thus designate "tubes" of airspace through which traffic could exit from the NTA. However, the details of the automatic take-off routing procedure have to be worked out.

2) Weather Disturbances. - The system in this thesis was designed assuming zero wind speed. This is a simplifying assumption because almost always there is a nonzero wind in the NTA.

We propose that at first the present deterministic nominal trajectories are studied, assuming there is a constant wind (magnitude and direction) blowing in the NTA. In other words, a study must be made of how the trajectories are altered if a wind speed is added to the aircraft velocity vector. Subsequently wind gusts could be studied assuming they can be modeled as white Gaussian noise.

What the study of the trajectories under the influence of wind should reveal, are the maximum expected errors in arrival times and IMS boundary positions. The geometry then could be changed accordingly to accommodate for these errors.

Presently when mean wind magnitude and direction is known, the pilots can adjust the aircraft's controls so that the indicated air speed reading is some value, from which if the mean wind speed is added or subtracted, according to some rule of thumb, the true air speed is known approximately.

3) Runway Rotation Due to Wind Shifts. - Since most airplanes have to land and take-off into the wind, when the latter changes direction, the runway has to be switched. This means switching the OM also to a new position. All landing traffic inside the NTA, at the time the switch is taking place, must be rescheduled and rerouted to the new OM. An automatic procedure for doing this seems very hard to derive, given that all aircraft have already been assigned nominal

trajectories.

A solution would be to assume that the switch will occur say in ten minutes, and start now rescheduling the aircraft that are entering the BZ so that they land on the "new" runway. Thus, after ten minutes all aircraft that were in the NTA and were scheduled to land on one runway will have done so, while all subsequent traffic will be arriving at the switched runway. The details of this scheme remain to be worked out.

4) Two Parallel Runways. - This problem that seems very hard to solve can be tackled with the geometry of the proposed scheme. The key idea would be to assign some altitude levels to traffic landing on one runway, and other altitude levels, possibly interspersed between the first ones, to traffic landing on the other runway. The hard problem would then be to choose the distances between the altitude levels so that traffic, bound toward one runway, does not interfere with that, bound toward the other one.

5) Intersecting Terminal Airspace from Two or More Airports. - This situation that presently constitutes a very difficult problem of ATC could be solved with the concepts developed here, provided that the airports' IMSes do not intersect. The idea would be again to assign different altitude levels to different airports. If however, the airports are so close together, that their IMSes intersect the problem becomes extremely complex. It is our feeling that this problem should be solved for each particular case, because the solution should depend very heavily on the proximity of the airports. The

solution should involve definition of new geometry and maybe new rules for the automatic choice of the nominal trajectories.

6) Hardware Requirements. - It would be very useful to know what kinds of computing and other equipment are necessary for the automatic communication between aircraft and ground as envisioned here. Since cost is always a crucial factor when a new system is proposed, the knowledge of necessary hardware should help determine the worth of a deterministic ATC system.

7) Automatic Feedback Controller. - An interesting topic for future research would be to try to build an automatic controller that corrects in a feedback fashion for the errors from the nominal trajectories. The idea would be to replace the box labeled "human controller" in figure 6.1 by a computer. The problem would be complicated by the fact that new correction maneuvers would have to be initiated every so often. It seems more promising to just adapt the already prescribed delay maneuvers, and speed profiles on line so that errors are corrected.

8) Simulation. - No ATC system deterministic or not can be fully understood without simulation. It is our feeling that a faster than real time simulation of the proposed system would not be hard to undertake. The system errors could be studied, when wind and other uncertainties are introduced in the simulation and a basis for comparison with other proposed schemes, as well as the present ATC system, established.

APPENDIX A

THE MINIMUM TIME PROBLEM IN THE OMS

In this appendix the solution to the minimum-time problem stated in 3.1.1 is presented. The theory of optimal control of nonlinear systems¹¹ is used to find the necessary conditions for optimality. Each candidate for the optimal control is then treated separately and the best solution is chosen.

I. Statement of the Problem

Given the three-state system:

$$\dot{x}(t) = v \cos \varphi(t) \quad (\text{A.1})$$

$$\dot{y}(t) = v \sin \varphi(t) \quad (\text{A.2})$$

$$\dot{\varphi}(t) = \frac{u(t)}{v} \quad (\text{A.3})$$

With the boundary conditions:

$$\begin{bmatrix} x(0) \\ y(0) \\ \varphi(0) \end{bmatrix} = \begin{bmatrix} x_0 \\ y_0 \\ \varphi_0 \end{bmatrix} \quad \begin{aligned} x_0^2 + y_0^2 &= R_N^2 \\ x^2(T) + y^2(T) &= L^2 \\ \tan \varphi(T) &= y(T)/x(T) \end{aligned}$$

Find the control $u_{[0,T]}$ such that $|u(t)| \leq A$ for $t \in [0,T]$ and such that it minimizes the cost functional $J = \int_0^T dt$.

II. Necessary Conditions for Optimality

Suppose $u^*(t)$, $t \in [0,T]$ is the optimal control which transfers the state of the system from $[x_0, y_0, \varphi_0]$ at time $t=0$, to $[x(T), y(T), \varphi(T)]$

at some time T , and minimizes J . Let $\underline{z}^\circ(t) = [x^\circ(t) \ y^\circ(t) \ \varphi^\circ(t)]$ be the trajectory of the system corresponding to $u^\circ(t)$. Then by the minimum principle of Pontryagin, it is necessary that there exists a vector $\underline{p}^\circ(t) = [p_x^\circ(t) \ p_y^\circ(t) \ p_\varphi^\circ(t)]$ such that the following conditions are satisfied.

a) State and co-state dynamics

$$\dot{\underline{z}}^\circ(t) = \frac{\partial H}{\partial \underline{p}} [\underline{z}^\circ(t), \underline{p}^\circ(t), u^\circ(t)] \quad (\text{A.4})$$

$$\dot{\underline{p}}^\circ(t) = -\frac{\partial H}{\partial \underline{z}} [\underline{z}^\circ(t), \underline{p}^\circ(t), u^\circ(t)] \quad (\text{A.5})$$

where the Hamiltonian function $H(\underline{z}, \underline{p}, u)$ is defined by

$$\begin{aligned} H(\underline{z}, \underline{p}, u) = & 1 + p_x(t)v \cos \varphi(t) + p_y(t)v \sin \varphi(t) \\ & + p_\varphi(t) \frac{u(t)}{v} \end{aligned} \quad (\text{A.6})$$

Conditions (A.4) and (A.5) thus become

$$\dot{x}^\circ(t) = v \cos \varphi^\circ(t) \quad (\text{A.7})$$

$$\dot{y}^\circ(t) = v \sin \varphi^\circ(t) \quad (\text{A.8})$$

$$\dot{\varphi}^\circ(t) = u^\circ(t)/v \quad (\text{A.9})$$

$$\dot{p}_x^\circ(t) = 0 \quad (\text{A.10})$$

$$\dot{p}_y^\circ(t) = 0 \quad (\text{A.11})$$

$$\dot{p}_\varphi^\circ(t) = p_x^\circ(t) v \sin \varphi^\circ(t) - p_y^\circ(t) v \cos \varphi^\circ(t) \quad (\text{A.12})$$

b) Boundary conditions

$$\underline{z}(0) = \begin{bmatrix} x^\circ(0) \\ y^\circ(0) \\ \varphi^\circ(0) \end{bmatrix} = \begin{bmatrix} x_0 \\ y_0 \\ \varphi_0 \end{bmatrix} \quad (x_0^2 + y_0^2 = R_N^2) \quad (\text{A.13})$$

$$g_1[\underline{z}^\circ(T)] = x^{\circ 2}(T) + y^{\circ 2}(T) - L^2 = 0 \quad (\text{A.14})$$

$$g_2[\underline{z}^\circ(T)] = \tan \varphi^\circ(T) - \frac{y^\circ(T)}{x^\circ(T)} = 0 \quad (\text{A.15})$$

$$\underline{p}^\circ(T) = a_1 \left. \frac{\partial g_1}{\partial \underline{z}} \right|_{\underline{z}^\circ(T)} + a_2 \left. \frac{\partial g_2}{\partial \underline{z}} \right|_{\underline{z}^\circ(T)} \quad (\text{A.16})$$

where a_1, a_2 are arbitrary constants. Notice that (A.13)-(A.15) provide five equations for the boundaries. If a_1 and a_2 are eliminated from the three equations (A.16), then the sixth equation at the boundary is obtained.

c) Hamiltonian minimization

$$H(\underline{z}^\circ(t), \underline{p}^\circ(t), u^\circ(t)) \leq H(\underline{z}^\circ(t), \underline{p}^\circ(t), u(t)) \quad (\text{A.17})$$

for all $t \in [0, T]$. (A.17) can be written explicitly:

$$\begin{aligned} & 1 + p_x^\circ(t) v \cos \varphi^\circ(t) + p_y^\circ(t) v \sin \varphi^\circ(t) + p_\varphi^\circ(t) \frac{u^\circ(t)}{v} \leq \\ & \leq 1 + p_x^\circ(t) v \cos \varphi^\circ(t) + p_y^\circ(t) v \sin \varphi^\circ(t) + p_\varphi^\circ(t) \frac{u(t)}{v} \end{aligned} \quad (\text{A.18})$$

$$\text{d) } H(\underline{z}^\circ(t), \underline{p}^\circ(t), u^\circ(t)) = 0, \quad \forall t \in [0, T]$$

or

$$1 + p_x^\circ(t) v \cos \varphi^\circ(t) + p_y^\circ(t) v \sin \varphi^\circ(t) + p_\varphi^\circ(t) \frac{u^\circ(t)}{v} = 0 \quad (\text{A.19})$$

e) Control constraint s

$$|u(t)| \leq A, \quad t \in [0, T] \quad (\text{A.20})$$

III. Candidates for Optimal Control

From (A.18) we obtain:

$$p_{\varphi}^{\circ}(t) u^{\circ}(t) \leq p_{\varphi}^{\circ}(t) u(t) \quad (\text{A.21})$$

hence

- i) If $p_{\varphi}^{\circ}(t) > 0$ then $u^{\circ}(t) = -A$
- ii) If $p_{\varphi}^{\circ}(t) < 0$ then $u^{\circ}(t) = A$
- iii) If $p_{\varphi}^{\circ}(t) = 0$ then $u^{\circ}(t)$ as given by (A.21) can be anything.

We now investigate this particular situation to see if the singular control $u^{\circ}(t)$ can be found. Thus suppose $p_{\varphi}^{\circ}(t) = 0$ for $t \in [t_1, t_2] \subset [0, T]$ ($t_1 \neq t_2$). Then in the same interval $\dot{p}_{\varphi}^{\circ}(t) = 0$ or from eq. (A.12)

$$p_x^{\circ}(t) v \sin \varphi^{\circ}(t) - p_y^{\circ}(t) v \cos \varphi^{\circ}(t) = 0 \quad (\text{A.22})$$

Differentiate both sides of (A.22) to obtain

$$\left[p_x^{\circ}(t) v \cos \varphi^{\circ}(t) + p_y^{\circ}(t) v \sin \varphi^{\circ}(t) \right] \frac{u^{\circ}(t)}{v} = 0 \quad (\text{A.23})$$

From (A.19) since $p_{\varphi}^{\circ}(t) = 0$, we have

$$p_x^{\circ}(t) v \cos \varphi^{\circ}(t) + p_y^{\circ}(t) v \sin \varphi^{\circ}(t) = -1 \quad (\text{A.24})$$

(A.23) and (A.24) readily yield $u^{\circ}(t) = 0$.

So the optimal control $u^{\circ}(t)$ is always defined and is equal to

$$u^{\circ}(t) = -A \operatorname{sgn} p_{\varphi}^{\circ}(t) \quad (\text{A.25})$$

where the signum function is defined by:

$$\text{sgn } x = \begin{cases} 1 & \text{if } x > 0 \\ -1 & \text{if } x < 0 \\ 0 & \text{if } x = 0 \end{cases}$$

To obtain some insight into the problem we derive the trajectories for the three values of the optimal control (see also Telson, p. 61).

i) If $u^\circ(t) = A$ then $\varphi^\circ(t) = \frac{A}{v} t + \varphi_1$, i.e., the aircraft is turning counterclockwise at the maximum possible rate.

ii) If $u^\circ(t) = -A$ then $\varphi^\circ(t) = -\frac{A}{v} t + \varphi_1'$ and the aircraft is turning clockwise at the maximum rate.

iii) If $u^\circ(t) = 0$ then $\varphi^\circ(t) = \text{constant}$ i.e., the aircraft is moving in a straight line.

Figure A.1 illustrates these trajectories.

We now try to find how many times the optimal control can switch between the three possible values $+A$, 0 , $-A$. This will depend on the nature of the function $p_\varphi^\circ(t)$.

From (A.25) we obtain that

$$\frac{u^\circ(t)}{v} p_\varphi^\circ(t) = -\frac{A}{v} [\text{sgn } p_\varphi^\circ(t)] p_\varphi^\circ(t) = -\frac{A}{v} |p_\varphi^\circ(t)| \quad (\text{A.26})$$

(A.26) combined with (A.19) give:

$$1 + p_x^\circ(t) v \cos \varphi^\circ(t) + p_y^\circ(t) v \sin \varphi^\circ(t) = \frac{A}{v} |p_\varphi^\circ(t)| \quad (\text{A.27})$$

From (A.10) and (A.11) we obtain that

$$p_x^\circ(t) = p_x = \text{constant} \quad (\text{A.28})$$

$$p_y^\circ(t) = p_y = \text{constant} \quad (\text{A.29})$$

Thus (A.27) becomes:

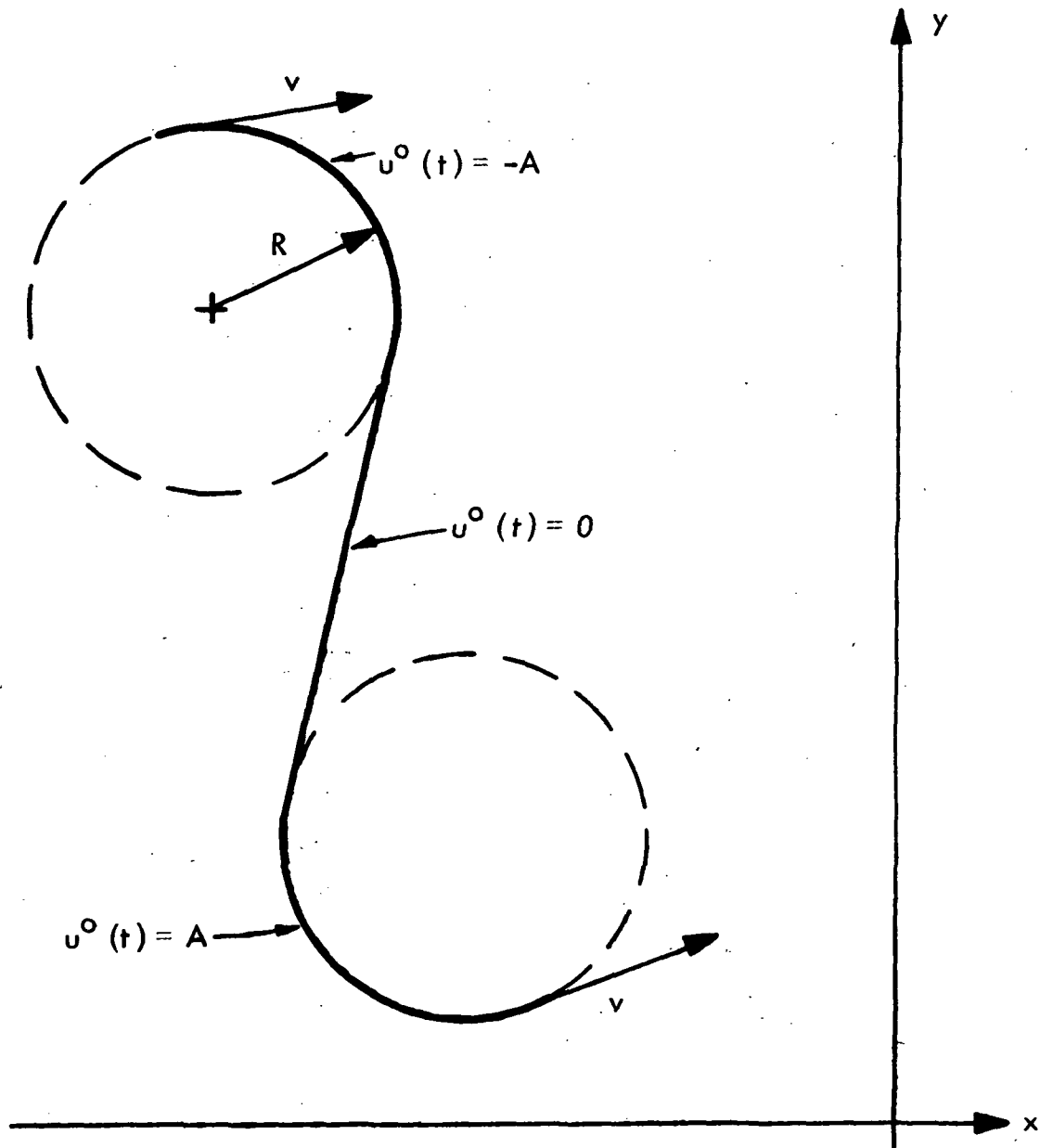


Fig. A.1 Acceptable Aircraft Trajectories for Minimum Time Operation

$$1 + p_x v \cos \varphi^\circ(t) + p_y v \sin \varphi^\circ(t) = \frac{A}{v} |p_\varphi^\circ(t)| \quad 154$$

or

$$1 + \frac{p_x v}{\cos \alpha} \cos[\varphi^\circ(t) - \alpha] = \frac{A}{v} |p_\varphi^\circ(t)| \quad (\text{A.30})$$

where

$$\tan \alpha = p_y/p_x \quad (\text{A.31})$$

Since the right-hand side of (A.30) is always non-negative, it must be true that $k = \frac{p_x v}{\cos \alpha} \geq 1$. If $k > 1$, then $p_\varphi^\circ(t)$ cannot switch, because $p_\varphi^\circ(t)$ is a continuous function of t and thus if $p_\varphi^\circ(t)$ is to go from positive to negative it must go through zero. Note that $k > 1$ gives no switching, in the optimal control sequence, namely $u^\circ(t) = 0$ or A or $-A$ for $t \in [0, T]$.

To investigate the case of switchings, assume $k = 1$. Then $p_\varphi^\circ(t)$ starts at some value $p_\varphi^\circ(0)$ which can be positive, negative or zero. If $p_\varphi^\circ(0)$ is non-zero then $p_\varphi^\circ(t)$ will tend toward zero in a sinusoidal fashion.[†] Once it reaches zero it will either stay there or leave. However, once $p_\varphi^\circ(t)$ leaves zero it cannot return to it until the cosine function in eq. (A.30) goes through a complete cycle. What this means is that $\varphi^\circ(t)$

[†]To see this solve (A.9) and (A.12).

$$\varphi^\circ(t) = \varphi_0 - \frac{At}{v} \operatorname{sgn} p_\varphi^\circ(t)$$

$$\dot{p}_\varphi^\circ(t) = \frac{p_x v}{\cos \alpha} \sin[\varphi^\circ(t) - \alpha] = \sin\left[\varphi_0 - \alpha - \frac{At}{v} \operatorname{sgn} p_\varphi^\circ(t)\right]$$

thus

$$\text{i) If } p_\varphi^\circ(0) > 0 \text{ then } p_\varphi^\circ(t) = p_\varphi^\circ(0) + \frac{v}{A} \left[\cos\left(\varphi_0 - \alpha - \frac{At}{v}\right) - \cos(\varphi_0 - \alpha) \right]$$

ii) If $p_\varphi^\circ(0) < 0$ then

$$p_\varphi^\circ(t) = p_\varphi^\circ(0) - \frac{v}{A} \left[\cos\left(\varphi_0 - \alpha + \frac{At}{v}\right) - \cos(\varphi_0 - \alpha) \right]$$

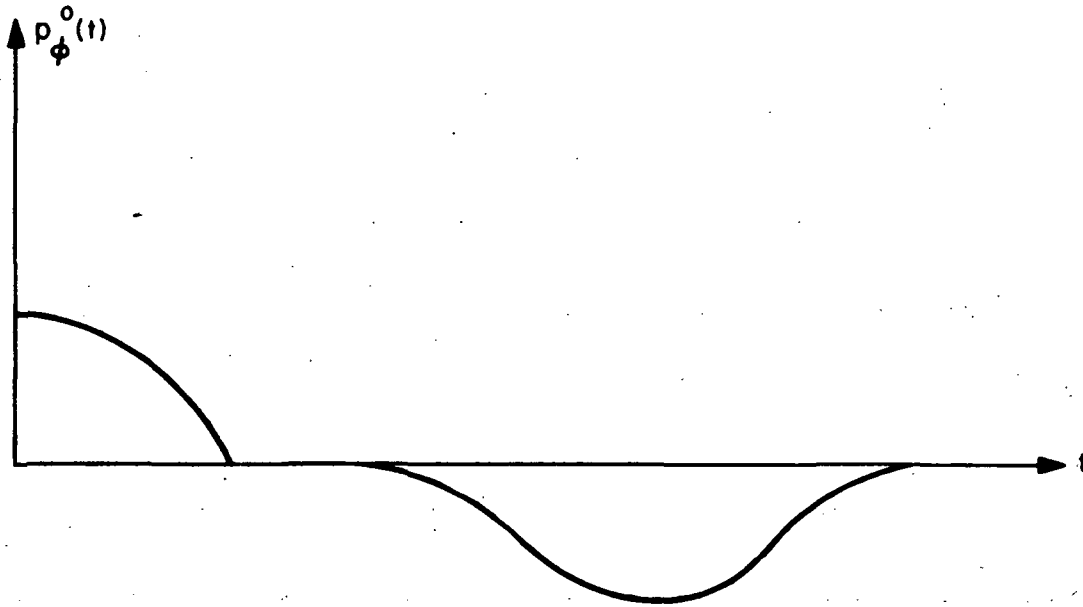


Fig. A.2 Behaviour of $p_{\phi}^0(t)$

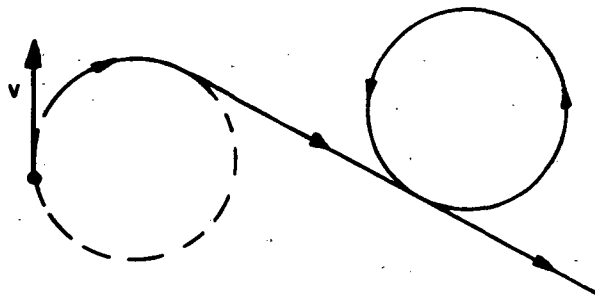


Fig. A.3 Aircraft Trajectory for $p_{\phi}^0(t)$ as in Fig. A.2

will have to increase (or decrease) by 2π , i.e., the aircraft must describe a full circle. The situation which is illustrated in Figs. A.2 and A.3 is clearly time suboptimal.

The conclusion thus is that the control $u^\circ(t)$ can switch at most twice in the interval $[0, T]$. This leaves as candidates for the optimal control law the following sequences:

- a) $u^\circ = 0$
 $-A$
 $+A$
- b) $u^\circ = (A, 0)$
 $(-A, 0)$
- c) $u^\circ = (0, A)$
 $(0, -A)$
- d) $u^\circ = (-A, A)$
 $(A, -A)$
- e) $u^\circ = (A, 0, A)$
 $(A, 0, -A)$
 $(-A, 0, A)$
 $(-A, 0, -A)$

IV. Examination of the Candidates for the Optimal Control Law

In this section we examine the trajectories that are enforced on an aircraft by each of the candidates for optimal control. Since the geometry has circular symmetry, it is seen (see Fig. A.4) that, as long as the velocity vector of the entering aircraft forms an angle θ with

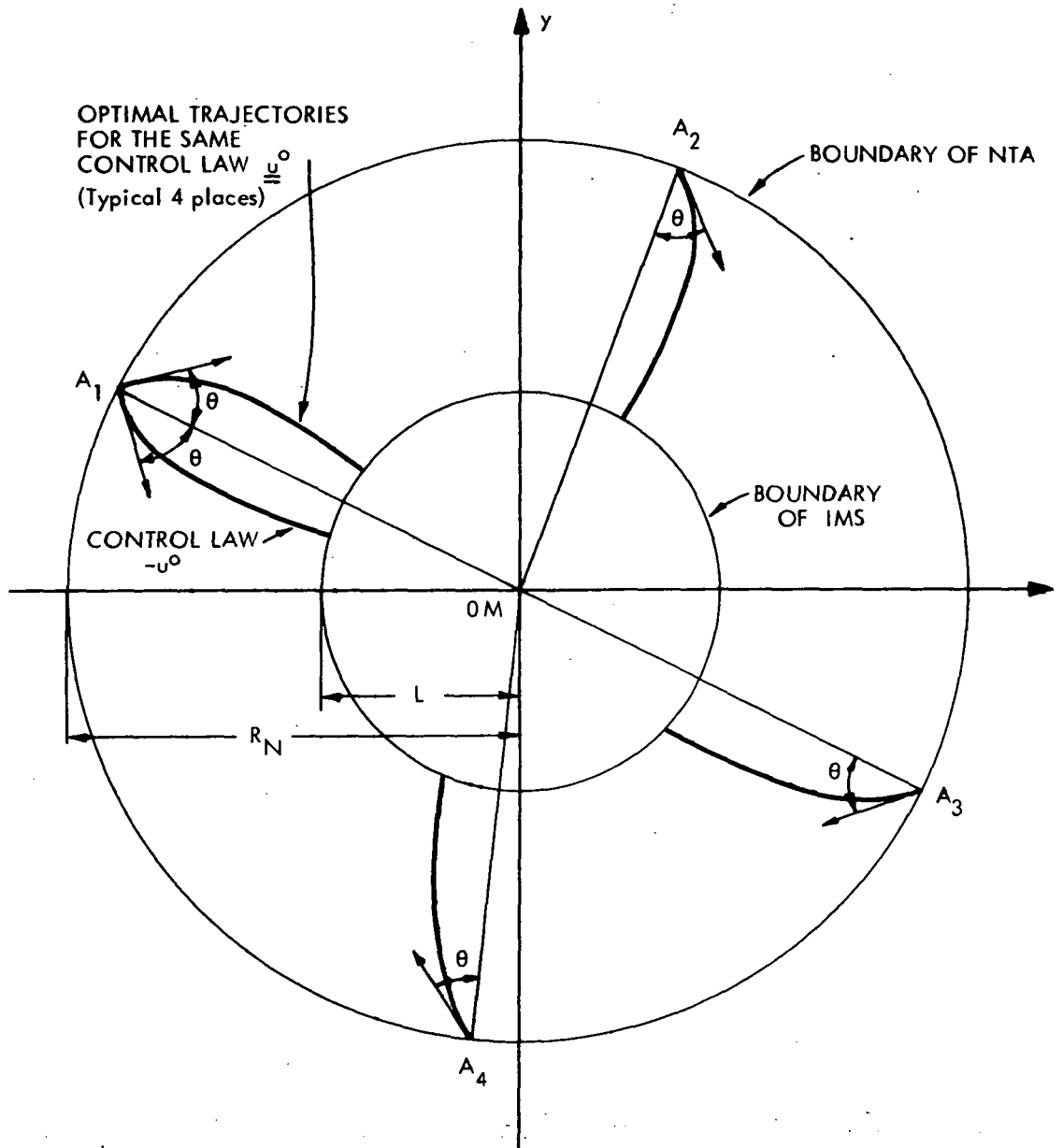


Fig. A.4 Symmetry of the Control Law

the radius of the NTA ending at the point of entry, then no matter where the entrance point is located on the boundary of the NTA, the control law is the same. Thus, we shall pick one point on the boundary of the NTA and will consider all possible θ 's. We shall assume that $-\frac{\pi}{2} < \theta < \frac{\pi}{2}$ which will represent an inbound aircraft. Radial symmetry also indicates that if u° is the optimal control law for a heading θ , then the optimal control law for an entrance heading $-\theta$ is $-u^\circ$ as illustrated in Fig. A.4. Thus we only need consider $0 \leq \theta < \pi/2$.

a) i) $u^\circ = 0$

This control law forces the aircraft to move along a straight line. It is obvious that the only case in which this trajectory will meet the boundary conditions is when the aircraft enters with $\theta = 0$ or, what amounts to the same thing, with a heading angle ϕ_0 such that:

$$\tan \phi_0 = y_0/x_0 \quad (\text{A.32})$$

Figure A.5 illustrates the situation. It is also apparent that if (A.32) is true about the initial conditions then this control is the optimal one. In this case the value of the cost J is readily found to be

$$J = T_{\min} = \frac{R_N - L}{v} \quad (\text{A.33})$$

ii) $u^\circ = \pm A$

This control law implies that aircraft will meet the boundary of the IMS before it completes a full turn. Let us calculate the radius of the turn. This can be found from the equation

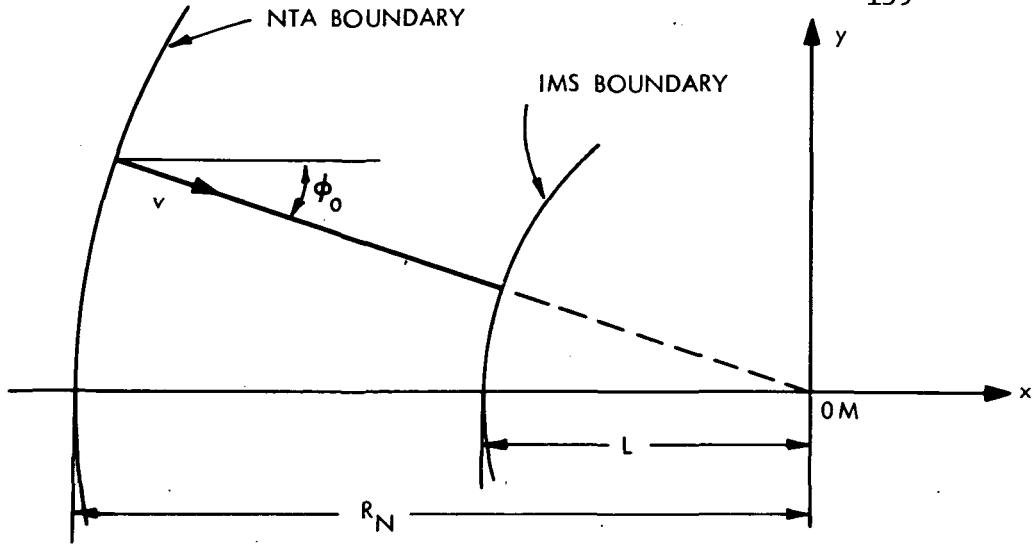


Fig. A.5 Trajectory for the $u^0 = 0$ Control Law

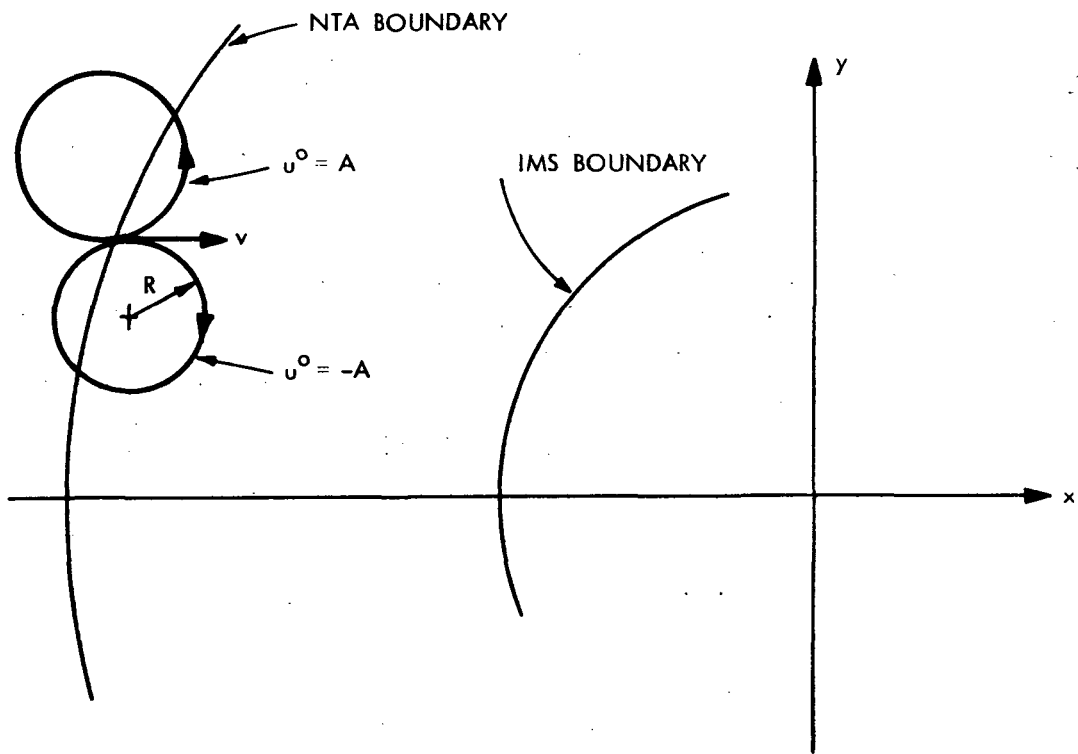


Fig. A.6 Trajectories for the Control Laws $u^0 = \pm A$

$$\frac{mv^2}{R} = mg|\tan \theta|$$

or

$$R = \frac{v^2}{g|\tan \theta|} \quad (\text{A.34})$$

For the maximum allowable entrance speed of 300 knots and maximum bank angle θ of 30° (which is what $u^\circ = \pm A$ signifies) we obtain

$$\begin{aligned} R &\simeq \frac{300^2 \times 1852 \times \sqrt{3}}{10 \times (3600)^2} \text{ n. miles} \simeq \\ &\simeq 2.21 \text{ n. miles} \end{aligned}$$

In this thesis L will be found to be of the order of 40 n. miles while R_N will be of the order of 70 n. miles. Thus it seems that this control law will never meet the boundary conditions.

b) i) $u^\circ = (-A, 0)$

It is easily seen that this control sequence can drive an aircraft with any initial condition $\theta \in (0, \pi/2)$,[†] to the boundary of the IMS with the proper heading. It will be seen shortly that this control law is also the optimal one if $\theta \in (0, \pi/2)$. Thus it seems proper to calculate the switch time t_s and the cost functional $J = T_{\min}$.

We first solve eqs. (A.7)-(A.9).

$$\dot{\varphi}^\circ(t) = \varphi_0 - \frac{A}{v} t \quad (\text{A.35})$$

$$\dot{x}^\circ(t) = v \cos(\varphi_0 - \frac{A}{v} t)$$

Then

[†]Under the assumption that the aircraft is inbound, the condition $\theta \in (0, \pi/2)$ is equivalent to $\theta > 0$. This, in turn, is equivalent to $\tan \varphi_0 > y_0/x_0$.

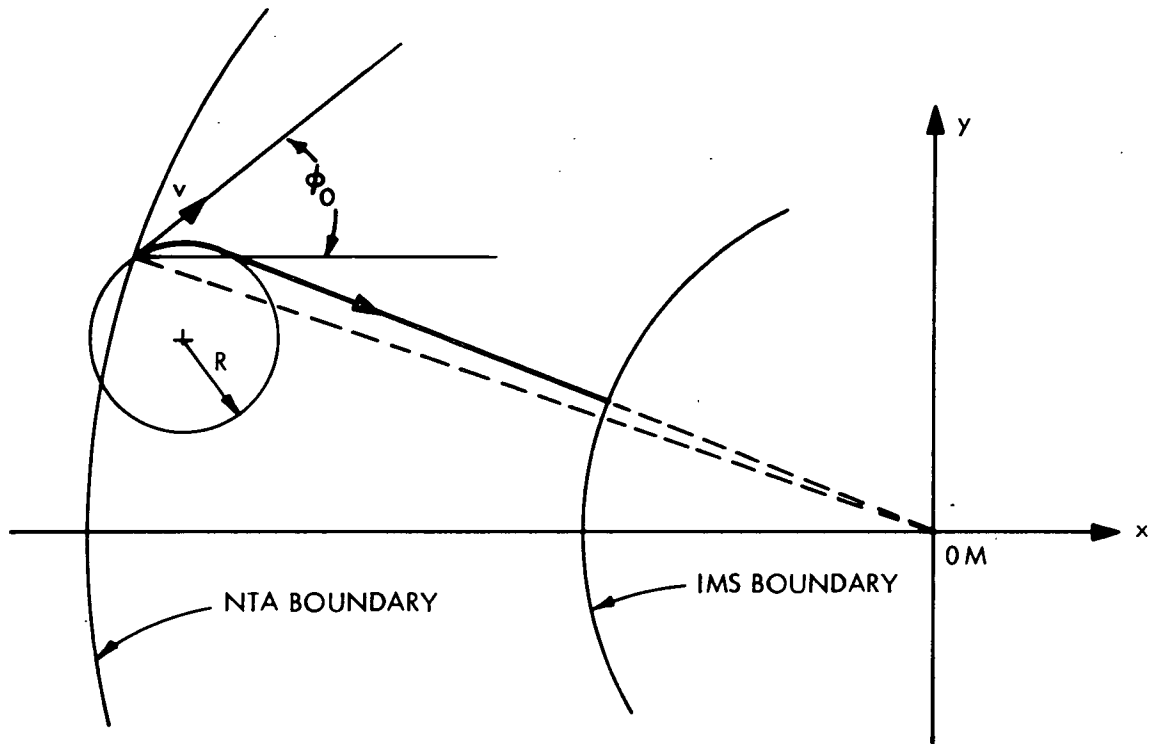


Fig. A.6 Trajectory for the Control Law $u^0 = (-A, 0)$

$$\begin{aligned} x^\circ(t) &= x_0 + \frac{v^2}{A} \sin \varphi_0 - \frac{v^2}{A} \sin\left(\varphi_0 - \frac{A}{v} t\right) \\ \dot{y}^\circ(t) &= v \sin\left(\varphi_0 - \frac{A}{v} t\right) \end{aligned} \quad (\text{A.36})$$

and, hence,

$$y^\circ(t) = y_0 - \frac{v^2}{A} \cos \varphi_0 + \frac{v^2}{A} \cos\left(\varphi_0 - \frac{A}{v} t\right) \quad (\text{A.37})$$

At time t_s the relation that must be satisfied is:

$$\tan \varphi^\circ(t_s) = \frac{y^\circ(t_s)}{x^\circ(t_s)} \quad (\text{A.38})$$

or,

$$\tan \varphi^\circ(t_s) = \frac{a + d \cos \varphi^\circ(t_s)}{b - d \sin \varphi^\circ(t_s)} \quad (\text{A.39})$$

where

$$a = y_0 - \frac{v^2}{A} \cos \varphi_0, \quad b = x_0 + \frac{v^2}{A} \sin \varphi_0, \quad d = \frac{v^2}{A}$$

Set $\varphi^\circ(t_s) = x$ and solve (A.39) for x .

$$\tan x = \frac{\sin x}{\cos x} = \frac{a + d \cos x}{b - d \sin x}$$

which yields

$$b \sin x - d \sin^2 x = a \cos x + d \cos^2 x \quad (\text{A.40})$$

or

$$b \sin x - a \cos x = d$$

Set $\tan \epsilon = a/b$, $-\pi/2 \leq \epsilon \leq \pi/2$. Then (A.40) becomes $\frac{b}{\cos \epsilon} \sin(x - \epsilon) = d$

so that

$$\sin(x - \epsilon) = \frac{d \cos \epsilon}{b} = \frac{d}{\sqrt{a^2 + b^2}}$$

and so

$$x = \epsilon + \sin^{-1} \frac{d}{\sqrt{a^2 + b^2}} \quad (\text{A.41})$$

or

$$x = \tan^{-1} \frac{y_0 - \frac{v^2}{A} \cos \varphi_0}{x_0 + \frac{v^2}{A} \sin \varphi_0} + \sin^{-1} \frac{\frac{v^2}{A}}{\left[\left(y_0 - \frac{v^2}{A} \cos \varphi_0 \right)^2 + \left(x_0 + \frac{v^2}{A} \sin \varphi_0 \right)^2 \right]^{\frac{1}{2}}} \quad (\text{A.42})$$

Equation (A.42) gives the value of the switch angle $\varphi^\circ(t_s)$ in terms of the initial conditions, the entrance speed, v , and the maximum value, A , of the control. To calculate the switch time t_s just set:

$$\varphi^\circ(t_s) = x$$

to obtain

$$\varphi_0 - \frac{A}{v} t_s = x \implies t_s = (\varphi_0 - x) \frac{v}{A} \quad (\text{A.43})$$

The value of the cost functional J is readily found to be:

$$J = T_{\min} = t_s + \frac{[x^{\circ 2}(t_s) + y^{\circ 2}(t_s)]^{\frac{1}{2}} - L}{v} \quad (\text{A.44})$$

where $x^\circ(t_s)$ and $y^\circ(t_s)$ are readily calculated by (A.36) and (A.37)

$$\text{ii) } u^\circ = (A, 0)$$

It is readily seen, considering the radial symmetry of the geometry, that if $-\pi/2 < \theta < 0$ (or equivalently if $\tan \varphi_0 < y_0/x_0$, and the aircraft is inbound) then this control law can meet the boundary conditions. The values of t_s and T_{\min} are given by the following formulas which are nothing but (A.43) and (A.44) with some sign changes.

$$\varphi^\circ(t) = x_0 + \frac{A}{v} t \quad (\text{A.45})$$

$$x^\circ(t) = x_0 - \frac{v^2}{A} \sin \varphi_0 + \frac{v^2}{A} \sin(\varphi_0 + \frac{A}{v} t) \quad (\text{A.46})$$

$$y^\circ(t) = y_0 + \frac{v^2}{A} \cos \varphi_0 - \frac{v^2}{A} \cos(\varphi_0 + \frac{A}{v} t) \quad (\text{A.47})$$

$$t_s = (x - \varphi_0) \frac{v}{A} \quad (\text{A.48})$$

where

$$x = \tan^{-1} \frac{y_0 + \frac{v^2}{A} \cos \varphi_0}{x_0 - \frac{v^2}{A} \sin \varphi_0} - \sin^{-1} \frac{\frac{v^2}{A}}{\left[\left(y_0 + \frac{v^2}{A} \cos \varphi_0 \right)^2 + \left(x_0 - \frac{v^2}{A} \sin \varphi_0 \right)^2 \right]^{\frac{1}{2}}} \quad (\text{A.49})$$

$$J = T_{\min} = t_s + \frac{[x^\circ{}^2(t_s) + y^\circ{}^2(t_s)]^{\frac{1}{2}} - L}{v} \quad (\text{A.50})$$

c) i) $u^\circ = (0, -A)$

This control law can drive the aircraft to the boundary of the IMS with radial heading only if $0 < \theta \leq \sin^{-1} \frac{L+R}{R_N}$, where R is the maximum turning radius given by (A.34) (see Fig. A.7). Before we plunge into any calculations it is easy to notice from Fig. A.7 that the path ADE-OM is longer than the path ABC-OM, because they are both on the same side of the straight line A-OM and the former path lies above the latter. Thus it is evident that the control law $u^\circ = (0, A)$ is inferior to the $(-A, 0)$ law.

ii) $u^\circ = (0, A)$

Symmetry and the reasoning above lead to the conclusion that for any initial conditions that the control law $u^\circ = (-A, 0)$ will drive to

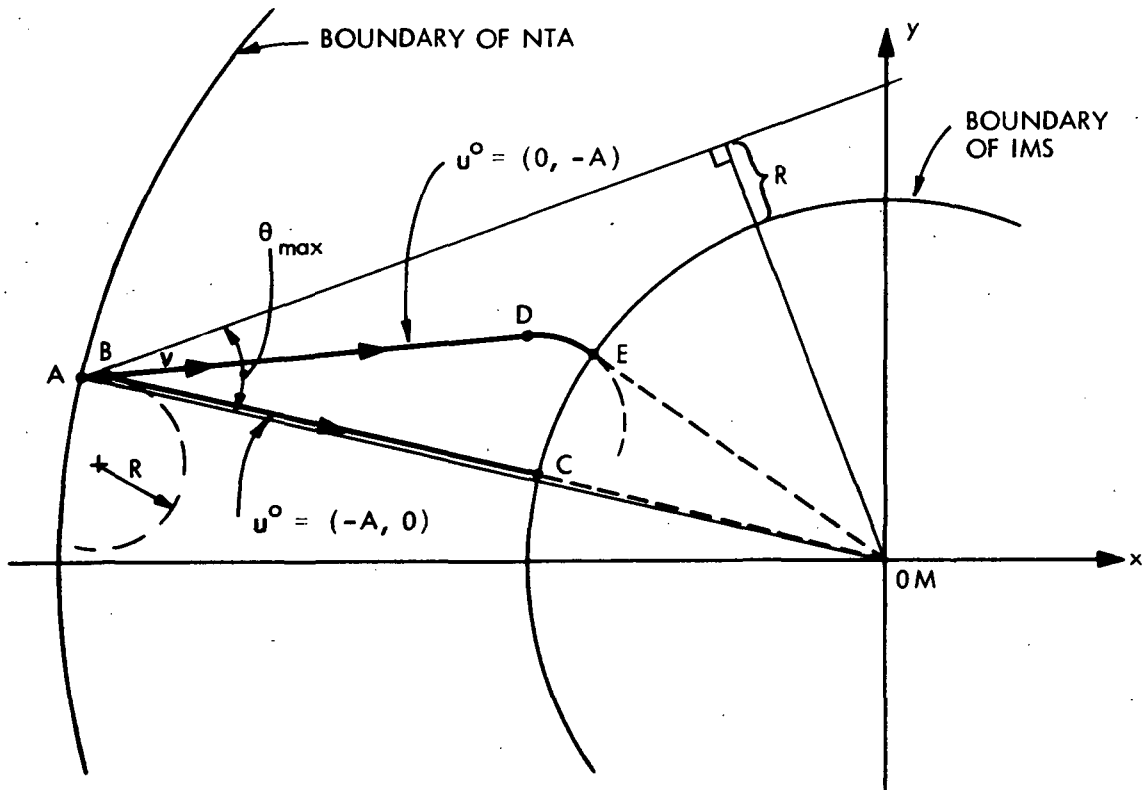


Fig. A.7 Trajectories for the Control Law $u^0 = (0, -A)$ and its Inferiority to the $(-A, 0)$ Control. For $\theta > \theta_{max}$ the Control Law $u = (0, -A)$ Cannot Lead the Aircraft to the Boundary of the IMS with Radial Heading

the boundary of the IMS with radial heading, the control law $u^\circ = (0, -A)$ is better.

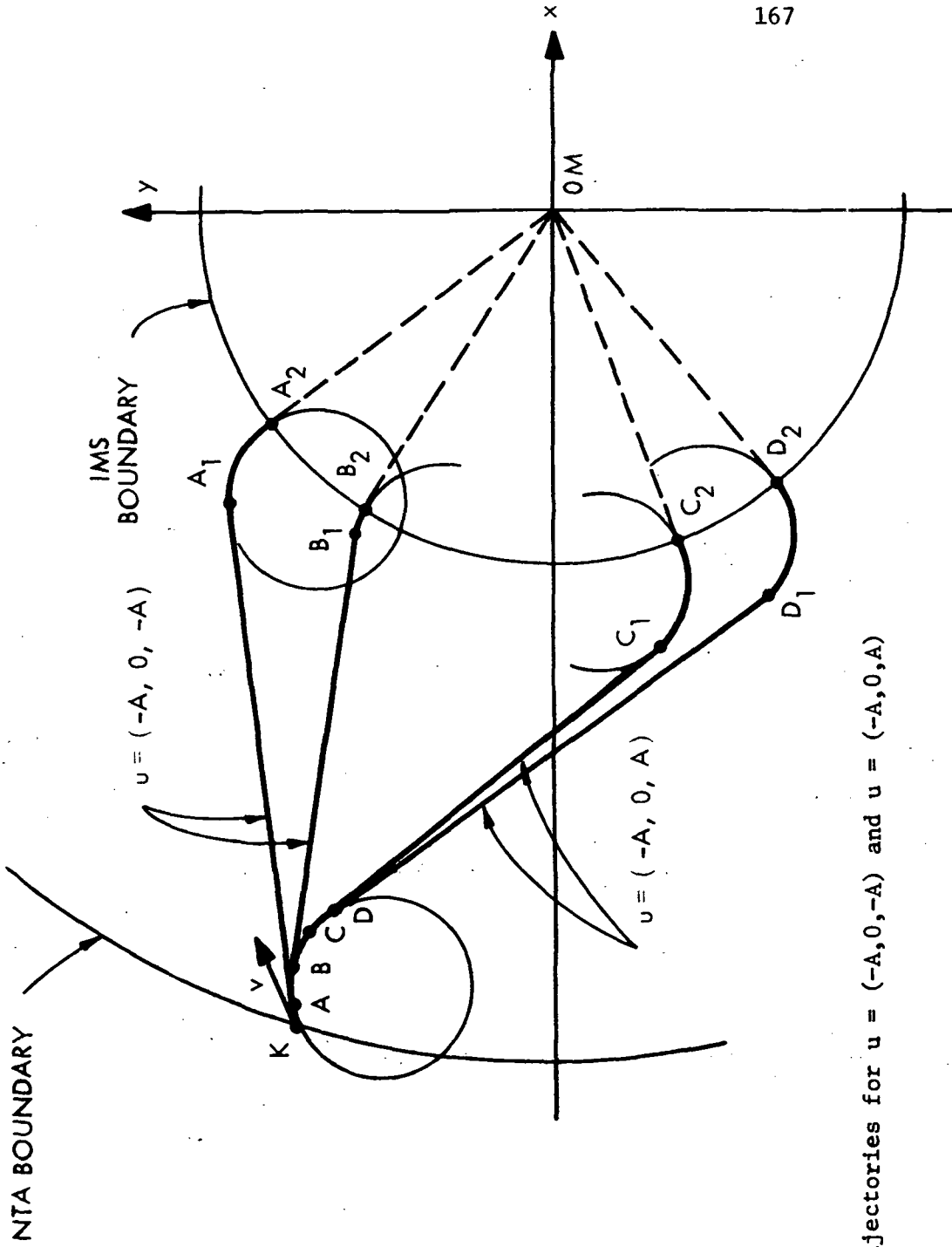
$$d) \quad u^\circ = (A, -A) \text{ or } (-A, A)$$

The reasoning that was used to exclude the control laws $u^\circ = A$ and $u^\circ = -A$ applies here too. In order for these control laws to give trajectories that will meet the boundary conditions, the difference $R_N - L$ must be very small (of the order of 4-5 n.miles). Since in the system proposed here, this is not the case, it seems futile to examine these control sequences.

$$e) \quad i) \quad u^\circ = (-A, 0, -A) \text{ or } (-A, 0, A)$$

It is easy to see that these control laws can drive any initial condition with $0 < \theta < \pi/2$ to the boundary of the IMS with radial heading. Furthermore, it can be seen that for any initial state, there are many possible ways that these laws can meet the boundary conditions (see Fig. A.8). We will show now that the control law $u = (-A, 0)$ is superior to any of the above control laws. To do this consider Fig. A.9. The trajectory $KABB_1-OM$ corresponds to the $(-A, 0)$ law. The trajectories KAA_1A_2-OM and $KABCC_1C_2-OM$ correspond to the $(-A, 0, -A)$ and $(-A, 0, A)$ laws respectively. The latter two trajectories are not picked in any specific way, but are just samples of all the possible trajectories which can be traced by the control laws $(-A, 0, \pm A)$.

Now it is obvious that the control law $(-A, 0)$ is superior. It is better than the $(-A, 0, -A)$ law because the path KAA_1A_2-OM is longer than the path $KABB_1-OM$. Also since the path BCC_1C_2-OM is longer than



Fig, A.8 Trajectories for $u = (-A, 0, -A)$ and $u = (-A, 0, A)$

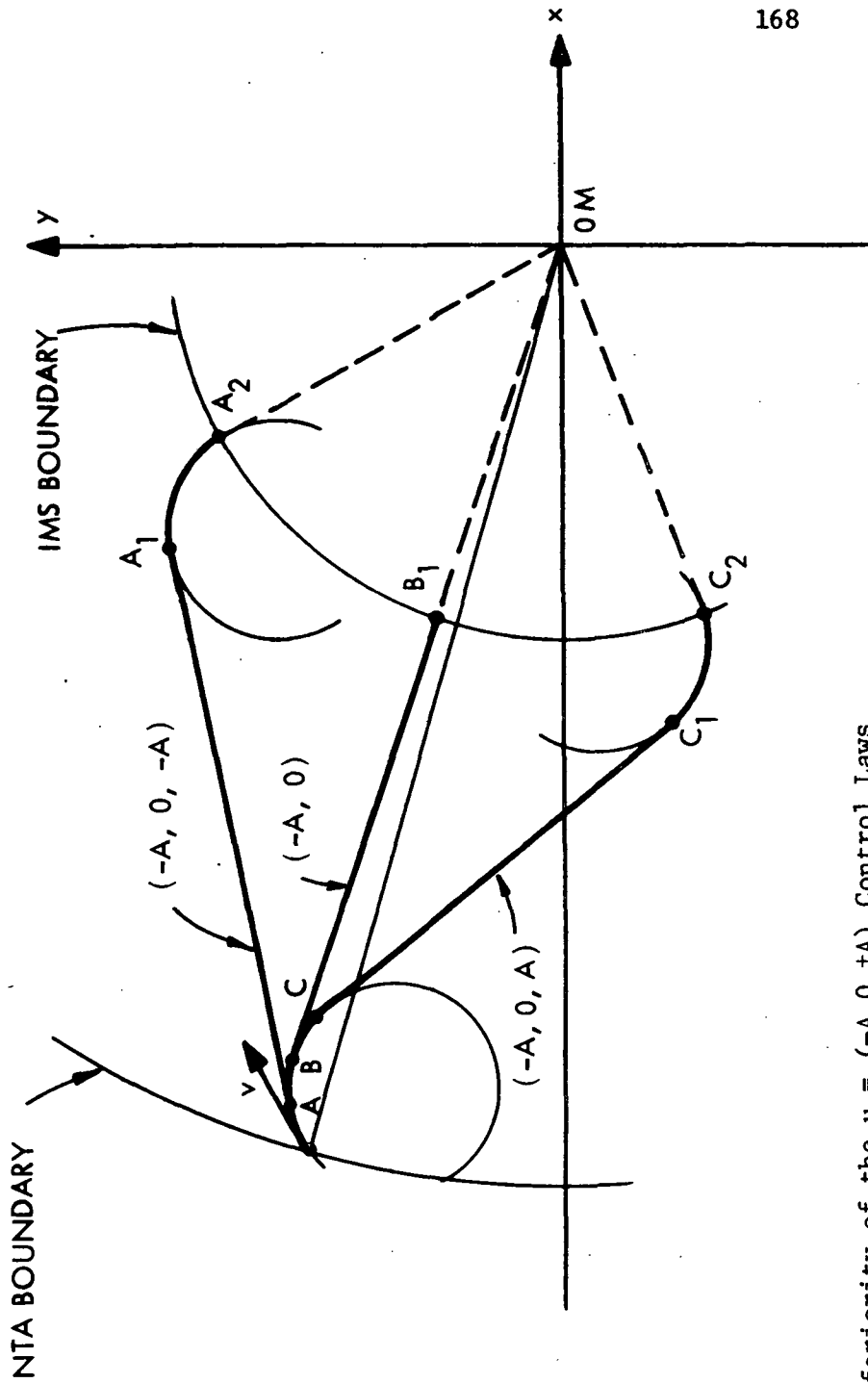


Fig. A.9 Inferiority of the $u = (-A, 0 \pm A)$ Control Laws

the straight line path BB_1-OM , the control law $(-A, 0, A)$ is clearly suboptimal.

$$\text{ii) } u^\circ = (A, 0, \pm A)$$

By symmetry and the observations made above, these control laws are inferior to the law $u^\circ = (A, 0)$.

V. The Optimal Control Law

Having analyzed all the possible candidates for optimality, we can state the optimal control law as follows.

Theorem: The optimal control law for the problem stated in section I is the following

a) If $\tan \phi_0 = y_0/x_0$ then $u^\circ = 0$. T_{\min} is calculated from eq. (A.33).

b) If $\tan \phi_0 > y_0/x_0$ then $u^\circ = (-A, 0)$. The switch time t_s and T_{\min} are calculated from eqs. (A.43) and (A.44) respectively.

c) If $\tan \phi_0 < y_0/x_0$ then $u^\circ = (A, 0)$. The switch time t_s and T_{\min} are calculated from eqs. (A.48) and (A.50) respectively.

BIBLIOGRAPHY

1. Simpson, R. W. An Analytical Investigation of Air Traffic Operations in the Terminal Area, Ph.D. Thesis, Dept. of Aeronautical Engineering, M.I.T., Cambridge, Mass. 1964.
2. Blumstein, A., An Analytical Investigation of Airport Capacity, Cornell Aeronautical Laboratory Report Number TA-1358-G-1, 1960.
3. Odoni, A., An Analytical Investigation of Air Traffic in the Vicinity of Terminal Areas, Ph.D. Thesis, Dept. of Electrical Engineering, M.I.T., Cambridge, Mass. 1969.
4. Report of the Department of Transportation Air Traffic Control Advisory Committee, Volumes 1 and 2, December 1969.
5. Special Issue on Air Traffic Control, Proc. IEEE, Vol. 58, No. 3, March 1970.
6. Computer Aided Metering and Spacing with ARTS III, Computer Systems Engineering Inc. Billerica, Mass. Study Report, Number FAA-RD-70-82, December, 1970.
7. Porter, L. W., On Optimal Scheduling and Holding Strategies for the Air Traffic Control Problem M.S. Thesis, Dept. of Electrical Engineering, M.I.T., Cambridge, Mass., September, 1969.
8. Athans, M. and Porter, L.W., An Approach to Semi-automated Optimal Scheduling and Holding Strategies for Air Traffic Control, M.I.T. Electronic Systems Laboratory, Rpt. ESL-P-437, December, 1970.
9. Telson, M. L., An Approach to Optimal Air Traffic Control During the Landing Phase, M.S. Thesis, Dept. of Electrical Engineering, M.I.T., Cambridge, Mass., August, 1969.
10. Erzberger, H. and Lee, H. Q., Optimum Guidance Techniques for Aircraft, NASA Rpt. 94035, Ames Research Center, Moffett Field, California, January 1971.
11. Athans, M. and Falb, P. L., Optimal Control, McGraw-Hill, New York, 1966.
12. Baran, G., Bateman, R. E., Benezra, J. N., Blumenthal, R. W., "Approach Airspace and Runway Capacity, Parametric Sensitivity Analysis", Boeing Company Report D6-24282, January 1970.